

CaCO_3 DISSOLUTION IN SO_2 SCRUBBING SOLUTION
MASS TRANSFER ENHANCED BY
CHEMICAL REACTIONS

BY

PUI-KUN ROLAND CHAN, B.S.

THESIS

Presented to the Faculty of the Graduate School of
The University of Texas at Austin
in Partial Fulfillment
of the Requirements
for the Degree of

MASTER OF SCIENCE IN ENGINEERING

THE UNIVERSITY OF TEXAS AT AUSTIN

May, 1981

ACKNOWLEDGMENTS

I would like to express my sincere appreciation and gratitude to Dr. D.M. Himmelblau and Dr. G.T. Rochelle for their helpful criticism and willingness to serve as members of the graduate supervising committee. Special thanks are due to Dr. G.T. Rochelle for his guidance, supervision, and support throughout this work; his suggestions and innovations are sincerely acknowledged.

I must also thank my colleague, Mr. P.K. Toprac for his work on the Coulter counter data.

Thanks are due to the U.S. Environmental Protection Agency for their financial support through EPA Grant No. R806251.

Finally, I wish to give my love to my family for giving me encouragement and support during all this years of my study. So many people have helped that I am sure to forget to mention some, but these also have my thanks.

Pui-Kun Roland Chan

February 1981

ABSTRACT

The rate of CaCO_3 dissolution in slurry scrubbers for flue gas desulfurization affects SO_2 absorption, $\text{CaSO}_3/\text{CaSO}_4$ scaling, and ultimate CaCO_3 utilization. The dissolution rate of reagent CaCO_3 has been measured in 0.1 M CaCl_2 at constant pH and CO_2 partial pressure by batch titration with HCl. A mass transfer model has been developed assuming that the calcite particles behave as spheres in an infinite stagnant solution. The model incorporates the effects of several equilibrium acid/base reactions and also includes the finite rate reaction involving CO_2 and HCO_3^- . The cumulative rate of mass transfer is calculated by integrating over a particle size distribution obtained by a Coulter counter.

The results of this investigation show that CaCO_3 dissolution is controlled by mass transfer and not surface reaction kinetics. The measured dissolution rate was about 25% higher(but not less than)than the calculated rate of mass transfer, probably because of the effect of turbulence. The enhancement and inhibition effects of buffers on CaCO_3 dissolution are predicted by the general mass transfer model. Buffer additives such as adipic, acetic, acrylic, and sulfosuccinic acid tend to enhance the rate of dissolution by buffering the solution pH and

increasing acidity transport to the limestone surface. Dissolution is enhanced at low sulfite concentration but inhibited at high sulfite concentration, indicating some kind of surface adsorption or crystallization phenomenon. The rate of dissolution is a strong function of pH and temperature as predicted by mass transfer. At high CO_2 partial pressure, the rate of dissolution is enhanced due to the CO_2 hydrolysis reaction. CO_2 partial pressure also determines the equilibrium pH for CaCO_3 dissolution.

TABLE OF CONTENT

	Page
ABSTRACT	v
TABLE OF CONTENTS	vii
LIST OF FIGURES	x
LIST OF TABLES	xii
CHAPTER I: INTRODUCTION	1
CHAPTER II: LITERATURE REVIEW	6
CHAPTER III: THEORY	10
GENERAL MASS TRANSFER MODEL	11
MASS TRANSFER MODEL NEGLECTING CO ₂	
REACTION	19
ACTIVITY COEFFICIENTS	20
DIFFUSIVITIES	22
SIMULATED RESULTS BY THE MASS	
TRANSFER MODEL	25
PARTICLE SIZE DISTRIBUTION	30
CHAPTER IV: APPARATUS AND PROCEDURE	35
METHODOLOGY	35
pH-STAT APPARATUS	35
PROCEDURE	40
PARTICLE SIZE DISTRIBUTION BY COULTER	
COUNTER	42
CHAPTER V: RESULTS AND DISCUSSION	43
EFFECT OF PARTICLE SIZE	45

EFFECTS OF pH, P_{CO_2} , AND TEMPERATURE	47
EFFECTS OF ORGANIC ACIDS	50
Acetic Acid	50
Adipic Acid	52
Other Buffers	52
EFFECTS OF SULFITE/BISULFITE	55
DISCUSSION	60
CONCLUSIONS AND RECOMMENDATIONS	62
APPENDIX A: MASS TRANSFER FOR A SPHERE IN AN INFINITE STAGNANT MEDIUM	64
APPENDIX B: TABULAR DATA	67
APPENDIX C: THE FISHER TITRIMETER II TITRATION SYSTEM	82
APPENDIX D: NOMENCLATURE	85
APPENDIX E: FORTRAN PROGRAM LISTINGS	88
PROGRAM I-MASS TRANSFER MODEL WITH CO_2 FINITE RATE REACTION	89
PROGRAM II-MASS TRANSFER MODEL NEGLECTING CO_2 REACTION	100
PROGRAM III-MASS TRANSFER MODEL FOR CALCULATING SURFACE $CaCO_3^0$ and $CaSO_3^0$ CONCENTRATIONS	107

PROGRAM IV-MASS TRANSFER MODEL WITH EQUILIBRIUM SHIFT OF CaSO_3^0 ON CaCO_3^0	114
PROGRAM V-SIMPLIFIED MASS TRANSFER MODEL SUMMING DISSOLUTION RATE OVER PARTICLE SIZE DISTRIBUTION	121
LITERATURE CITED	124
VITA	129

LIST OF TABLES

Table	Page
3-1 Activity Coefficient Parameters	21
3-2 Self Diffusion Coefficients at 25° and 55°C	23
3-3 Diffusivities of Organic Acid Additives at 25°C	24
3-4 Size Distribution Determined by Coulter Counter for CaCO ₃ (Reagent Grade)	32
B-1 Calculated Effects of Particle Diameter, 25°C at pH 5.0, [Ca ⁺⁺] = 0.01 M, P _{CO₂} = 1 atm (Figure 3-1)	68
B-2 Contribution to Dissolution by Individual Chemical Species (Figure 3-2)	69
B-3 Calculated Effects of P _{CO₂} , 25°C, [Ca ⁺⁺] = 0.01 M, D _p = 8.856 μm (Figure 3-3)	70
B-4 Values of kt/kt ₅₀ versus Percent Remaining Calculated by Simplified Mass Transfer Model (Figure 3-4)	71
B-5 Data from pH-Stat Experiments at 25°C in 0.1 M CaCl ₂ Sparged with N ₂ (Figure 5-1)	72

5-3.	Dissolution Rate of Reagent Grade CaCO_3	
	with N_2 Sparging in 0.1 M CaCl_2	49
5-4.	CaCO_3 Dissolution at 25°C in 0.1 M CaCl_2 ,	
	Effects of Acetic Acid	51
5-5.	Dissolution Rate of CaCO_3 in 0.1 M CaCl_2	
	with N_2 Sparging at 25°C , and 3 mM	
	Adipic Acid	53
5-6.	Effect of Organic Acids on Dissolution	
	Rate in 0.1 M CaCl_2 with N_2 Sparging,	
	25°C and pH 5	54
5-7.	Effect of Sulfite, N_2 Sparging, 25° and	
	55°C .	56
5-8.	Effect of Acetate on Dissolution Rate	
	with 3 mM of Total Sulfite, pH 5	
	and 25°C	58
5-9.	Calculated Solution Composition at CaCO_3	
	Surface, N_2 Sparging and 25°C	59

LIST OF FIGURES

Figure	Page
1-1. Simple Slurry Scrubbing	2
1-2. Double Alkali Process	4
3-1. Effect of Particle Diameter on Dissolution Rate, pH 5.0, $[Ca^{++}] = 0.01 M$, and $P_{CO_2} = 1 \text{ atm}$	26
3-2. Flux Contribution to Dissolution Rate with $P_{CO_2} = 1 \text{ atm}$, $[Ca^{++}] = 0.01 M$, and $25^\circ C$	28
3-3. Effects of P_{CO_2} and pH on Dissolution Rate	29
3-4. Calculated Dissolution Curve for Reagent Grade $CaCO_3$	33
4-1. pH-Stat Apparatus	36
4-2. Detail Components of Reactor	37
4-3. Top View of Reactor Showing Different Orientations of Each Component	39
5-1. Dissolution Curves for Reagent Grade $CaCO_3$ at $25^\circ C$ with N_2 Sparging	36
5-2. Dissolution rate of Reagent $CaCO_3$ with CO_2 Sparging in 0.1 M $CaCl_2$	48

B-6 Integrated Mass Transfer Model Data for Monodisperse Particle Size Distribution (Figure 5-1)	73
B-7 Calculated versus Measured Rate Constant for Reagent Grade Calcite at 25°C and 55°C with CO ₂ Sparging (Figure 5-2)	74
B-8 Calculated versus Measured Rate Constant for Reagent Grade Calcite at 25°C and 55°C with N ₂ Sparging (Figure 5-3)	75
B-9 Dissolution of Reagent CaCO ₃ at 25°C, 0.1 M CaCl ₂ , 5 mM CaCO ₃ , and various Acetate Concentration (Figure 5-4)	76
B-10 Calculated and Measured Rate k(cm ² /sec) for 3 mM Total Adipate at Low P _{CO₂} and 25°C (Figure 5-5)	77
B-11 Measured and Calculated Rate k(cm ² /sec) for Reagent Grade CaCO ₃ with Organic Acid Additives, pH 5, 25°C, N ₂ Sparging and 0.1 M CaCl ₂	78
B-12 Experimental Rate of Dissolution k(cm ² /sec) of Reagent Grade CaCO ₃ with Organic Acid Additives, pH 5, 25°C, N ₂ Sparging, 0.1 M CaCl ₂ (Figure 5-6)	79

B-13	Reagent Grade CaCO_3 Dissolution in the Presence of Dissolved Sulfite (Figure 5-7)	80
B-14	Effects of Total Acetate and Sulfite on Rate of Dissolution at 25°C (Figure 5-8)	81

CHAPTER I

INTRODUCTION

The dominant commercial technology for stack gas desulfurization is aqueous scrubbing using limestone (CaCO_3) to neutralize the SO_2 and produce $\text{CaSO}_3/\text{CaSO}_4$ waste solids. Such typical throwaway processes use either slurry scrubbing or clear solution scrubbing.

The typical slurry scrubbing process is represented by the flowsheet in Figure 1-1. It consists of a scrubber, a crystallizer, and a solid/liquid separator. The SO_2 waste gas is absorbed with a slurry of product solids and unreacted limestone at pH 4 to 6. The alkalinity for SO_2 absorption is provided by CaSO_3 dissolution or by limited CaCO_3 dissolution in the scrubber. Slurry is recycled from the crystallizer to the scrubber and a small portion containing 10 to 15 wt.% suspended solids is withdrawn for solid/liquid separation (Rochelle and King, 1978). To avoid CaSO_3 and CaSO_4 crystallization and scaling in the scrubber, the crystallizer vessel must provide adequate residence time to control supersaturation of CaSO_3 and CaSO_4 (Rochelle and King, 1978). Some of the CaCO_3 dissolution must also occur in the crystallizer to avoid CaSO_3 scaling in the scrubber. The $\text{CaSO}_3/\text{CaSO}_4$ solid product is disposed of as a solid waste in ponds

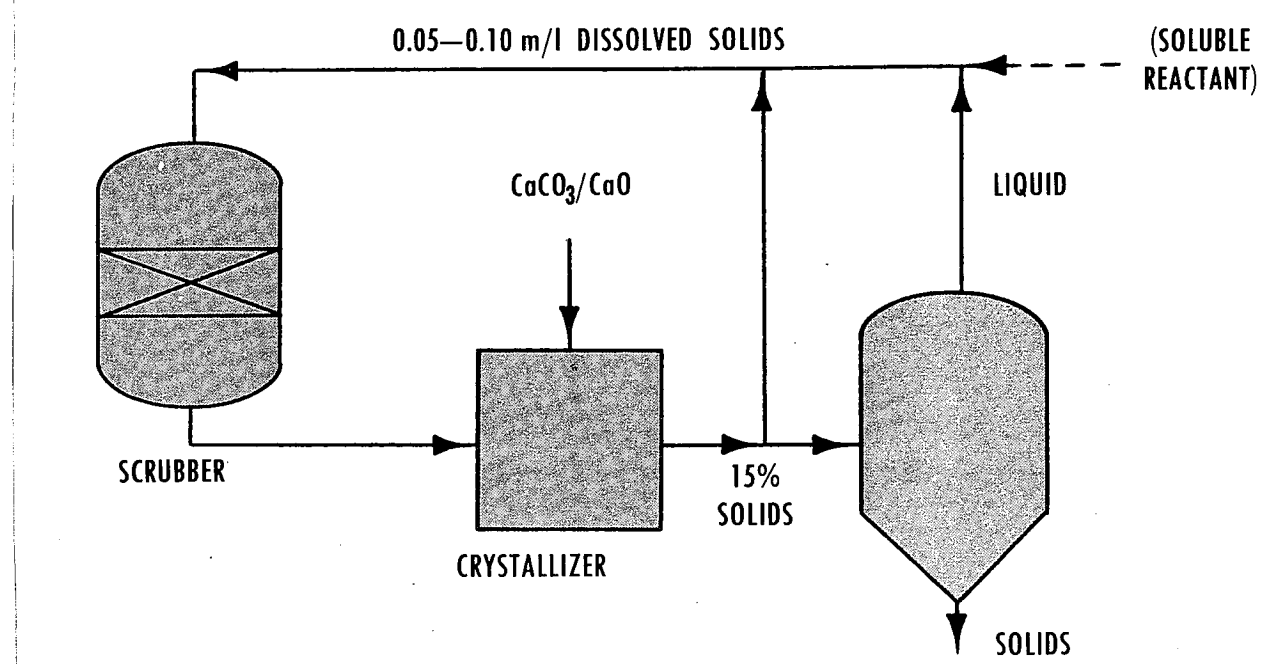
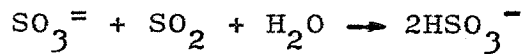


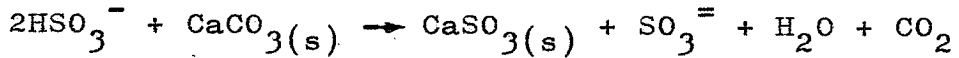
Figure 1-1. Simple Slurry Scrubbing

or landfills.

In the double-alkali processes(Figure 1-2) (Kaplan, 1973), SO_2 is absorbed into a clear solution of soluble alkali such as Na_2SO_3 :



The solution is reacted with CaCO_3 in a separate vessel to precipitate CaSO_3 and regenerate $\text{SO}_3^=$:



The CaSO_3 solids are separated for disposal, and clear solution is recycled to the scrubber. The advantage of the double-alkali process over that of slurry scrubbing is that the problem of handling slurry in the scrubber are avoided. However, high levels of dissolved alkalinity are required to minimize the amount of liquid that must be processed for liquid/solid separation.

The use of additives such as soluble alkalis or buffering acids has been shown to enhance SO_2 removal efficiency of limestone slurry. Organic acids with pK_a values of 4.5 to 5.0 can accelerate the rate of SO_2 absorption at concentration as low as 3 to 10 mmoles/liter (Rochelle and King, 1977; Chang and Rochelle, 1980). These additives act as buffers to limit the drop in pH that normally occurs at the gas/liquid interface during SO_2 absorption.

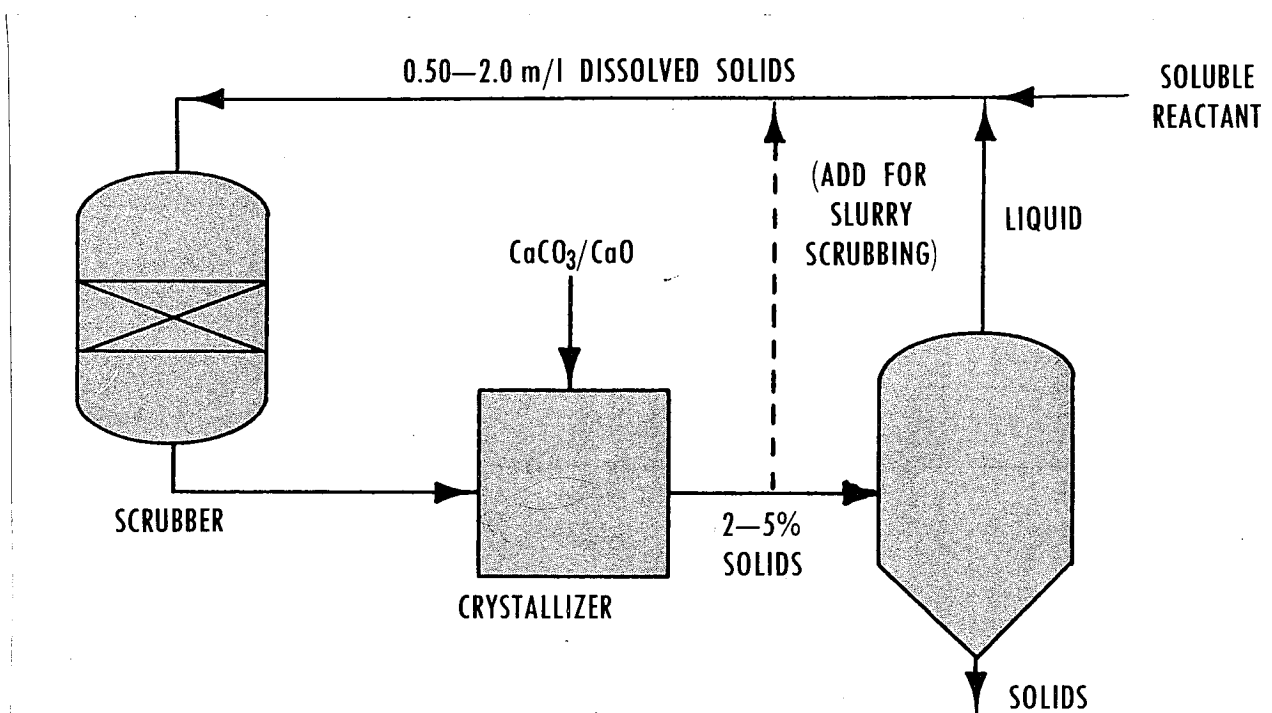


Figure 1-2. Double Alkali Process

The purpose of this investigation is to characterize limestone dissolution at conditions representative of slurry and double alkali scrubbers for stack gas desulfurization. The dissolution rate of reagent CaCO_3 (calcite) has been measured. A mass transfer model assuming spherical CaCO_3 particles in an infinite stagnant medium is proposed to predict the experimental rates. The results of this work should provide for more reliable, economic scrubber and reactor designs for both simple slurry and double-alkali processes.

CHAPTER II

LITERATURE REVIEW

CaCO_3 dissolution has been partially characterized by investigators interested in geochemistry, mine water disposal, and stack gas desulfurization. The most representative work being that of Berner and Morse (1974) and Plummer et al. (1978).

Berner and Morse (1974) used the pH-stat method to study the rate of dissolution of finely crystalline calcite (reagent or precipitated CaCO_3) in sea water. They report three regions of pH dependence. At pH less than 4, calcite dissolution appears to be controlled by diffusion of H^+ to the crystal surface. Near equilibrium, ΔpH (pH at equilibrium minus solution pH) of 0.0 to 0.4, the dissolution is sensitive to phosphate ion inhibition. At intermediate pH values the dissolution rate was a function of CO_2 partial pressure. At pH greater than 4, the dissolution rate was found to be distinctly less than that predicted for control by ionic diffusion.

Plummer et al. (1978) used the free drift and pH-stat method to study the dissolution of coarse Iceland spar. The pH-stat method identified three forward rate dependencies far from equilibrium: (1) linear dependence on the bulk fluid activity of H^+ , (2) linear dependence on bulk

fluid P_{CO_2} , and (3) a constant forward rate in the near absence of H^+ and dissolved CO_2 . Similar results were obtained when reaction approached equilibrium by the free drift method. In addition, the free drift method shows that the reverse reaction at constant P_{CO_2} and temperature is a linear function of the bulk fluid product activities of Ca^{++} and HCO_3^- in solution. A model of heterogeneous reaction in the adsorption layer was used and expanded by the authors to interpretate the rate expression.

Barton and Natanatham (1976) report a first order dependence on H^+ of the rate of dissolution of limestone in H_2SO_4 in the pH range of 2-6, indicating a mass transport reaction. Some investigators report dependence of dissolution on agitation which implies at least a certain degree of mass transfer resistance (Sjoberg, 1976; Erga and Terjesen, 1956; Ottmers *et al.*, 1974). It appears that dissolved CO_2 does not participate in the mass transfer (Berner and Morse, 1974), probably because it does not react sufficiently fast at the limestone surface. Other buffering acidic components such as HSO_3^- or organic acids could substitute for H^+ by providing for mass transfer of acidity to the limestone surface (Rochelle, 1977).

Only limited work has been done on the temperature dependence of calcite dissolution. Sjöberg (1976)

measured an activation energy of 8.4 kcal/mol for dissolution at pH 8-10. Ottmers et al. (1974) found an activation energy of 14 kcal/mol at pH 5-6. Barton and Vatanatham (1976) reported a value of 3.6 kcal/mol for dissolution at pH 2-6. Plummer et al. (1978) gave values of 2.0 and 10.0 kcal/mol for dissolution at low and moderate pH. At high pH, an activation energy of 7.9 kcal/mol is reported for temperature greater than 25 °C and 1.5 kcal/mol for temperature less than 25 °C.

Particle size distribution and surface area are both important parameters for evaluating dissolution rate irrespective of the controlling mechanisms. Neglecting the surface area change during the experiment can lead to erroneous kinetics. It will also make the data incomparable for different runs and different limestone sources. Berner and Morse (1974) determined the initial particle size distribution by measuring several hundred individual crystal diameters under a high power microscope using a random sampling technique. Plummer et al. (1978) obtained the size distribution of coarse Iceland spar by wet sieving and estimated surface area by representing the particles as rhombohedra. Mean particle diameter was used to calculate the corresponding geometrical surface area. Sjöberg (1976) utilized the nitrogen adsorption method (BET) to

measure the reactive surface area. He found that the effective BET surface area was a factor of 2-3 times the area estimated from particle size assuming spherical shape.

CHAPTER III

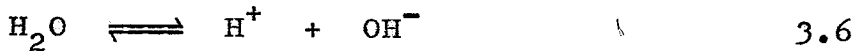
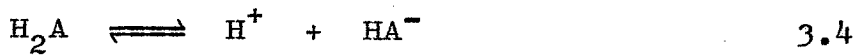
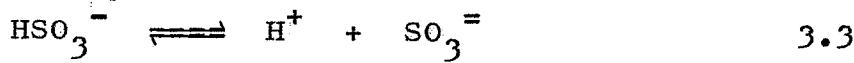
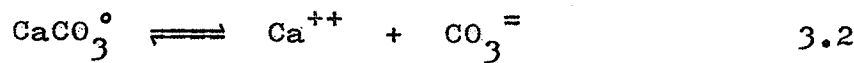
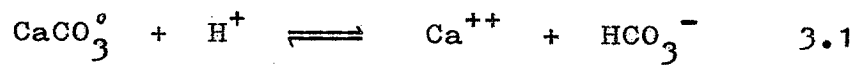
THEORY

The dissolution of CaCO_3 in aqueous solution can be modeled by mass transfer assuming spherical particles suspended in an infinite stagnant medium. For spheres dissolving in a stagnant medium, the mass transfer coefficient is given by the asymptotic limit of a Sherwood number ($k_c d/D$) of 2 (Appendix A). A simplified mass transfer model integrated over the particle size distribution is used to calculate the theoretical dissolution constant k (cm^2/sec).

GENERAL MASS TRANSFER MODEL

A mass transfer model based on steady-state theory is proposed to describe limestone dissolution in aqueous solution. The calcite particles are assumed to be spheres suspended in an infinite stagnant medium. The model is limited to mass transfer with homogenous reaction rates and does not account for surface reaction rates. It usually assume liquid/solid equilibrium at the limestone surface.

When calcium carbonate is dissolved into aqueous solution of difunctional buffer(H_2A) in the pH range from 4 to 7, the following six reversible reaction should be considered:



All of the above reaction are essentially instantaneous (Weems, 1981). The values of the equilibrium constants for all but reaction 3.4 and 3.5 at 25 °C and infinite dilutions are:

$$K_1 = \frac{a_{\text{Ca}}^{++} a_{\text{HCO}_3^-}}{a_{\text{CaCO}_3^0} a_{\text{H}^+}} = 1.34 \times 10^7 \text{ (estimated from } K_2 \text{ and } K_3 \text{)}$$

$$K_2 = \frac{a_{\text{Ca}}^{++} a_{\text{CO}_3^2-}}{a_{\text{CaCO}_3^0}} = 6.3 \times 10^{-4} \text{ (Garrels and Thompson, 1962)}$$

$$K_3 = \frac{a_{\text{H}^+} a_{\text{CO}_3^2-}}{a_{\text{HCO}_3^-}} = 4.69 \times 10^{-11} \text{ (Harned and Scholes, 1941)}$$

$$K_4 = \frac{a_{\text{H}^+} a_{\text{SO}_4^{2-}}}{a_{\text{HSO}_3^-}} = 6.24 \times 10^{-8} \text{ (Tartar and Garretson, 1941)}$$

$$K_w = a_{\text{H}^+} a_{\text{OH}^-} = 1.008 \times 10^{-14}$$

At 55 °C, K_w was taken to be 7.26×10^{-14} and the other equilibrium constants were evaluated by relations given in Lowell et al. (1970). Activities of each species were calculated as the product of concentration and activity coefficient.

In order to account for CaSO_3^0 ion pair an effective K_4' is defined

$$K_4' = K_4 \left(1 + \frac{a_{\text{Ca}}^{++}}{K_s} \right) \quad 3.7$$

$$K_s = \frac{a_{\text{Ca}^{++}} a_{\text{SO}_3^-}}{a_{\text{CaSO}_3^0}} = 4.0 \times 10^{-4} \text{ (Lowell et al., 1970)}$$

at 25°C and infinite dilution.

For reactions 3.4 and 3.5

$$K_{A_1} = \frac{a_{\text{H}^+} [\text{HA}^-]}{[\text{H}_2\text{A}]} = 1.05 \times 10^{-4} \text{ M (Cavanaugh, 1978)}$$

$$K_{A_2} = \frac{a_{\text{H}^+} [\text{A}^=]}{[\text{HA}^-]} = 1.38 \times 10^{-5} \text{ M (Cavanaugh, 1978)}$$

These values are equilibrium constants in terms of concentrations for adipic acid in 0.1 M CaCl_2 . For acetic and acrylic acids, K_{A_1} is estimated to be 3.55×10^{-5} and 9.54×10^{-5} M, respectively. The K_{A_1} and K_{A_2} values for sulfosuccinic acid are 7.94×10^{-4} and 3.98×10^{-5} M (Cavanaugh, 1978).

The material balance for CO_2 species at steady state in spherical coordinates gives:

$$\begin{aligned} & \frac{1}{r^2} \left[D_{\text{CO}_2} \frac{\partial}{\partial r} \left(r^2 \frac{\partial [\text{CO}_2]}{\partial r^2} \right) + D_{\text{HCO}_3^-} - \frac{\partial}{\partial r} \left(r^2 \frac{\partial [\text{HCO}_3^-]}{\partial r^2} \right) + \right. \\ & \left. D_{\text{CaCO}_3^0} \frac{\partial}{\partial r} \left(r^2 \frac{\partial [\text{CaCO}_3^0]}{\partial r^2} \right) + D_{\text{CO}_3^=} = \frac{\partial}{\partial r} \left(r^2 \frac{\partial [\text{CO}_3^=]}{\partial r^2} \right) \right] = 0 \quad 3.8 \end{aligned}$$

Substituting $x = (1 - R_o/r)$ where R_o is the particle diameter and r the distance from the center of the sphere, equation 3.8 reduces to

$$D_{CO_2} \frac{\partial^2 [CO_2]}{\partial x^2} + D_{HCO_3^-} \frac{\partial^2 [HCO_3^-]}{\partial x^2} + D_{CaCO_3^o} \frac{\partial^2 [CaCO_3^o]}{\partial x^2} + \\ D_{CO_3^{=}} \frac{\partial^2 [CO_3^{=}]}{\partial x^2} = 0 \quad 3.9$$

Integrating equation 3.9 with respect to x gives

$$D_{CO_2} [CO_2] + D_{HCO_3^-} [HCO_3^-] + D_{CaCO_3^o} [CaCO_3^o] + \\ D_{CO_3^{=}} [CO_3^{=}] = \alpha_1 + \beta_1 x \quad 3.10$$

where α_1 ($M \text{ cm}^2 \text{ sec}^{-1}$) and β_1 ($M \text{ cm}^2 \text{ sec}^{-1}$) are constants of integration.

Similarly, other steady-state balances give for Ca^{++} species,

$$D_{Ca^{++}} [Ca^{++}] + D_{CaCO_3^o} [CaCO_3^o] = \alpha_2 + \beta_2 x \quad 3.11$$

for a charge balance of diffusing species,

$$\begin{aligned}
 & D_H^+ [H^+] + 2D_{Ca^{++}} [Ca^{++}] - D_{HCO_3^-} [HCO_3^-] - 2D_{CO_3^{=}} [CO_3^{=}] \\
 & - D_{HA^-} [HA^-] - 2D_A [A^-] - D_{HSO_3^-} [HSO_3^-] - 2D_{SO_3^{=}} [SO_3^{=}] \\
 & - D_{OH^-} [OH^-] = \alpha_3 + \beta_3 x
 \end{aligned} \quad 3.12$$

for H_2A species,

$$D_{H_2A} [H_2A] + D_{HA^-} [HA^-] + D_A [A^-] = \alpha_4 + \beta_4 x \quad 3.13$$

and for sulfite species,

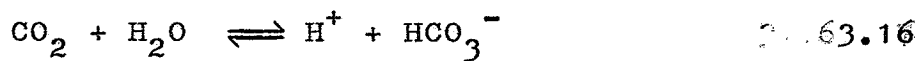
$$D_{HSO_3^-} [HSO_3^-] + D_{SO_3^{=}} [SO_3^{=}] = \alpha_5 + \beta_5 x \quad 3.14$$

By reaction stoichiometry, the flux of calcium must equal to the flux of CO_2 :

$$\frac{\partial}{\partial x} \left(D_{Ca^{++}} [Ca^{++}] + D_{CaCO_3^\circ} [CaCO_3^\circ] \right) = \frac{\partial}{\partial x} \left(D_{CO_2} [CO_2] + D_{HCO_3^-} [HCO_3^-] + D_{CaCO_3^\circ} [CaCO_3^\circ] \right) \quad 3.15$$

Therefore $\beta_1 = \beta_2 = \beta$. Since the net fluxes of H_2A species, sulfite species, and charge species are zero, β_3, β_4 , and β_5 are zero. The constants $\alpha_1, \alpha_2, \alpha_3, \alpha_4$, and α_5 can be obtained from the compositions of the bulk solution ($x = 1.0$).

The finite-rate reversible CO_2 hydrolysis reaction



is also considered in the mass transfer model. The rate of this reaction is given by:

$$\frac{d[\text{CO}_2]}{dt} = k_f \left(\frac{\gamma_{\text{H}^+} [\text{H}^+] \gamma_{\text{HCO}_3^-} - [\text{HCO}_3^-]}{K_5 \gamma_{\text{CO}_2}} \right) - [\text{CO}_2] \quad 3.17$$

where k_f is the forward rate constant and K_5 is the equilibrium constant for reaction 3.16. At 25°C and infinite dilution, the value of k_f and K_5 are 0.026 sec^{-1} (Pinsent *et al.*, 1956) and $4.45 \times 10^{-7} \text{ M}$ (Harned and Bonner, 1954), respectively. The k_f and K_5 values at 55°C are 0.127 sec^{-1} (Pinsent *et al.*, 1956) and $5.12 \times 10^{-7} \text{ M}$ (Lowell *et al.*, 1970)

A steady-state differential material balance for CO_2 gives:

$$\frac{D_{\text{CO}_2} x^4 R_o^{-2}}{\partial x} \frac{\partial^2 [\text{CO}_2]}{\partial x} + k_f \left(\frac{\gamma_{\text{H}^+} [\text{H}^+] \gamma_{\text{HCO}_3^-} - [\text{HCO}_3^-]}{K_5 \gamma_{\text{CO}_2}} \right) - [\text{CO}_2] = 0 \quad 3.18$$

The solubility of $\text{CaCO}_3(s)$ gives us the concentration of CaCO_3 at the limestone surface. The concentration of the

bulk species can be calculated from the pH, partial pressure of CO_2 , total buffer and calcium concentrations, and the equilibrium relations 3.1 to 3.6. Therefore under slurry scrubbing conditions CaCO_3 dissolution becomes a process of simultaneous mass transfer with multiple equilibrium reactions and a single finite-rate reversible reaction.

Due to the non-linearity of the equilibrium equations, the concentration of chemical species at the limestone surface is calculated by trial and error using a modified interval halving method. If a value for β is guessed, the constants $\alpha_1, \alpha_2, \alpha_3, \alpha_4$, and α_5 can be calculated from the bulk composition(at $x=1.0$) and diffusivities by equations 3.10 to 3.14. The surface concentration of all species is calculated given the equilibrium solubility of CaCO_3^o at the surface:

$$[\text{CaCO}_3^o]_s = 6.80 \times 10^{-6} \text{ M} \quad (\text{Lowell et al., 1970})$$

Given CO_2 concentration at the surface ($x=0.0$) and a guess value for β , the CO_2 differential rate expression 3.17 is integrated numerically from $x=0.0$ to $x=1.0$ by the Simpson-Kutta method(Nielsen, 1964). A cubic equation fit of $[\text{CO}_2]$ from $x=0.7$ to $x=0.85$ is used to extrapolate the values of $[\text{CO}_2]$ from $x=0.86$ to $x=1.0$ as $r \rightarrow \infty$. If

$[CO_2]_b$ does not agree with its calculated value, a new value of β is guessed until the solution converges within 1% of CO_2 . Due to the nonlinearity of the $[H^+] [HCO_3^-]$ in equation 3.16, each step of the numerical integration requires numerical solution of equilibria and material balance equations. The interval numerical solution iterates on $[H^+]$ until it is known within 1%.

If the rate of the CO_2 hydrolysis reaction is negligible, the rate per unit radius is approximately constant and is given by β . The rate of limestone dissolved per unit surface area is given by

$$\text{Rate/unit area} = \frac{\beta}{(R_o \times 1000)} \left(\frac{\text{gmol}}{\text{cm}^2 \text{sec}} \right) \quad 3.19$$

where β is in $(M \text{ cm}^2 \text{ sec}^{-1})$ and R_o in cm. This mass transfer model can also be employed with other buffers by substituting the appropriate equilibrium constants and diffusivities.

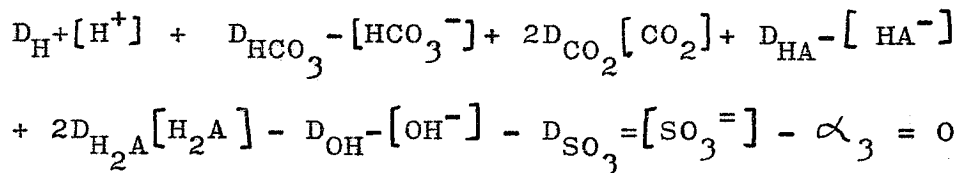
A FORTRAN listing of the model is given in Appendix D.

MASS TRANSFER MODEL NEGLECTING CO₂ REACTION

For low P_{CO₂}, the CO₂ finite rate reaction is insignificant. Therefore the mass transfer model can be simplified by neglecting the CO₂ differential equation material balance. By specifying values for the dissolution flux (β), pH, P_{CO₂}, buffer concentration, and [Ca⁺⁺] in the bulk, the constants α_1 , α_2 , α_3 , α_4 , and α_5 can be readily calculated. While applying the condition

$$[CO_2]_b = [CO_2]_s,$$

and specifying [CaCO₃[°]] at the surface, a trial and error calculation is made on [H⁺] until the following condition converges within 2% :



One can also calculate solution composition at the surface from a measured β (experimentally obtained rate data). Thus effects of surface kinetics or equilibria can be separated from mass transfer. We have used this mode of calculation to correlate [CaCO₃[°]] as a function of [CaSO₃[°]] at the surface.

A FORTRAN listing is given in Appendix D.

ACTIVITY COEFFICIENTS

Individual ion activity coefficients are calculated by a modified Debye-Hückel Limiting Law (Lowell et al., 1970)

$$\log \gamma_j = AZ_j^2 \left(\frac{-I^{\frac{1}{2}}}{1 + B a_j I^{\frac{1}{2}}} + b_j I \right) \quad 3.20$$

where I is the ionic strength, Z_j is the charge on the j th ion, a_j and b_j are the characteristic parameters for each ion species. The values of the constants A and B in equation 3.20 are given by Hamer (1968):

$$A = \frac{1.8248 \times 10^6}{D_o \cdot T^{1.5}} \left(M^{-\frac{1}{2}} \right) \quad 3.21$$

$$B = \frac{50.292}{D_o \cdot T^{1.5}} \left(M^{-\frac{1}{2}} \right) \quad 3.22$$

where D_o is the dielectric constant of water (82.04, 468.30 at 25° and 55°C) and T is the absolute temperature in K.

Values of a_j and b_j are given in Table 3-1.

The ionic strength I in equation 3.20 is given by

$$I = \frac{1}{2} \sum_i M_i Z_i^2 \quad 3.23$$

Table 3-1 Activity Coefficient Parameters

<u>Species</u>	<u>a_j</u>	<u>b_j</u>
H ⁺	6.0	0.4
Ca ⁺⁺	4.5	0.1
SO ₃ ⁼	4.5	0.0
HSO ₃ ⁼	4.5	0.0
CO ₃ ⁼	4.5	0.0
HCO ₃ ⁼	4.5	0.0
OH ⁻	3.0	0.0
Buffer species	3.0	0.0

The sum in equation 3.23 is over all charged species.

For uncharged species, the activity coefficients are given to a good approximation by the following equation (Harned and Owen, 1958)

$$\log \gamma_i = U_i I \quad 3.24$$

in which U_i is an empirical constant taken to be 0.076.

DIFFUSIVITIES

Values of diffusivities used in the model are given in table 3-2 and 3-3. Interactions between ions are neglected, possibly resulting in errors as large as 40%.

Diffusivities for ions are taken to be those in absence of a potential gradient, since there is usually a large excess of CaCl_2 to disperse any potential gradient. At 25°C and infinite dilution, ionic diffusivities are given by:

$$D = \frac{RT\lambda_0}{n_j(Fa)^2} \quad 3.25$$

where Fa is the Faraday number, n_j is the charge on the j th ion, and λ_0 is the equivalent ionic conductivity at infinite dilution.

Diffusivities at 55°C were estimated by the Stokes-Einstein relationship:

Table 3-2 Self Diffusion Coefficients at
25° and 55°C

<u>Species</u>	<u>Diffusivity x 10⁵</u> (cm ² /sec)	<u>25°C^a</u>	<u>55°C</u>
CO ₂		2.00 ^b	3.89
HCO ₃ ⁻		1.20	2.33
CO ₃ ⁼		0.70	1.36
Ca ⁺⁺		0.79	1.54
H ⁺		9.30	18.1
CaCO ₃ ^o		0.75 ^c	1.46
SO ₃ ⁼		0.70	1.36
HSO ₃ ⁻		1.33	2.59
OH ⁻		5.27	10.30

a Landolt-Bornstein, 1960

b Sherwood et al., 1975

c Estimated as average of D_{Ca⁺⁺} and D_{CO₃⁼}

Table 3-3 Diffusivities of Organic Acid
additives at 25 °C

<u>Organic Acids</u>	<u>acid species</u>	<u>basic species</u>	Diffusivity $\times 10^5$ (cm^2/sec)
Adipic acid	0.736 ^a	0.705 ^b	
Acetic acid	1.19 ^c	1.09 ^d	
	$\underline{\text{H}_2\text{A}}^-$	$\underline{\text{HA}}=$	$\underline{\text{A}}^=$
Sulfosuccinic acid	0.73 ^a	0.53 ^e	0.41 ^e

a Albery et al., 1967

b Jeffrey and Vogel, 1935

c Lewis, 1955

d Landolt-Bornstein, 1960

e Weems, 1981

$$\frac{D_1 \eta_1}{T_1} = \frac{D_2 \eta_2}{T_2} \quad 3.26$$

For the basic and monohydrogen species of sulfosuccinic acid, the diffusivities were reduced by 45% and 25% respectively to account for Ca^{++} interaction (Weems, 1981).

SIMULATED RESULTS BY THE MASS TRANSFER MODEL

The computer model of CaCO_3 dissolution limited by mass transfer has been used to calculate dissolution rates at 25°C and 0.3 ionic strength as a function of pH, P_{CO_2} , particle diameter(d), and dissolved Calcium($[\text{Ca}^{++}]$).

Figure 3-1 shows the effects of particle diameter on the dissolution flux. With small particles or low P_{CO_2} the dissolution flux varies inversely with particle diameter, because the CO_2 reaction with CaCO_3 is negligible. However, as shown in Figure 3-1, with larger particles(20 μm) and high P_{CO_2} (1 atm), the predicted dissolution flux is greater because the increased volume of solution around a single particle permits a greater amount of CO_2 reaction with CaCO_3 .

Figure 3-2 shows the contributions of different species to the total dissolution rate at P_{CO_2} of 1 atm, d of 9 μm , and $[\text{Ca}^{++}]$ of 0.01 M. The relative contribution for each species is in ($\text{M cm}^2 \text{ sec}^{-1}$). The total rate is

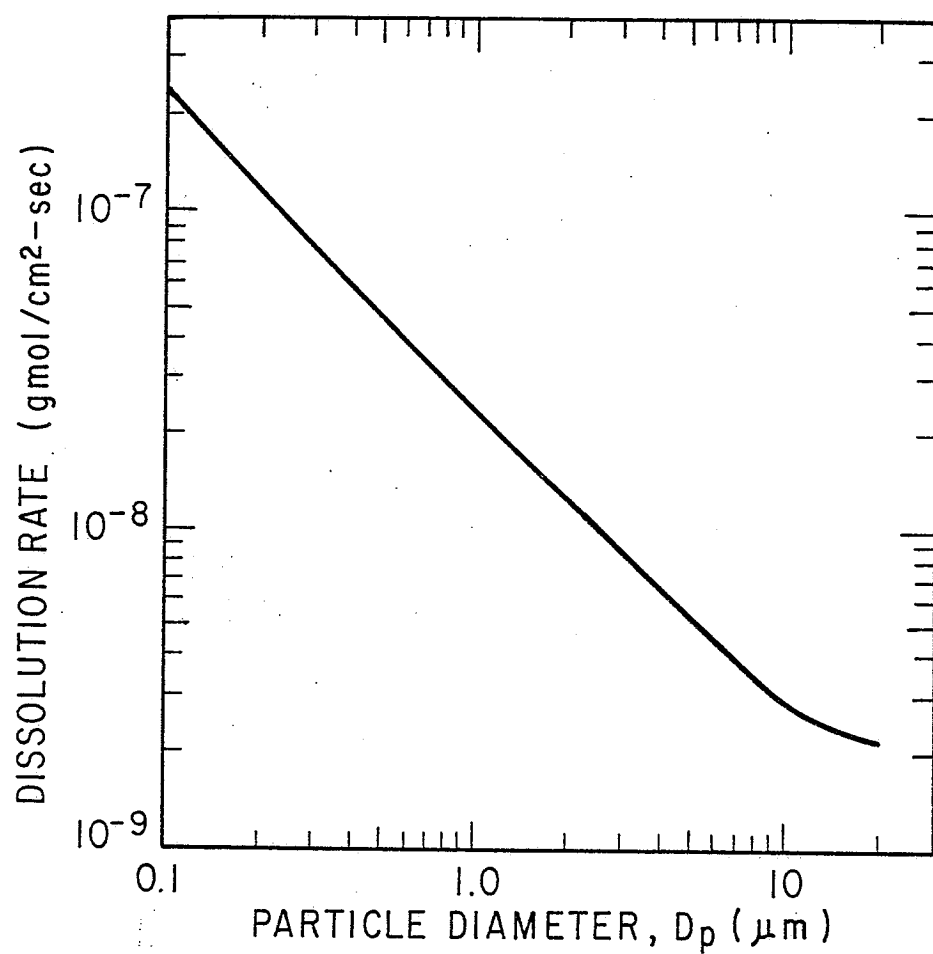


Figure 3-1. Effects of Particle Diameter on Dissolution Rate, pH 5.0, $[Ca^{++}] = 0.01M$, and $P_{CO_2} = 1 \text{ atm}$

represented by $-\beta$:

$$\begin{aligned} -\beta &= D_{CO_3^=} \Delta [CO_3^=] + D_{CaCO_3^o} \Delta [CaCO_3^o] - D_{H^+} \Delta [H^+] \\ &\quad - D_{CO_2} \Delta [CO_2] \end{aligned} \quad 3.27$$

where $\Delta[j]$ is the concentration difference (M) between the $CaCO_3$ surface and the bulk solution.

As shown in Figure 3-5, the contribution of $CaCO_3^o$ and $CO_3^=$ is small and nearly constant as a function of pH, but decreasing near equilibrium. The contribution of CO_2 diffusion dominates near equilibrium and increases to a maximum at pH 4.75. However, below pH 4.75 the CO_2 contribution decreases sharply and even becomes negative at pH 4.0. At low pH, the reverse reaction of HCO_3^- with H^+ reduces the availability of H^+ for $CaCO_3$ dissolution. The contribution of H^+ increases almost linearly with 10^{-pH} and dominates below pH 5.5. At pH 5.0, the total dissolution rate includes contributions of 66% from H^+ , 28% from CO_2 , and 7% from $CaCO_3^o$ and $CO_3^=$.

Figure 3-3 gives calculated data on the effects of pH and P_{CO_2} . At pH 4.5 to 5.5, P_{CO_2} of 1 atm increases the rate of dissolution by as much as 60% because of the indirect reaction of CO_2 with $CaCO_3$. However, at low pH(4.0) the effect of P_{CO_2} is significantly less. On the other hand, P_{CO_2} is dominant in determining the equilibrium pH at which dissolution stops.

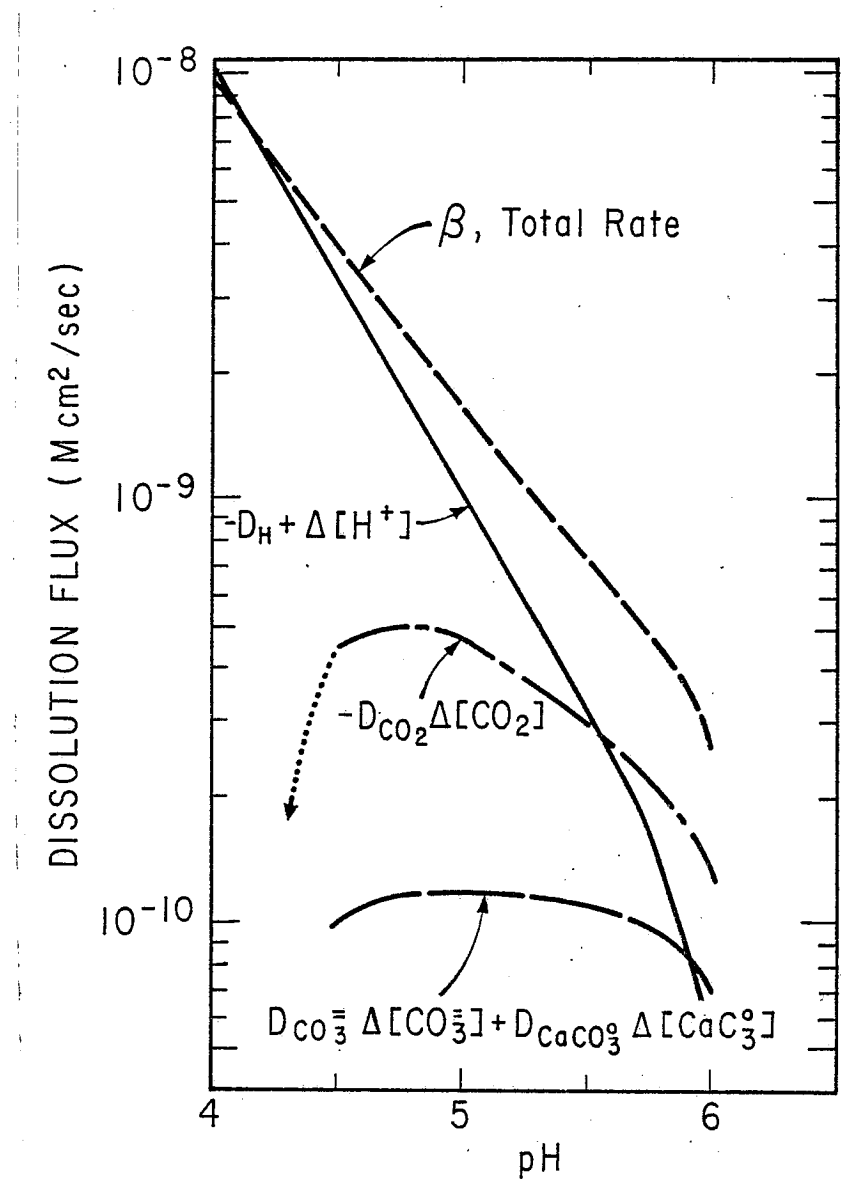


Figure 3-2. Flux Contribution to the Dissolution Rate with $P_{CO_2} = 1$ atm, $[Ca^{++}] = 0.01$ M and $25^\circ C$

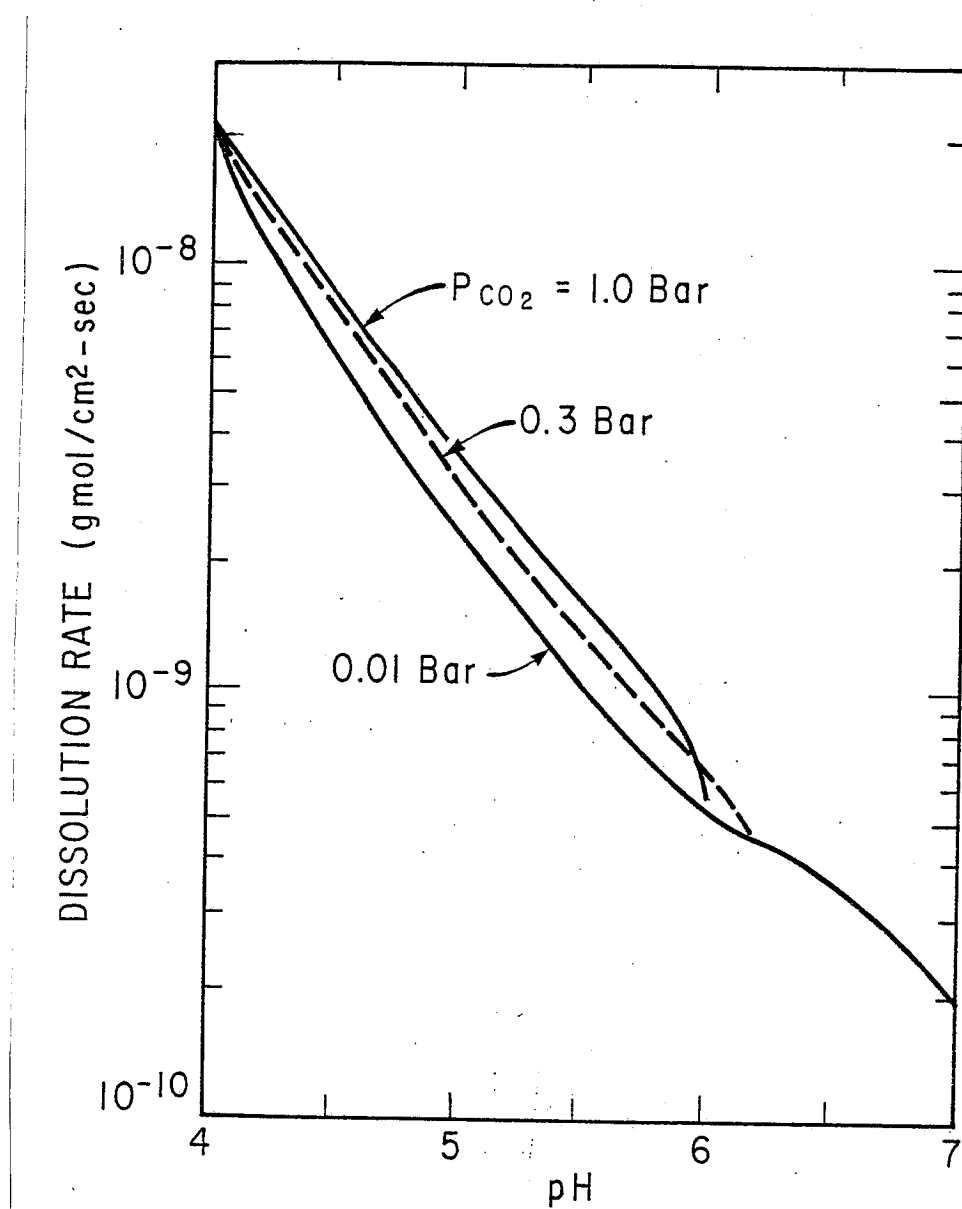


Figure 3-3. Effects of P_{CO_2} and pH on Dissolution Rate

PARTICLE SIZE DISTRIBUTION

If we neglect the finite-rate reaction involving CO_2 , the rate of dissolution of a single spherical particle can be represented by the proportionality

$$\frac{dV}{dt} \hat{=} d \hat{=} V^{1/3} \quad 3.28$$

where V is the volume of the particle and the proportionality constant varies with solution composition(pH) but is independent of particle diameter. This observation is confirmed by model simulation of rate of dissolution with different particle diameters. In order to account for the various particle size distributions, a simplified mass transfer model is used to integrate the size distribution of reagent grade CaCO_3 from Coulter counter measurement. The fraction remaining of a single particle after time t is given by integration of equation 3.28 to get

$$F = \frac{V}{V_0} = \left(1 - \frac{kt}{d^2} \right)^{1.5} \quad 3.29$$

where k is the proportionality constant (cm^2/sec), t is the time(sec) to dissolve a given fraction f , and d is the particle diameter in cm.

The comprehensive mass transfer model gives k equal to $4.71 \times 10^{-10} \text{ cm}^2/\text{sec}$ at pH 5 for particles less than 10 to 20

μ_m . The proportionality constant, k , includes effects of solution composition, but is approximately independent of d .

With a polydisperse size distribution, the total fraction remaining, F , can be determined by summing over the differential size distribution ϕ where ϕ_i is the fraction of total particle mass with diameters from d_i to d_{i+1} :

$$F = \sum_{i=1}^n \phi_i \left(1 - \frac{kt}{d_i d_{i+1}} \right)^{1.5} \quad 3.30$$

The fraction remaining of a given size range is taken to be zero when kt is greater than $d_i d_{i+1}$.

A FORTRAN program based on the above theory is written and listed in Appendix D. The program gives F as a function of kt or normalized time, t/t_{50} , where t_{50} is the time required for 50% of the limestone to dissolve. Figure 3-4 gives calculated values of total percent remaining ($100 \cdot F$) for reagent grade CaCO_3 based on the Coulter counter distribution in table 3-4. At 50% remaining the value of kt is $43.8 \times 10^{-8} \text{ cm}^2$.

If a batch experiment gives the fraction remaining, F , as a function of time at constant composition, the

Table 3-4 Size Distributions Determined by
 Coulter Counter for CaCO_3
 (Reagent Grade)

Size (microns)	Volume %	
	<u>Differential</u> ^a	<u>Cumulative</u> ^b
4.00	0.2	100.4
5.04	1.4	100.2
6.35	6.7	98.8
8.00	22.1	92.1
10.08	39.2	70.0
12.7	25.6	30.8
16.0	4.6	5.2
20.2	0.4	0.6
25.4	0.2	0.2
32.0	0.0	0.0

^aFraction of total volume between the given diameter and the next largest diameter.

^bFraction of total volume in sizes larger than the given diameter.

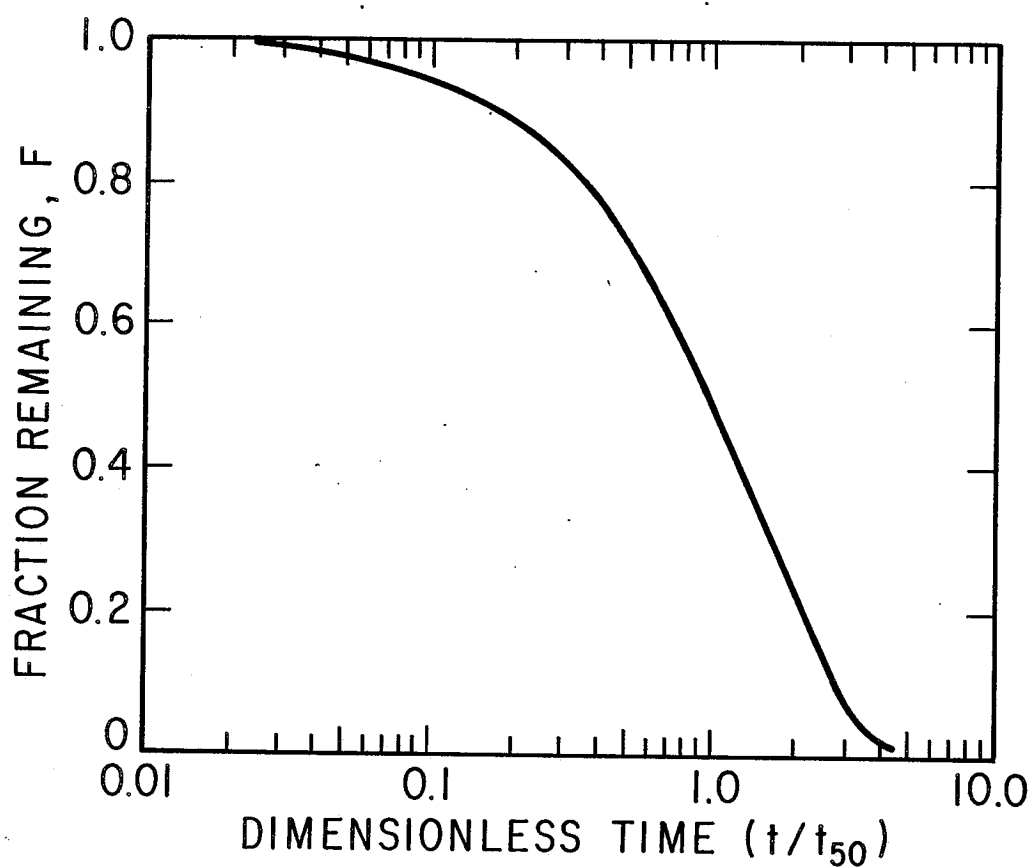


Figure 3-4. Calculated Dissolution Curve
for Reagent Grade CaCO_3

rate constant, k , can be calculated from the experimental data and the mass transfer model. Two experimental data points (F_1, t_1) and (F_2, t_2) can be combined with two calculated data points at F_1 and F_2 with $[F_1, (kt)_1]$ and $[F_2, (kt)_2]$ to get the rate constant k_{exp} :

$$k_{exp} = \frac{(kt)_2 - (kt)_1}{t_2 - t_1} \quad 3.31$$

If the experimental data at $t=0.0$ are reliable, k_{exp} can be obtained from a single data point of constant F :

$$k_{exp} = \frac{(kt)_2 - 0}{t_2 - 0} = \frac{(kt)_2}{t_2} \quad 3.32$$

For example, with 50% remaining:

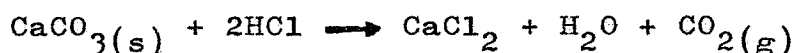
$$k_{exp} = \frac{(kt)_{50}}{t_{50}} \quad 3.33$$

CHAPTER IV

APPARATUS AND PROCEDURE

METHODOLOGY

Rates were measured in a pH-stat with batch dissolution of CaCO_3 at constant pH and solution composition (Morse, 1974). The pH was controlled by HCl titration with the stoichiometry:



Either CO_2 or N_2 were sparged into the solution to maintain a constant P_{CO_2} and HCO_3^- concentration. The relative change in calcium concentration was minimized by dissolving a small amount of CaCO_3 in solution with a high initial Ca^{++} concentration.

pH-STAT APPARATUS

A schematic representation of the pH-stat apparatus is shown in Figure 4-1. It consisted of a three-liter plexiglass batch reactor, an automatic burette/dispenser, an electrometer, and a titrate demand module. Nitrogen and carbon dioxide were supplied by two large gas cylinders.

The reactor was 15 cm in diameter and height with an o-ring sealed lid. It was baffled on four sides to eliminate vortex effects. The detail components of the reactor are shown in Figure 4-2. A variable speed agitator

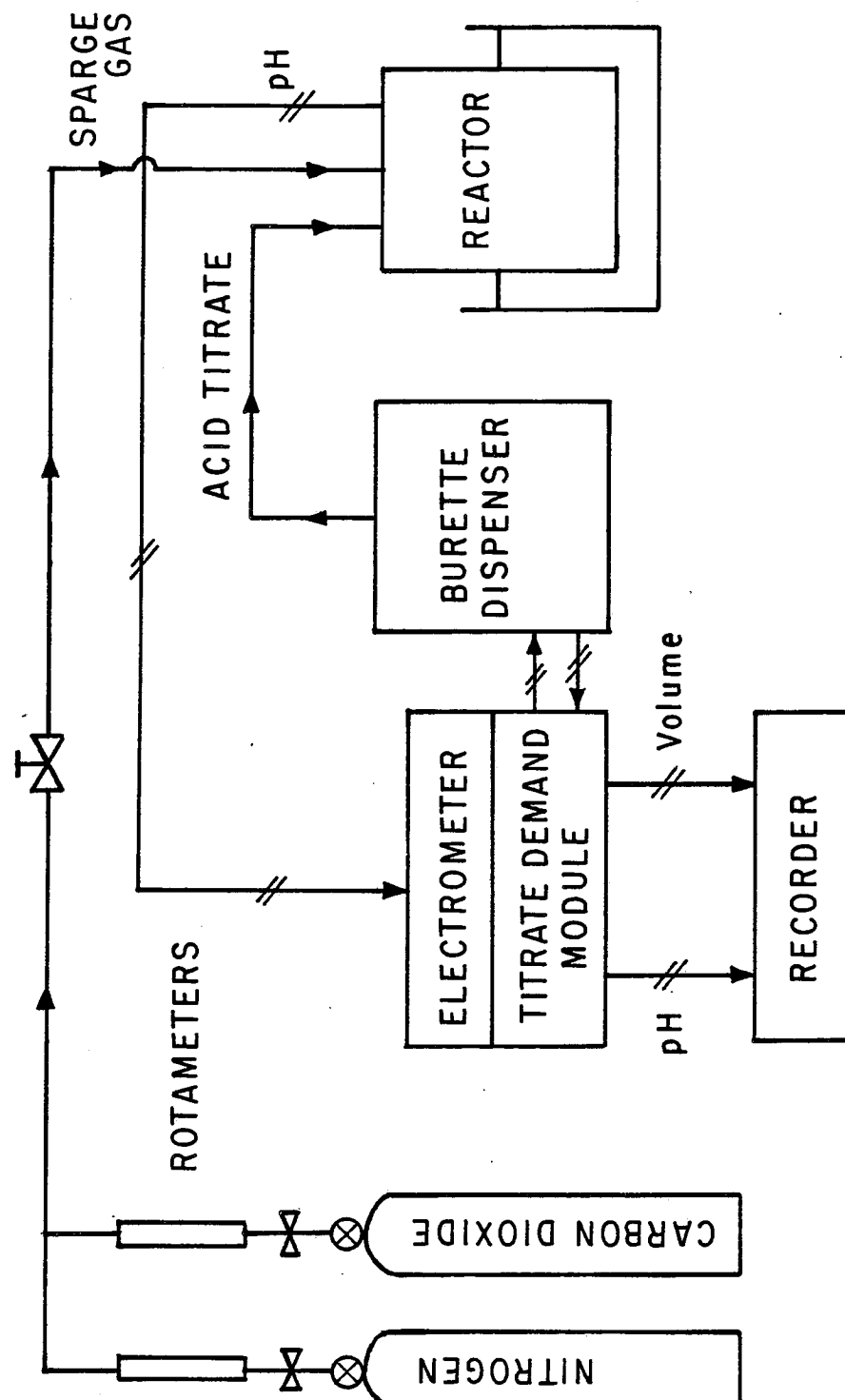


Figure 4-1. pH-Stat Apparatus

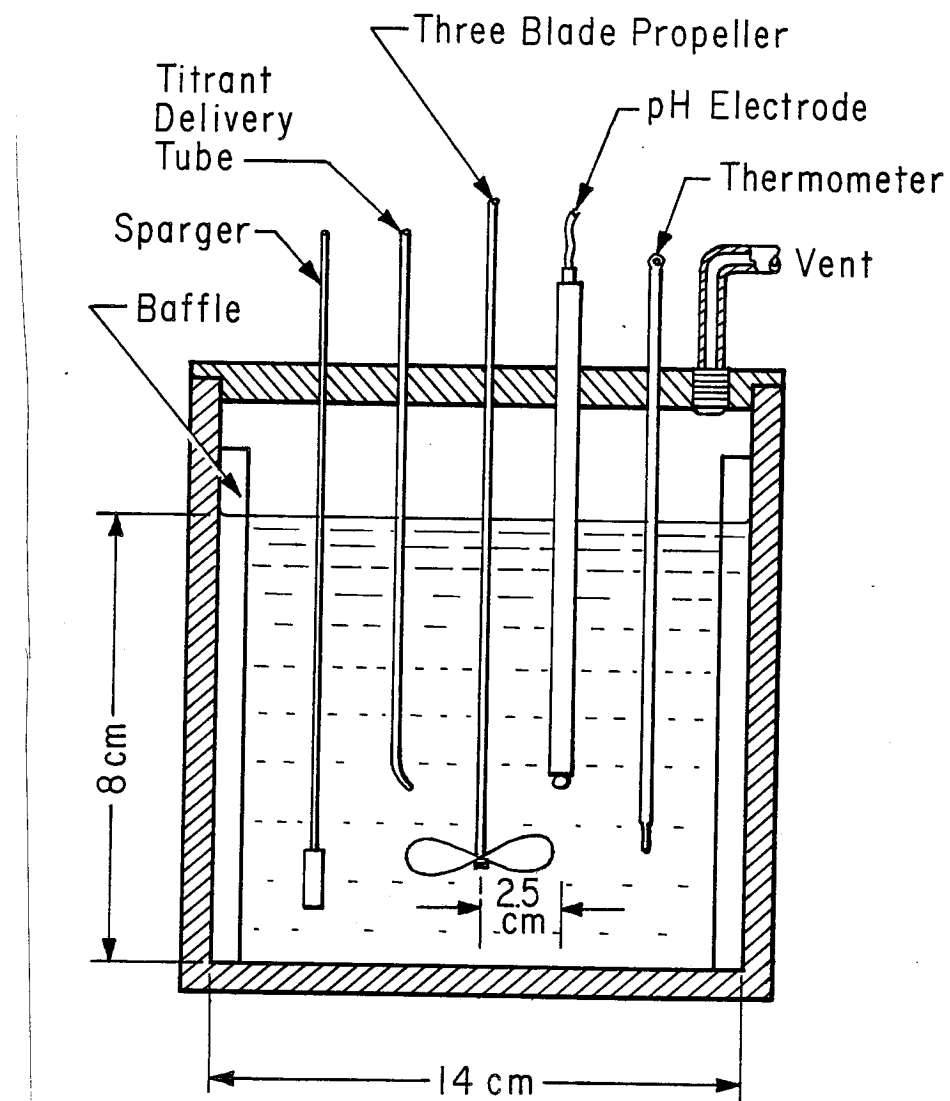


Figure 4-2. Detail Components of
Reactor

with a three-bladed 2.5 cm marine propeller was used to keep the limestone in suspension. The variable speed agitator was kept constant at 720 rpm for all runs.

The pH of the solution was measured by a combination electrode calibrated with standardized pH 4 phthalate and pH 7 phosphate buffers. The acid titrant was added through a slanted glass-delivery tube.

Carbon dioxide or nitrogen was supplied to the reactor by fritted-glass tubing for better gas-liquid mass transfer. The flow rate of the gas was controlled by a needle valve and measured by a rotameter. The flow rate was maintained at about 1750 ml/min (at 1 atm and 70°F) for all experimental runs.

For runs at 55°C, the temperature of the reactor was kept constant within 2°C by a water bath with a mercury on/off thermoregulator. The heat was supplied by an electric heating coil submerged in the bath. The temperature of the solution in the reactor was measured by a thermometer. The cold gas was presaturated with water at 55°C to eliminate evaporation of water in the reactor.

Figure 4-3 shows the orientation of the various components in the reactor. All devices were fastened to reactor lid by means of number three and four rubber stoppers.

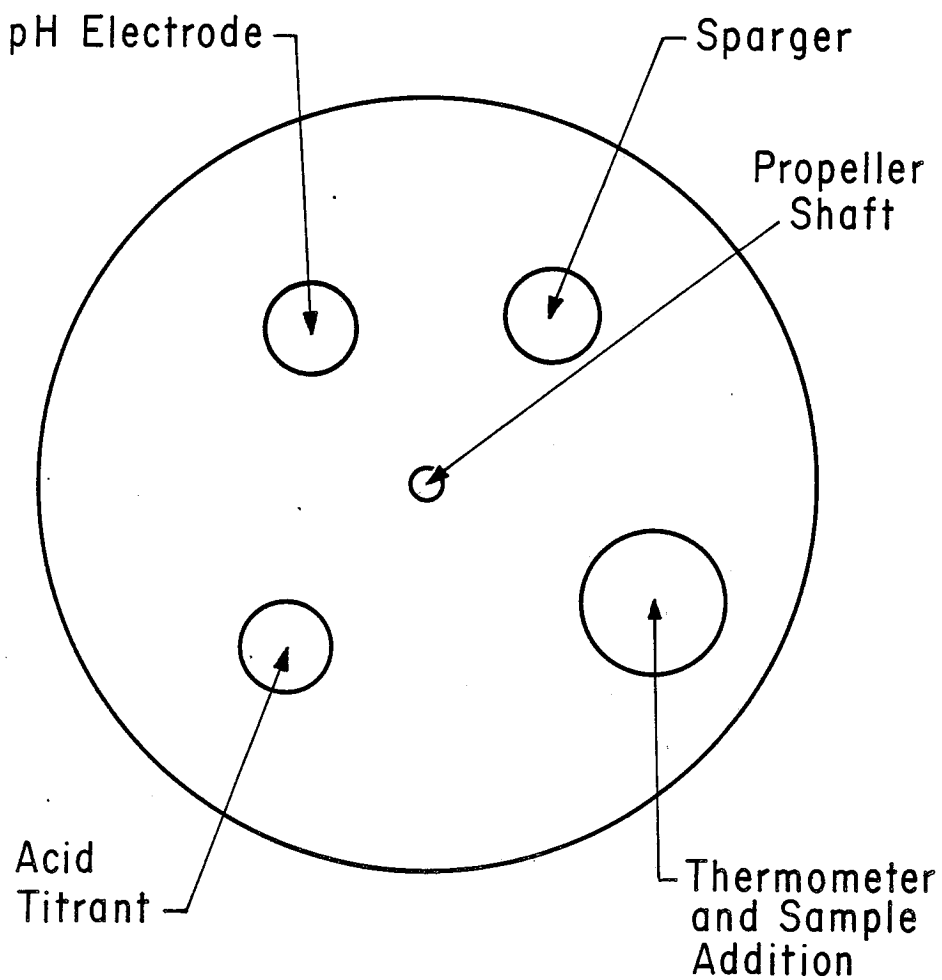


Figure 4-3. Top View of Reactor showing
different orientations of
each component

The Fisher Electrometer and Titrate Demand Module consisted of a pH controller with proportional or on/off functions. A 50 ml digital burette was used for acid addition with a 10 mv recorder output and a two-pen linear recorder for pH and cumulative volume versus time. A detailed description of the system is given in Appendix C.

PROCEDURE

The plexiglass reactor was filled with one liter of 0.1 M CaCl_2 solution. The solution was sparged by either CO_2 or N_2 depending on whether high or low P_{CO_2} was chosen for the experiment. The solution was sparged by either CO_2 or N_2 for about 20 minutes to presaturate the solution with the gas. During this time, the pH electrode was calibrated and a nominal pH was chosen. The agitator was turned on and 0.5 ± 0.01 g of limestone was added to the reactor. The automatic burette/dispenser was started as soon as the limestone was added and the pH was controlled automatically within 0.02 pH. Cumulative titrant volume and pH were recorded versus time on a two pen linear chart recorder.

For CO_2 sparging, the pH controller was operated in the on/off mode (with a 0% proportioning band) since $\text{CO}_2/\text{HCO}_3^-$ acts as a buffer for the solution. However, with N_2 sparging, on-off control gave cyclic pH variations.

Therefore, the pH controller was used with a 50-60% proportioning band and a set point of almost one pH below the target value. The set point was adjusted manually to get the desired pH after the limestone was added and during the experiment. The use of the proportioning band eliminated the problem of pH fluctuating when a buffer is not present.

For runs at 55°C, the same procedures were followed except that the electrode was calibrated with standardized solutions preheated at 55°C. The 0.1 M CaCl₂ solution was preheated to about 57°C before adding to the reactor. The above procedure was necessary to reduce the time for reaching thermal equilibrium.

In experiments with buffers, an appropriate amount of organic acid or sodium salt was added to the 0.1 M CaCl₂ solution and the procedure for simple solutions was followed. With HSO₃⁻/SO₃⁼ buffer, a known sample of solution was drawn from the reactor before and after the run. The samples were quenched with excess iodine and backtitrated with thiosulfate to determine the amount of sulfite oxidized during the run.

PARTICLE SIZE DISTRIBUTION BY COULTER COUNTER

The Coulter counter determines the number and size of particles suspended in a conductive liquid by forcing the suspension to flow through a small aperture and monitoring an electrical current which also passes through the aperture. As a particle passes through the aperture, it changes the resistance between the electrodes. This produces a current pulse of short duration having a magnitude proportional to the particle volume. The measurements obtained from the Coulter counter are different percent volume versus volumetric size, and cumulative percent volume versus volumetric size. A single aperture can generate a size distribution with 14 fractions from 2 to 40% of the aperture diameter.

The particle size distribution of reagent CaCO_3 was measured with a $100 \mu\text{m}$ aperture in 0.18 M CaCl_2 electrolyte (Table 3-4). Preliminary measurements with NaCl electrolyte were unsuccessful because of CaCO_3 dissolution during size analysis. Dissolution was avoided by using CaCl_2 electrolyte or by using $1 \text{ mM Na}_3\text{PO}_4$ in 1 wt.\% NaCl .

CHAPTER V

RESULTS AND DISCUSSION

The rate of calcite dissolution in 0.1 M CaCl_2 solution was measured and predicted by the general mass transfer model as a function of pH, P_{CO_2} , temperature, and buffer additives. The effect of P_{CO_2} is significant only in determining the equilibrium pH for dissolution due to buffer reaction. Acetic, adipic, acrylic, and sulfosuccinic acids enhance the rate of CaCO_3 dissolution at concentrations as low as 2 mM. However, sulfopropionic, hydroxypropionic, and polyacrylic acids inhibit the rate of CaCO_3 dissolution. Low sulfite concentrations enhance CaCO_3 dissolution. However, at high sulfite concentrations, crystallization or adsorption of CaSO_3 on the limestone surface tends to inhibit the rate. An equilibrium shift of $[\text{CaCO}_3^\circ]$ as a function of $[\text{CaSO}_3^\circ]$ on the limestone surface is used to model these effects. The enhancement of dissolution at low pH and high temperature is also observed.

The above results are modeled by mass transfer from a spherical particle to an infinite stagnant medium with enhancement by chemical reaction. This mass transfer model always predicts a rate that is about 25% lower than the experimental rate. Therefore, the model results in this chapter have been uniformly increased by 25% to

account for nonideality of the model. This nonideality may be the results of turbulence or non-spherical particles. Even for particles as small as 5 to 10 μm , the effect of turbulence may increase mass transfer as much as 25%. Furthermore, the model and Coulter counter measurement assume that the calcite particles are spheres instead of rhombhedra.

EFFECT OF PARTICLE SIZE

Figure 5-1 gives measured and calculated results of typical experiments as the fraction remaining versus dimensionless time. The integrated mass transfer model (polydisperse and monodisperse) is compared to that of runs at pH 4 and 5 with N_2 sparging. The results show that the integrated mass transfer model for polydisperse particles can predict the general dissolution shape for $CaCO_3$ dissolution at different solution compositions. The monodisperse (uniform particle size distribution) data also show that reagent grade $CaCO_3$ has a very uniform particle size distribution. However, for $t/t_{50} > 1.0$, the monodisperse model does not give as good a fit as the polydisperse model.

To obtain the experiment rate constant, k , equation 3.29 is used. From the general mass transfer model integrated over the size distribution (polydisperse),

$$kt_{56} - kt_{50} = 6.14 \times 10^{-8} \text{ cm}^2/\text{sec},$$

for the experimental run at pH 5, $t_{50} = 11.3 \text{ min}$.

From Figure 5-1:

$$t_{50} - t_{56} = (1 - \frac{t_{56}}{t_{50}}) \cdot 11.3 \text{ min} = 96.8 \text{ sec}$$

Therefore $k_{exp} = 6.34 \times 10^{-10} \text{ cm}^2/\text{sec}$.

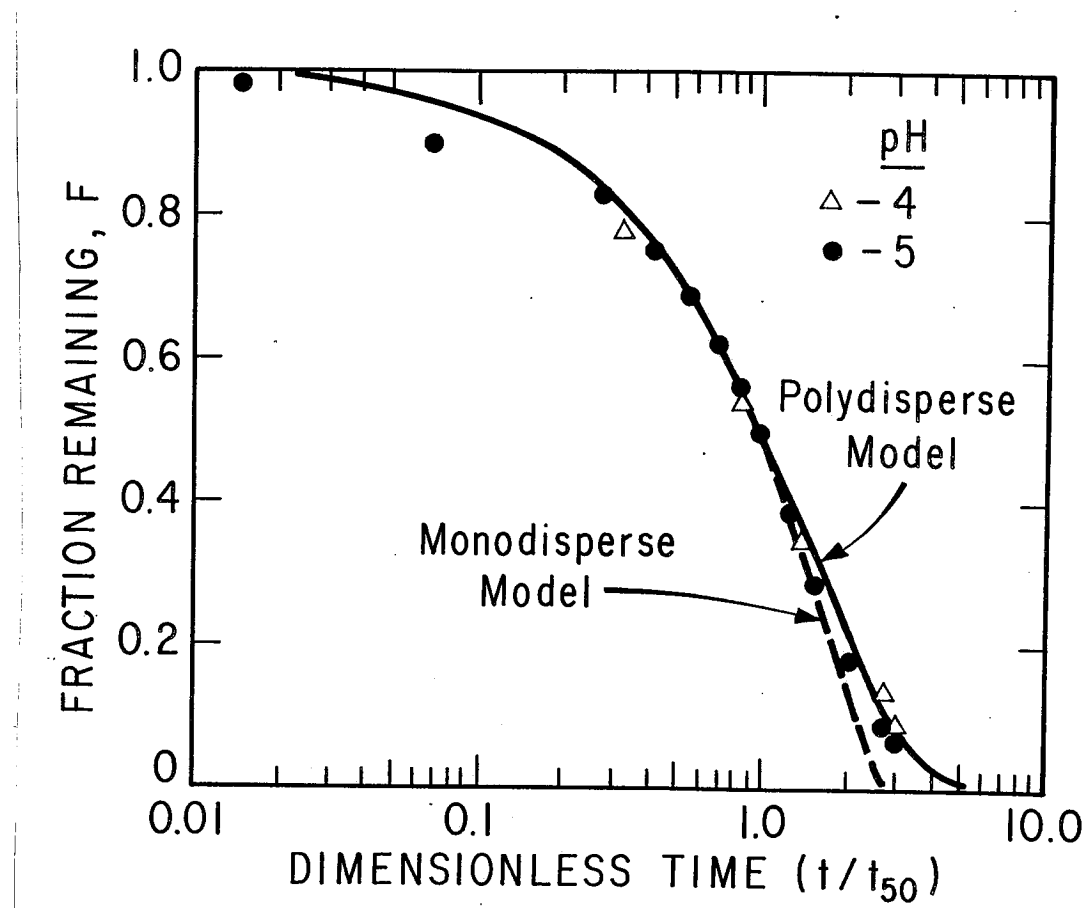


Figure 5-1. Dissolution Curves for Reagent
Grade CaCO_3 at 25°C with
 N_2 Sparging

EFFECT OF pH, P_{CO_2} , AND TEMPERATURE

Figure 5-2 and 5-3 give calculated and measured dissolution rates at 25 °C and 55 °C and pH 4 to 7 with CO₂ or N₂ sparging, respectively. Rates shown by the curves were calculated by the general mass transfer model assuming a particle diameter of 10 μm. The calculated rates were arbitrarily increased by 25% to account for nonideality of the model. The model works well for both CO₂ and N₂ sparging.

With CO₂ sparging, the model predicts a 6.7-fold increase in rate from pH 4 to 5. At 55 °C, the rates are 1.7 times than that at 25 °C for both high and low P_{CO₂}. The CO₂ reaction tends to increase the rate of dissolution 1.15 times below pH 5. With CO₂ sparging, the equilibrium pH is 5.6 at 25 °C and 5.4 at 55 °C.

With N₂ sparging, the model predicts rates at pH 7 which are 15% to 68% lower than experimental data at 25 °C and 55 °C respectively. These deviations are probably due to the sensitivity of the model to solution and surface equilibrium constants at high pH. At pH 6.5, the rate is three times higher at 55 °C than at 25 °C. However, at pH 5.0, the rate at 55 °C is about twice that at 25 °C. These effects were also predicted by the mass transfer model. The temperature dependence at high pH is probably due to the OH⁻ contribution to mass transfer.

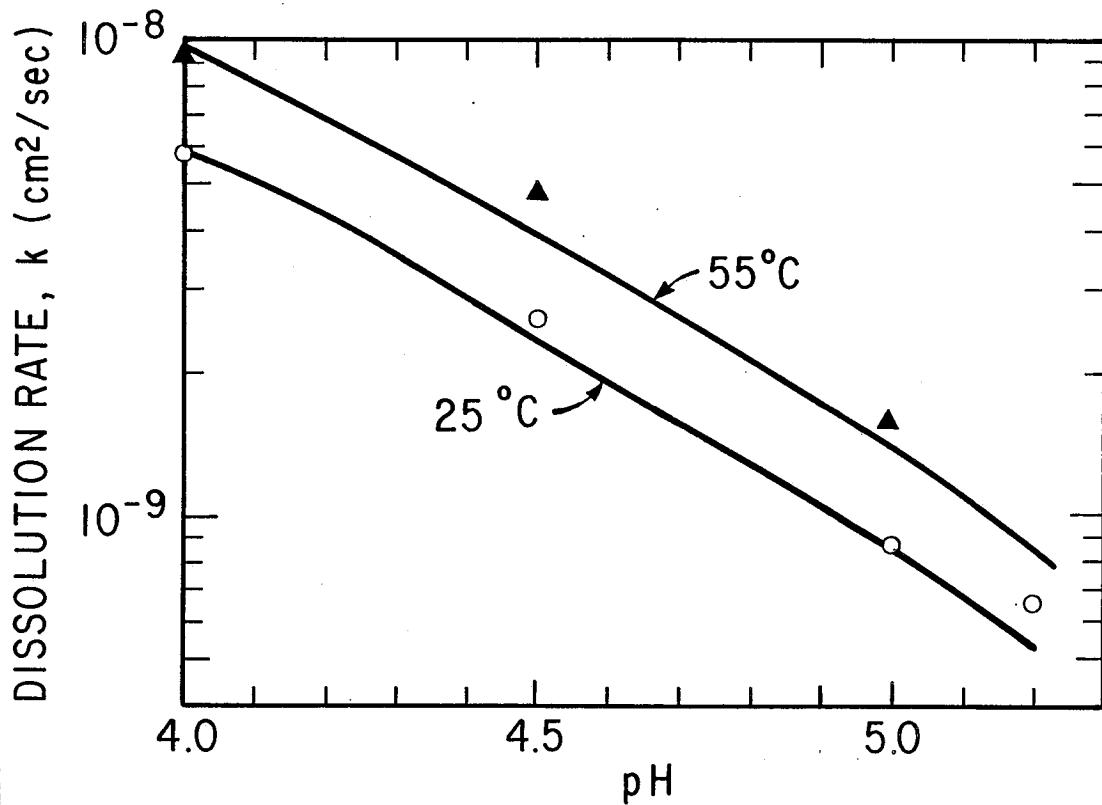


Figure 5-2. Dissolution Rate of Reagent CaCO_3 with CO_2 Sparging in 0.1 M CaCl_2 . Curves Calculated by the General Mass Transfer Model

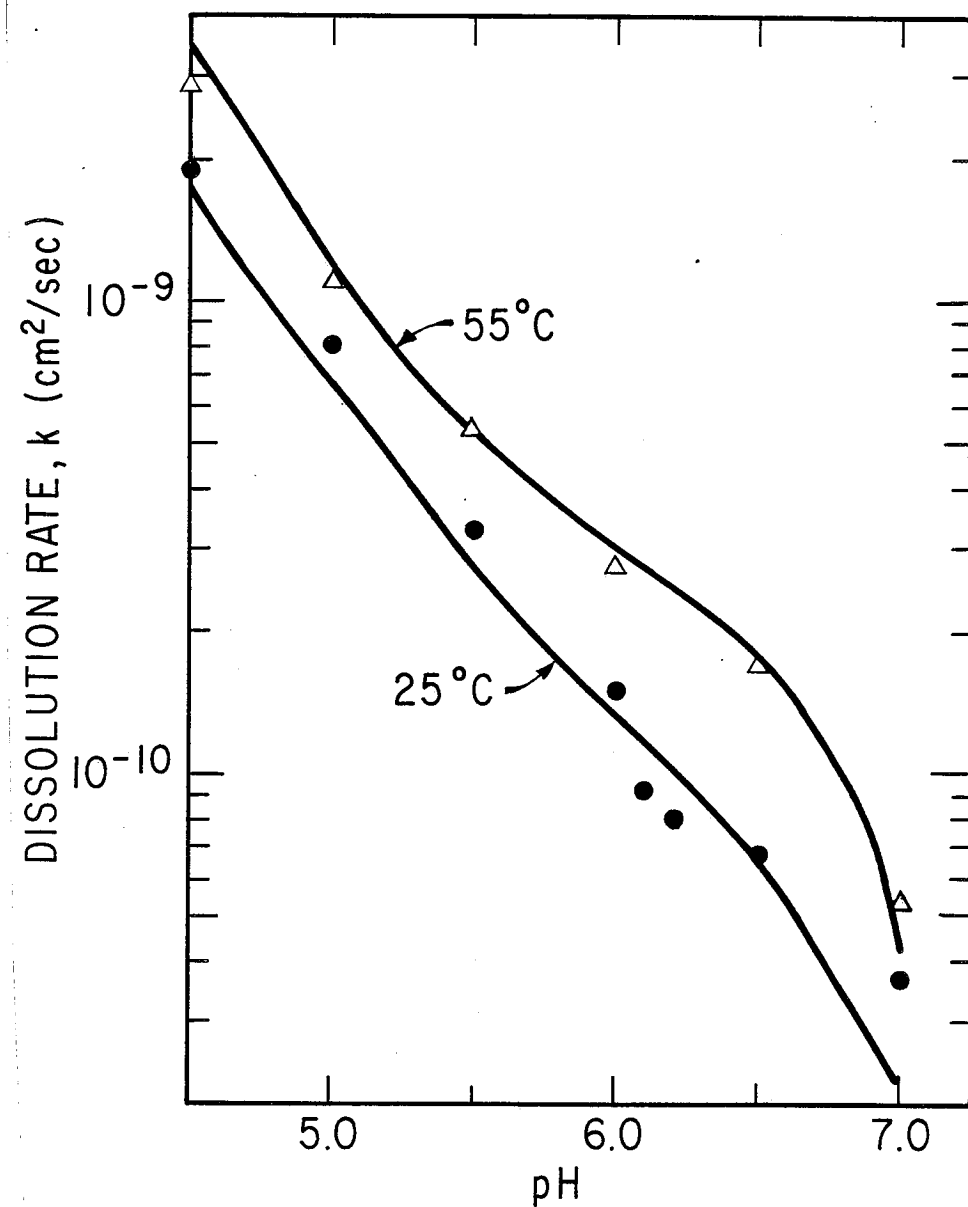


Figure 5-3. Dissolution Rate of Reagent Grade CaCO_3
with N_2 Sparging in 0.1 M CaCl_2 .
Curves Calculated by Mass Transfer Model
Neglecting CO_2 Reaction

EFFECTS OF ORGANIC ACIDS

The rate constants for the various buffer systems were measured in 0.1 M CaCl_2 at 25 °C with N_2 and CO_2 sparging. Organic buffer additives such as acetic, adipic, acrylic, and sulfosuccinic acids enhance the rate of calcite dissolution by buffering the solution pH and providing for mass transfer of acidity to the limestone surface.

Acetic acid - The effects of 1, 3, and 10 mM acetic acid were measured at pH 4 to 6 with N_2 and CO_2 sparging. Figure 5-4 shows that the enhancing effects are predicted accurately by the mass transfer model. The enhancement of the dissolution rate with 1 mM acetic acid varies from 1.5 at pH 4 to 3.5 at pH 6. The buffer is more effective at high pH where H^+ diffusion has little effect on the rate. At pH 5 and 6, the dissolution rates are 2.8 and 3.5 times faster with 1 mM acetate than without acetate. At pH 5, the effect of CO_2 is insignificant in the presence of acetic acid.

Figure 5-4 shows results at pH 5.5 with CO_2 sparging. The calculated rates are 2-3 times higher than the measured rates. These deviations may be due to the presence of impurities in the solution. Phosphate (Berner and Morse, 1974) and certain metal ions (Terjesen *et al.*, 1961)

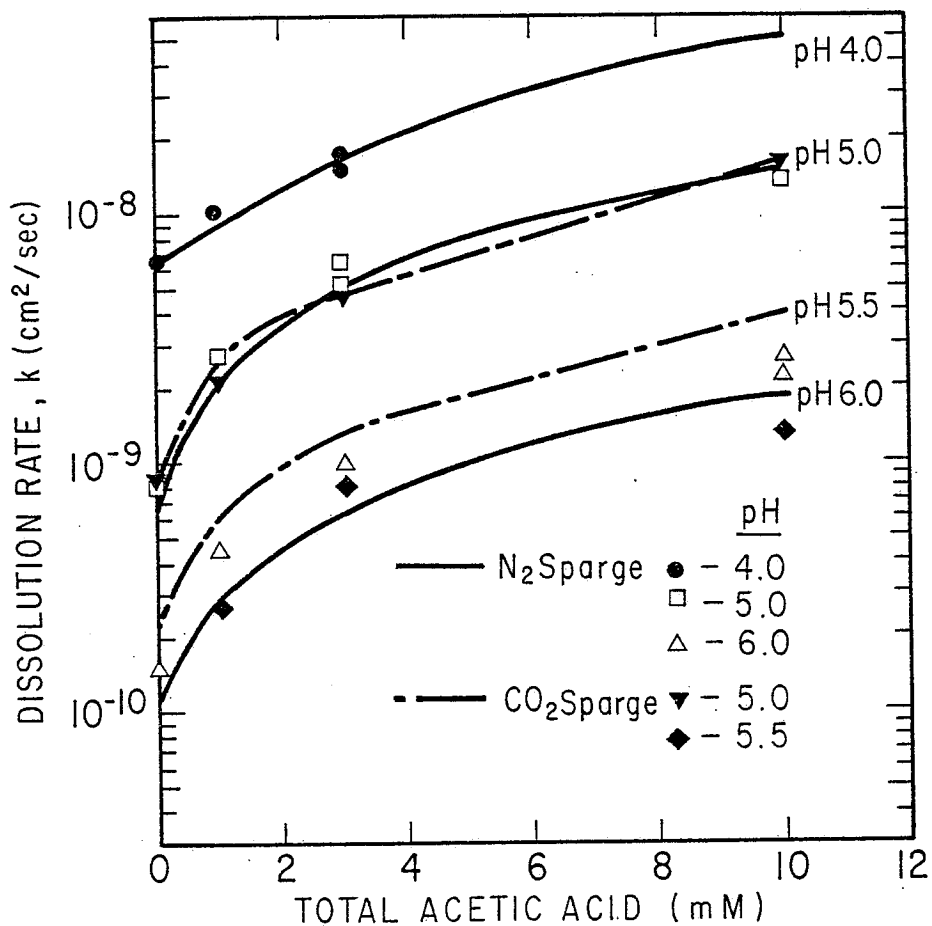


Figure 5-4. CaCO_3 Dissolution at 25°C in $0.1 \text{ M } \text{CaCl}_2$,
Effect of Acetic Acid

shown some kind of inhibition by surface adsorption. Since the measured rates are extremely sensitive to pH near equilibrium, any inhibitors could cause a large deviation from the calculated rates. Furthermore, at pH close to equilibrium, the rates are very sensitive to the surface equilibrium and the values of the physical constants used in the mass transfer model.

Adipic acid - The effects of 3 mM adipic acid on the rate of dissolution are given in Figure 5-5. The calculated rate is within 5% of the experimental rate at pH 4 and 30% at pH 5 and 6. The rate data show that adipic acid is equivalent on a molar basis to acetic acid at pH 4, but gives 25% to 35% faster dissolution rates at pH 5 and 6.

Other buffers - The effects of acrylic, sulfo-succinic, hydroxypropionic, sulfopropionic and polyacrylic acids were measured at pH 5 with N_2 sparging(Figure 5-6). The acrylic and polyacrylic acids used were commercially available reagent grade materials. The other organic acids were synthesized from acrylic or maleic acid. Hydroxy-propionic acid was synthesized from 2 M acrylic acid by heating with 1 M H_2SO_4 at $100^\circ C$ for 10-20 hours. Sulfo-propionic acid was synthesized by reaction of Na_2SO_3 with

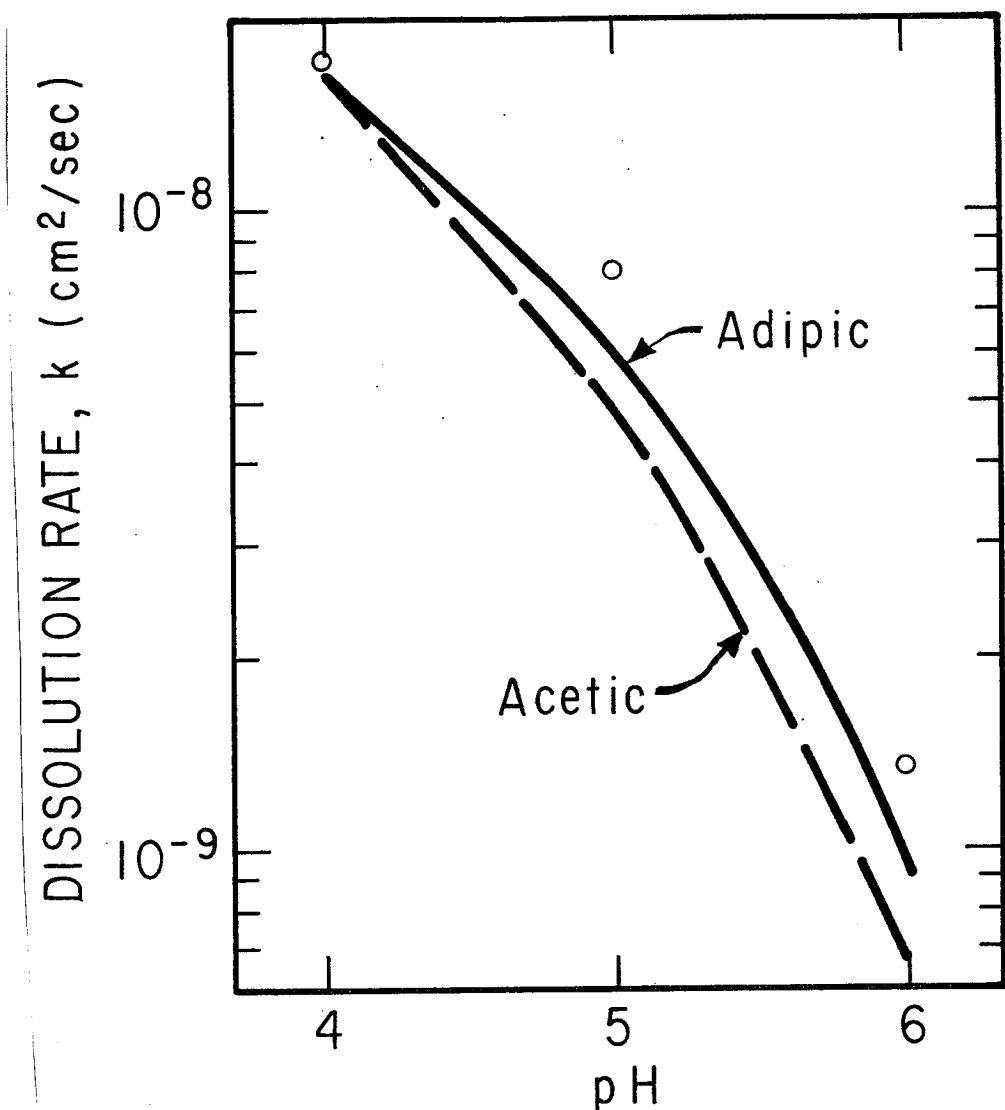


Figure 5-5. Dissolution Rate of CaCO_3 in 0.1 M CaCl_2 with N_2 Sparging at 25°C , and 3 mM Adipic Acid.

Curves Calculated by Mass Transfer Model Neglecting CO_2 Reaction

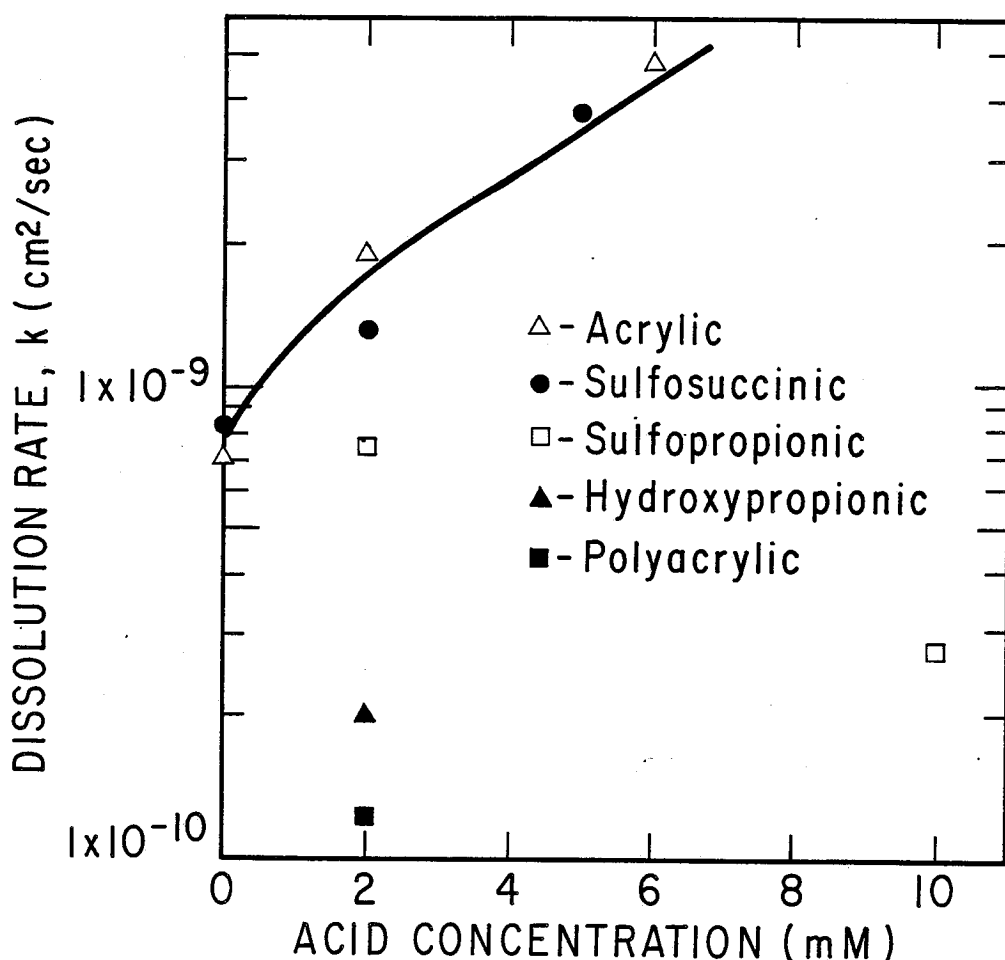


Figure 5-6. Effect of Organic Acids on Dissolution Rate in 0.1 M CaCl_2 with N_2 Sparging, 25°C and pH 5.
 Curve for Acrylic and Sulfosuccinic Acid Calculated by Mass Transfer Model Neglecting CO_2 Reaction

acrylic acid at ambient temperature. Sulfosuccinic acid was synthesized by reaction of Na_2SO_3 with maleic anhydride at 25°C (Smith, 1981).

The calculated rates for acrylic and sulfosuccinic acids happened to be about equal and agreed well with the measured data except at 2 mM sulfosuccinic acid. The diffusivity of acetic acid was used for acrylic acid. Polyacrylic acid(2 meq/liter) inhibited the dissolution rate probably by adsorption on the CaCO_3 . Both sulfopropionic and hydroxypropionic acids also inhibited the rate, probably due to the presence of polyacrylic acid formed by the synthesis processes.

EFFECTS OF SULFITE/BISULFITE

The effects of sulfite/bisulfite on CaCO_3 dissolution were measured from pH 4.5 to 6.0 at 25°C. Rate data at pH 5 and 55°C were also measured. The experimental and calculated results are shown in Figure 5-7.

From the experimental data in Figure 5-7, one can see that sulfite enhances at low concentration but inhibits at high concentration. The inhibition starts at about 10 mM at pH 4.5 and at about 1 mM at pH 6.0. These concentrations correspond to those of calcium sulfite solubility at pH 4.5 and pH 6.0 respectively. The inhibition phenomenon suggests some sort of reversible blinding

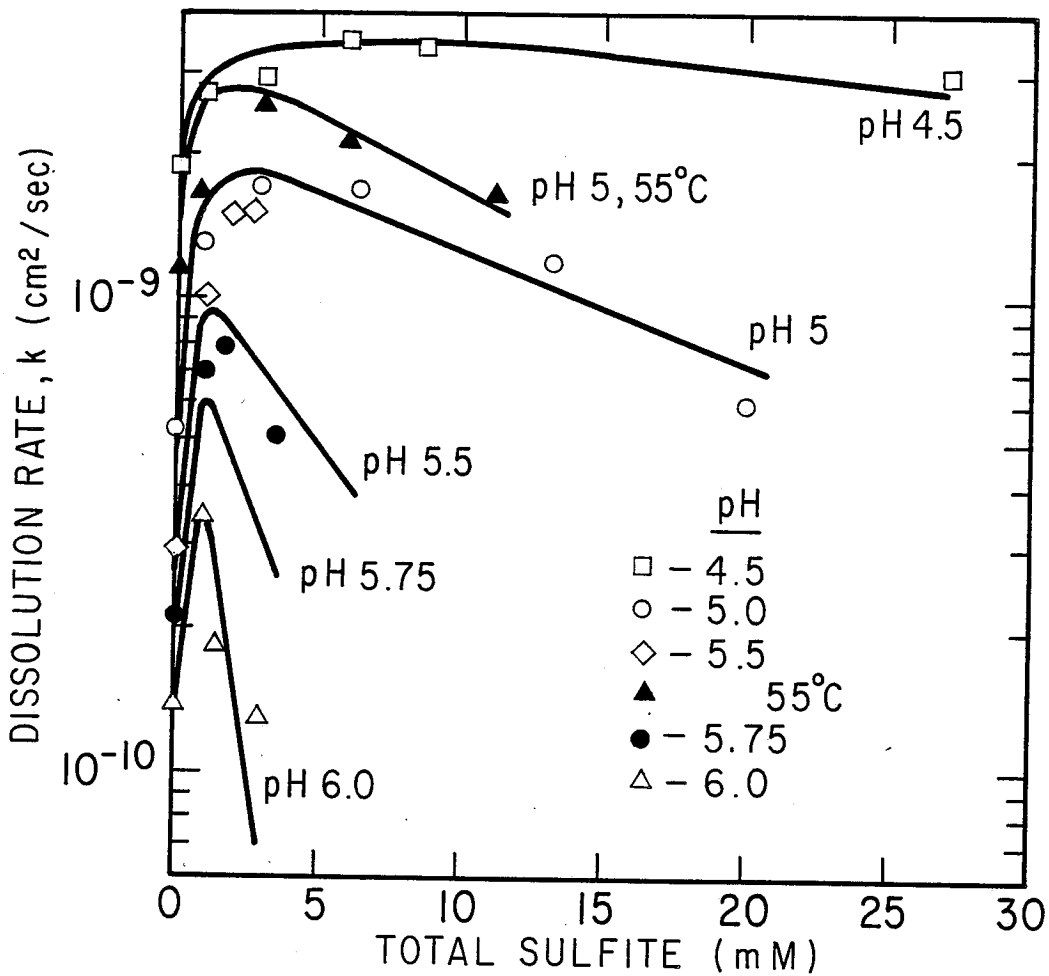


Figure 5-7. Effect of Sulfite, N_2 Sparging, 25°C and 55°C . Curves Calculated from Mass Transfer Model Neglecting CO_2 Reaction and Including $\text{CaCO}_3^\circ / \text{CaSO}_3^\circ$ Solid Solution

of the CaCO_3 surface by CaSO_3 adsorption or crystallization. Thus the present mass transfer model had to be modified to take into account the inhibition effect.

Figure 5-8 gives the combined effects of acetate and sulfite buffers on the rate of dissolution. The rates are enhanced from 0 to about 1.5 mM acetate with 3 mM sulfite but inhibited at higher acetate concentration.

The enhancing and inhibiting effect of sulfite in 0.1 M CaCl_2 solution can be modeled as a shift in equilibrium at the calcite surface. Thus the equilibrium CaCO_3° concentration is reduced by increased CaSO_3° concentration, much like a solid solution at the CaCO_3 surface. Using the simplified mass transfer model which neglects the $\text{CO}_2/\text{HCO}_3^-$ reaction, the solution composition at the CaCO_3 surface was calculated from the experimental rate data.

Figure 5-9 shows a correlation of the surface concentration of CaCO_3° and CaSO_3° given by:

$$\log [\text{CaCO}_3^\circ] = -10.76 - 1.29 \log [\text{CaSO}_3^\circ]$$

Thus CaSO_3° concentration quantitatively reduces the equilibrium solubility of CaCO_3° , probably by forming a solid solution at the calcite surface. For $[\text{CaSO}_3^\circ]$ less than 0.05 mM, $[\text{CaCO}_3^\circ]$ at the surface is equal to its normal equilibrium value, 6.80×10^{-7} M. The calculated rate is obtained by successive trial and error with β until the above solid solution equilibrium is satisfied.

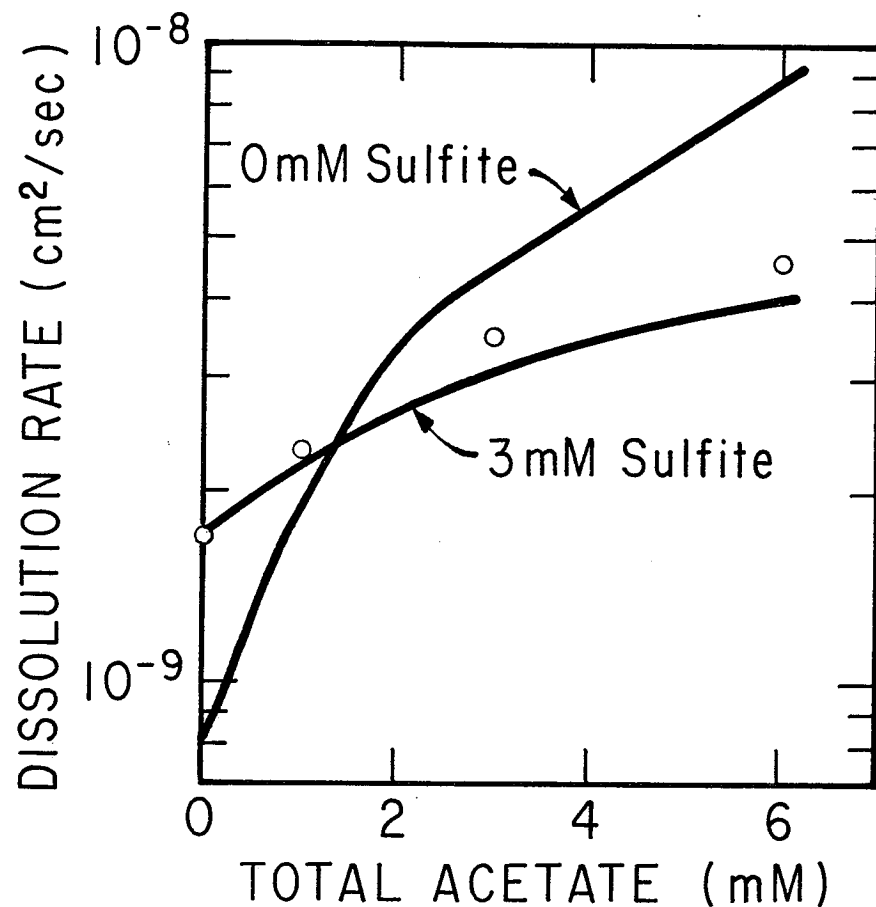


Figure 5-8. Effect of Acetate on Dissolution
Rate with 3 mM of Total Sulfite,
pH 5 and 25 °C.
Curves Calculated by Mass Transfer
Model

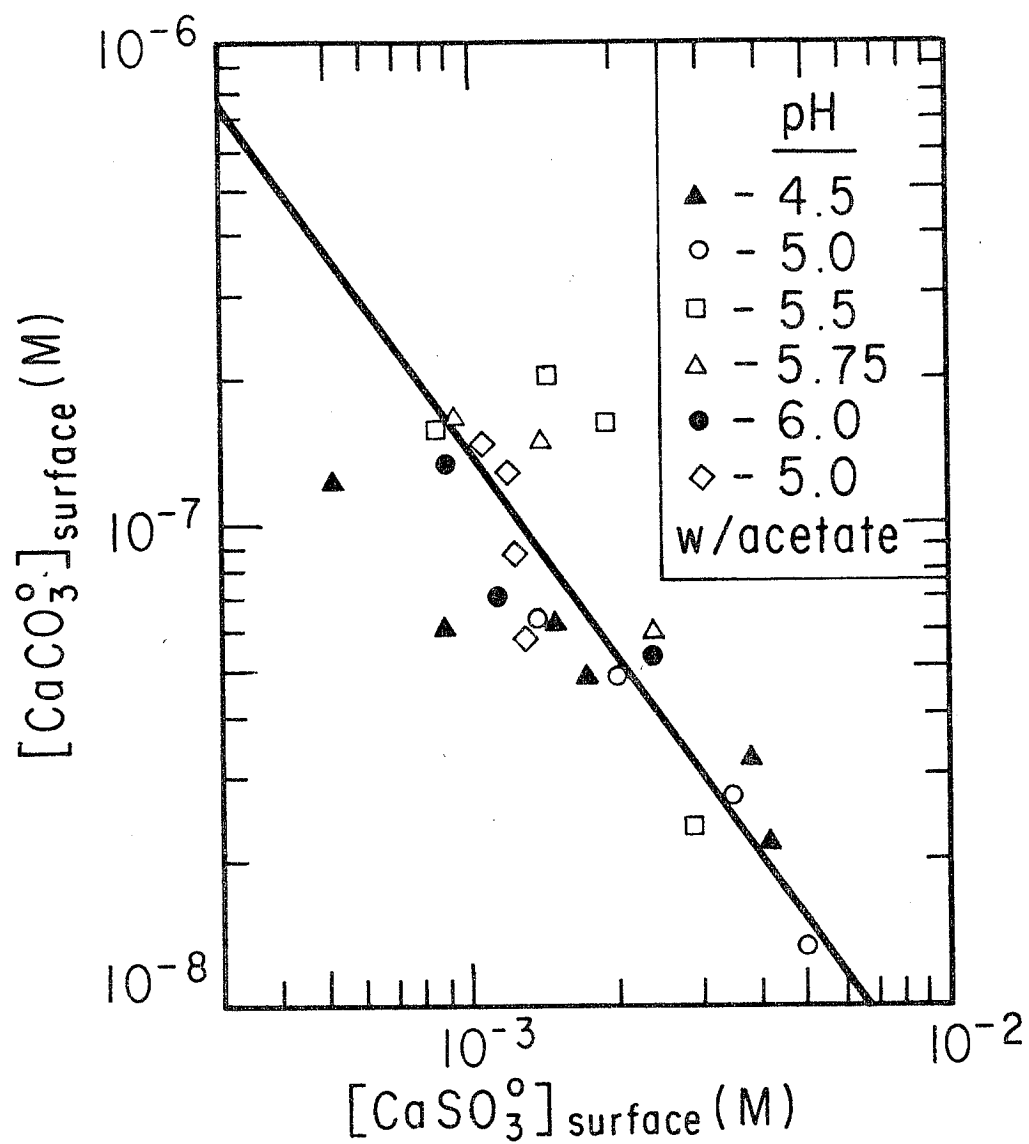


Figure 5-9. Calculated Solution Composition
at CaCO_3 Surface, N_2 Sparging and
 25°C

As shown in Figure 5-7, the modified mass transfer model predicts the measured rate well at pH 4.5, 5.0, and 6.0 but deviates significantly at pH 5.5 and 5.75. These deviations may result from the sensitivity of the calculated rates to the estimated equilibrium constants and diffusivities used in the model. The maximum dissolution rates at each pH correspond roughly to the CaSO_3 solubility, shifting to higher sulfite concentrations at lower pH. A higher dissolution rate was observed at 55°C, but the rates are still modeled well by mass transfer with the same $\text{CaSO}_3^\circ/\text{CaCO}_3^\circ$ equilibrium.

DISCUSSION

Several previous investigators (Plummer *et al.*, 1978; Berner and Morse, 1974; Barton and Vatanatham, 1976; Sjoberg, 1976; Erga and Terjesen, 1956; and Ottmers *et al.*, 1974) showed that CaCO_3 dissolution is controlled by H^+ diffusion at low pH. However, Plummer *et al.*, (1978) and Berner and Morse(1974) found it necessary to model in terms of surface kinetics at moderate and high pH.

By using a more comprehensive mass transfer model than previous investigators, we have shown that the dissolution rate is modeled by mass transfer even at high pH. Berner neglected the effects of OH^- and the CO_2 reaction.

Our model has taken into account the effects of CO_2 , OH^- , CaOH^+ , and buffer additives. The general mass transfer model shows that at low pH, the diffusion of H^+ is the controlling mechanism for dissolution. At high pH, however, the contribution of OH^- dominates, especially at high temperature.

Present experimental work on limestone dissolution also goes beyond that of the previous investigators. The enhancement effect of buffer additives on CaCO_3 dissolution was observed as predicted by mass transfer. The buffer additives increase dissolution rate by providing acidity to the limestone surface. The inhibition of sulfite is analogous to inhibition by phosphate (Berner and Morse, 1974) and metal ions (Terjesen *et al.*, 1961; Koss and Moller, 1974). Our results show that sulfite inhibits by surface adsorption, an equilibrium process, and not by an effect on surface kinetics. We also provide better particle size distribution data from Coulter counter than those determined optically (Berner and Morse, 1974) and by wet sieving (Plummer *et al.*, 1978).

Finally, the effect of temperature can also be modeled by mass transfer as shown in this work. The temperature dependence shows an apparent ΔH of 4.4 kcal/gmol from pH 4.0 to 5.5. However at pH 6.0 to 6.5, an apparent ΔH of 7.1 kcal/gmol is observed. Berner and Morse did not report the effect of temperature on the rate of CaCO_3 .

dissolution. Plummer et al., however, reported high activation energy at pH close to equilibrium and proposed a surface kinetics mechanism. Our model enables the dissolution of calcite to be calculated even at high pH.

CONCLUSIONS AND RECOMMENDATIONS

1. Limestone dissolution in throwaway scrubbing can be modeled by mass transfer. For particles less than $10-20 \mu\text{m}$, the mass transfer coefficient can be obtained by assuming a sphere in an infinite stagnant medium.
2. Organic buffer additives such as acetic, adipic, acrylic, and sulfosuccinic acid enhance the rate of calcite dissolution by buffering the solution pH and providing for mass transfer of acidity to the limestone surface.
3. At pH 4.5 to 5.5, P_{CO_2} of 1 atm increases the rate of dissolution by 15% because of the indirect reaction of CO_2 with CaCO_3 . However, at low pH(4.0), the effect of P_{CO_2} is insignificant. High P_{CO_2} is also a dominant factor in determining the equilibrium pH at which dissolution stops.
4. The rate of dissolution is enhanced at low sulfite concentration and inhibited at high sulfite concentration. These phenomena are modeled by mass transfer with

a solid solution equilibrium of CaSO_3^0 and CaCO_3^0 .

5. The dissolution of calcite is a function of the solution composition and particle size distribution. The rate should be independent of surface roughness, surface area, and shape.

6. The effects of temperature are predicted by the mass transfer model with appropriate physical constants. High temperature dependence at high pH results from the effect of temperature on OH^- equilibrium.

7. More experimental data are needed to establish the validity of the mass transfer model near equilibrium pH.

APPENDIX A
MASS TRANSFER FOR A SPHERE IN AN INFINITE
STAGNANT MEDIUM

The equation of continuity for mass transfer in spherical coordinates (Bird, Stewart, and Lightfoot, 1960) gives

$$\frac{\partial}{\partial r} \left(r^2 \frac{\partial c}{\partial r} \right) = 0 \quad A-1$$

where c is the concentration and r is the radius of particle.

Integrating equation A-1 gives

$$c = \frac{-A_1}{r} + A_2 \quad A-2$$

where A_1 and A_2 are constants of integration.

For the dissolution of a sphere in a stagnant medium, the following B.C. apply:

$$\text{at } r = r_o, \quad c = c_i$$

$$\text{and at } r = \infty, \quad c = c_\infty$$

where r_o is the radius of the sphere, c_i is the surface concentration, and c_∞ is the bulk concentration.

Solving for A_1 and A_2 in equation A-2, one gets

$$c = \frac{-(c_i - c_\infty) r_o}{r} + c_\infty \quad A-3$$

From Fick's first law

$$N = -D \frac{\partial c}{\partial r} \Big|_{r=r_o} \quad A-4$$

where N is the flux at $r=r_o$ and D is the diffusivity.

Differentiating equation A-3 with respect to r and substituting in equation A-4 gives

$$N = \frac{D(c_i - c_\infty)}{r_o} \quad A-5$$

Rearranging equation A-5 gives

$$\frac{Nr_o}{D(c_i - c_\infty)} = 1 \quad A-6$$

$$\text{since } N = k_c(c_i - c_\infty) \quad A-7$$

where k_c is the mass transfer coefficient.

Equation A-6 becomes

$$\frac{2Nr_o}{D(c_i - c_\infty)} = \frac{2k_c r_o}{D} = \frac{k_c d_p}{D} = 2 \quad A-8$$

where d_p is the diameter of the sphere.

Thus for spheres dissolving in a stagnant medium the Sherwood number ($k_c d_p / D$) is 2. This condition represents the asymptotic limit of small particles in an agitated vessel.

APPENDIX B

TABULATED DATA

Table B-1 Calculated Effects of Particle
 Diameter, 25°C at pH 5.0
 $[Ca^{++}] = 0.01M$, $P_{CO_2} = 1 \text{ atm}$,
 (Figure 3-1)

$D_p (\mu m)$	Dissolution Rate $\times 10^9$ $(\text{gmol/cm}^2\text{-sec})$
0.1	232.00
1.0	23.60
9.0	3.61
10.0	2.90
20.0	2.13

pH	$\text{DCO}_3^- \text{ CO}_3^=$ + $\text{DCaCO}_3^\circ \Delta \text{CaCO}_3^\circ$	$-\text{DH}^+ \Delta \text{H}^+$	$-\text{DCO}_2^- \Delta \text{CO}_2^-$	$-\beta$
	(M cm ⁻² /sec)	(M cm ⁻² /sec)	(M cm ⁻² /sec)	(M cm ⁻² /sec)
6.00	6.934×10^{-11}	6.429×10^{-11}	1.30×10^{-10}	2.636×10^{-10}
5.75	9.923×10^{-11}	1.639×10^{-10}	2.26×10^{-10}	4.890×10^{-10}
5.50	1.085×10^{-10}	3.194×10^{-10}	2.94×10^{-10}	7.221×10^{-10}
5.25	1.114×10^{-10}	5.839×10^{-10}	3.62×10^{-10}	1.058×10^{-9}
5.00	1.118×10^{-10}	1.047×10^{-9}	4.40×10^{-10}	1.598×10^{-9}
4.75	1.114×10^{-10}	1.867×10^{-9}	4.96×10^{-10}	2.476×10^{-9}
4.50	1.099×10^{-10}	3.324×10^{-9}	4.48×10^{-10}	3.881×10^{-9}
4.00	1.061×10^{-9}	1.052×10^{-8}	7.06×10^{-10}	9.914×10^{-9}

Table B-2 Contribution to Dissolution by Individual Chemical Species
(Figure 3-2)

Table B-3 Calculated effect of P_{CO_2} , 25 °C,
 $[Ca^{++}] = 0.01 M$, $D_p = 8.856 \mu m$
(Figure 3-3)

Dissolution Rate $\times 10^{10}$ (gmol/cm²sec)

pH	$P_{CO_2} = 1 \text{ atm}$	$P_{CO_2} = 0.3 \text{ atm}$	$P_{CO_2} = 0.1 \text{ atm}$
7.205	-----	-----	equil.
7.00	-----	-----	1.95
6.50	-----	-----	3.72
6.467	-----	equil.	-----
6.205	equil.	-----	-----
6.20	-----	4.68	-----
6.00	5.95	-----	5.37
5.75	11.04	9.74	7.151
5.50	16.31	-----	10.33
5.25	23.89	20.20	15.97
5.00	36.09	30.94	-----
4.75	55.91	48.72	-----
4.5	87.65	-----	-----
4.0	223.9	214.1	209.5

**Table B-4 Values of kt/kt_{50} versus Percent Remaining
Calculated by Simplified Mass Transfer
Model (Figure 3-4)**

kt/kt_{50}	Per Cent Remaining
.02283	99.04342
.04566	97.69510
.06849	96.35510
.09132	95.02351
.11416	93.70039
.13699	92.38583
.15982	91.07992
.18265	89.78275
.20548	88.49440
.22831	87.21498
.45662	74.94130
.68493	63.70998
.91324	53.64720
1.14155	44.69400
1.36986	37.07484
1.59817	30.28641
1.82648	24.58535
2.05479	20.26973
2.28311	16.36684
4.56621	1.44915
6.84932	.29189
9.13242	.11332
11.41553	.04919
13.69863	.02679
15.98174	.01034
18.26484	.00040
20.54795	0.00000
22.83105	0.00000

kt_{50}	Per Cent Remaining
43.80000	50.09767

Table B-5 Data from pH-Stat Experiments at
 25°C in 0.1 M CaCl_2 Sparged with
 N_2 (Figure 5-1)

Reagent Grade 100% available CaCO_3

Run 1a pH 5
 $t_{50} = 11.27 \text{ min}$

Run 2a pH 4
 $t_{50} = 1.5 \text{ min}$

Time (min)	Fraction CaCO_3 Remaining	Time (min)	Fraction CaCO_3 Remaining
0.13	0.985	0.50	0.78
0.80	0.900	1.30	0.538
3.20	0.825	2.10	0.344
4.80	0.755	3.70	0.136
6.40	0.688	4.50	0.095
8.00	0.624	5.30	0.072
9.60	0.562	6.10	0.064
11.27	0.500	6.90	0.056
12.80	0.450	7.70	0.055
14.4	0.390	9.70	0.045
16.00	0.340	11.30	0.036
17.60	0.294	14.50	0.030
20.00	0.240	18.10	0.022
23.20	0.180		
26.40	0.134		
30.40	0.094		
34.40	0.070		
37.60	0.060		
40.80	0.050		
44.00	0.040		
48.00	0.034		
52.80	0.028		
66.40	0.013		
74.40	0.010		

Table E-6 Integrated Mass Transfer Model data
for Monodisperse Particle Size
Distribution (Figure 5-1)

Fraction Remaining(F)	Dimensionless time(t/t_{50})
0.978	0.04
0.967	0.06
0.956	0.08
0.945	0.10
0.891	0.20
0.838	0.30
0.786	0.40
0.736	0.50
0.686	0.60
0.590	0.80
0.500	1.00
0.415	1.20
0.335	1.40
0.261	1.60
0.193	1.80
0.133	2.00
0.080	2.20
0.037	2.40
0.007	2.60

Table B-7 Calculated versus Measured Rate Constant
for Reagent Grade Calcite at 25 °C and 55 °C
with CO₂ Sparging (Figure 5-2)

Temperature(°C)	pH	k(cm ² /sec) x 10 ⁹	
		Calculated	Measured
25	4.0	5.8	5.8
25	4.5	2.3	2.6
25	5.0	0.86	0.87
25	5.2	0.53	0.65
55	4.0	9.8	9.3
55	4.5	3.9	4.9
55	5.0	1.4	1.6

Table B-8 Calculated versus Measured Rate Constant
for Reagent Grade Calcite at 25° and 55° C
with N₂ Sparging (Figure 5-3)

Temperature (°C)	pH	k (cm ² /sec) x 10 ¹⁰	
		Calculated	Measured
25	4.5	17.3	19.3
25	5.0	6.8	8.1
25	5.5	2.7	3.3
25	6.0	1.3	1.5
25	6.1	1.2	0.99
25	6.2	1.0	0.80
25	6.5	0.69	0.67
25	7.0	0.22	0.37
55	4.5	34.0	28.0
55	5.0	12.0	11.0
55	5.5	5.2	5.4
55	6.0	3.4	2.8
55	6.5	2.0	1.7
55	7.0	0.45	0.53

Table B-9 Dissolution of Reagent CaCO_3 at 25°C ,
 0.1 M CaCl_2 , 5mM CaCO_3 , and various
 Acetate Concentration³(Figure 5-4)

N_2 sparge

pH	Total Acetate concentration (mM)	Calculated $k(\text{cm}^2/\text{sec}) \times 10^9$	Measured
4	1	8.8	10.5
4	3	16.4	17.4
			15.0
4	10	41.6	--
5	1	2.1	2.6
5	3	4.9	5.2
			6.4
5	10	14.4	13.1
6	1	0.30	0.40
6	3	0.64	0.90
6	10	1.81	2.3
			2.0

CO_2 sparge

5	1	2.6	2.3
5	3	4.5	4.6
5	10	15.4	15.7
5.5	1	0.26	0.63
5.5	3	0.80	1.4
5.5	10	1.30	3.6

Table B-10 Calculated and Measured Rate $k(\text{cm}^2/\text{sec})$
for 3 mM Total Adipate at Low P_{CO_2} and
 25°C (Figure 5-5)

pH	$k(\text{cm}^2/\text{sec}) \times 10^9$	
	Calculated	Measured
4	16.7	17.4
5	6.2	8.1
6	0.89	1.3

Table B-11 Measured and Calculated Rate $k(\text{cm}^2/\text{sec})$
 for Reagent Grade CaCO_3 with Organic Acid
 Additives, pH 5, 25 °C, N_2 Sparging and
 0.1 M CaCl_2 (Figure 5-6)

Organic Acid	Concentration (mM)	$k(\text{cm}^2/\text{sec}) \times 10^9$	
		Measured	Calculated
Acrylic Acid	0	0.69	0.77
	2	1.9	1.7
	6	4.8	4.4
Sulfosuccinic Acid	0	0.82	0.77
	2	1.3	1.7
	5	3.8	3.4

Table B-12 Experimental Rate of Dissolution k (cm^2/sec)
 of Reagent Grade CaCO_3 with Organic Acid
 Additives, pH 5, 25°C, N_2 Sparging,
 0.1 M CaCl_2 (Figure 5-6)

Organic Acid	Concentration (mM)	Measured $k \times 10^9$ (cm^2/sec)
Sulfopropionic	0	0.69
	2	0.72
	10	0.27
Hydroxypyropionic	2	0.20
Polyacrylic	2 (meq)	0.12

Table B-13 Reagent Grade CaCO_3 Dissolution in the Presence of Dissolved Sulfite (Figure 5-7)

N_2 sparging, 25 °C

pH	Total Sulfite Concentration (mM)	k (cm^2/sec) $\times 10^9$	Measured	Calculated
4.5	0	1.9	1.9	
4.5	0.9	2.7	2.9	
4.5	3.0	2.9	3.3	
4.5	5.8	3.5	3.4	
4.5	8.7	3.4	3.4	
4.5	27.0	3.5	2.8	
4.5	38.0	2.8	2.4	
5.0	0	0.53	0.46	
5.0	0.9	1.3	1.7	
5.0	3.2	1.7	1.8	
5.0	6.3	1.7	1.6	
5.0	13.2	1.2	1.1	
5.0	20.0	0.60	0.73	
5.5	0	0.29	0.26	
5.5	1.0	1.0	0.93	
5.5	1.8	1.5	0.86	
5.5	2.6	1.5	0.75	
5.5	5.8	0.33	0.40	
5.75	0	0.14	0.18	
5.75	1.0	0.35	0.61	
5.75	1.7	0.18	0.51	
5.75	3.5	0.13	0.27	
6.0	0	0.14	0.13	
6.0	1.0	0.35	0.34	
6.0	1.4	0.18	0.27	
6.0	3.1	0.13	0.07	

N_2 sparging, 55 °C

5.0	0	1.2	1.3
5.0	0.7	1.7	2.6
5.0	2.8	2.6	2.7
5.0	5.8	2.7	2.3
5.0	11.1	1.7	1.6

Table B-14 Effects of Total Acetate and Sulfite on
Rate of Dissolution at 25°C (Figure 5-8)

N_2 sparging	3.0 mM Total Sulfite		
pH	Total Acetate Concentration (mM)	$k(cm^2/sec) \times 10^9$	
	Measured	Calculated	
5.0	0	1.7	1.7
5.0	1	2.3	2.2
5.0	3	3.5	3.1
5.0	6	4.6	3.9

APPENDIX C

THE FISHER TITRIMETER II TITRATION SYSTEM

The Fisher Titrimeter II Titration System consists of a burette/dispenser, an electrometer, and a titrate demand module. A linear two pen recorder is used to record the signals from the electrometer and burette/dispenser. The burette/dispenser is a 50 ml clear glass syringe which enables acid titrant to be added to the reactor at a continuous rate. The burette/dispenser refills after 50 ml is used.

The Fisher Electrometer Model 380 has controls for temperature 0/slope 0, standardize 0/zero 0, zero adjustment and mv/pH function. Four precision-calibrated scales are provided on the meter face for normal 0-14 pH measurements in the normal operating mode. The ± 5 , ± 3.5 , and ± 1 scales are employed for pH measurements in the expanded operating mode, and measure the pH deviation (± 5 , ± 3.5 , and ± 1 pH units full-scale, respectively) of a sample from a preset reference value.

The Fisher Titrate Demand Model 381 acts as a remote automatic proportional or on/off controller for the automatic dispenser system. Two end point settings which enable targets between zero and 19.99 be set to the closest 0.01 pH unit. The second endpoint setting is used only when dual-endpoint analysis are desired. A proportioning band control is used to set the endpoint deviation at

which proportioning will ensue. The rate of slow-down is always proportioning to the proximity of the endpoint target. The minimum delivery control places a lower limit on the extent to which the titrant delivery rate may be reduced by proportioning, and thus acts to enhance titration speed. The minimum delivery rate is maintained through approximately the final 5% of the proportioning band. When using the automatic demand module, the pH electrode act as a sensor for the titrate demand module. Acid titrant will be delivery if the pH is higher than the pre-set target endpoint. Acid delivery will be stopped once the target pH is reached. Signals from the burette/dispenser and the electrometer are sent to a two pen recorder where the pH and acid titrant volume are recorded versus time.

APPENDIX D

NOMENCLATURE

A,B - constants defined by equation 3.21 and 3.22

a - activity, M

a_j, b_j - characteristic parameters for each ion species
for estimation of activity coefficient

$\Delta[]$ - concentration difference between the limestone
surface and the bulk solution, M

D - diffusivity, cm^2/sec

D_o - dielectric constant of water

d - particle diameter, cm

F_a - Faraday Number, 23,062 cal/volt-equiv

f - fraction remaining of a given size fraction

F - total fraction remaining

ΔH - apparent heat of reaction, kcal/mol

I - ionic strength, M

k - dissolution rate constant, cm^2/sec

k_c - mass transfer coefficient, cm/sec

M - molar, gmol/liter

n_j - charge on the jth ion

P_{CO_2} - partial pressure of CO_2 , bar

pH - negative logarithm of hydrogen ion activity

ΔpH - pH at equilibrium minus solution pH

R - universal gas constant, 0.08205 liter-atm/gmol-K

R_o - diameter of sphere, cm

r - distance from center of sphere, cm

T - temperature, K

t - time, sec

t_{50} - time for 50% of CaCO_3 remaining, sec

t_{56} - time for 50% of CaCO_3 remaining, sec

U - activity coefficient for uncharged species

V - volume of particle, cm^3

x - dimensionless distance $(1-R_0/r)$

z_j - charge on the jth ion

β - rate of dissolution per unit radius, $\text{M cm}^2 \text{ sec}^{-1}$

α_i, β_i - constants of integration, $\text{M cm}^2 \text{ sec}^{-1}$

γ - activity coefficient

λ_o - equivalent ionic conductivity at infinite dilution
 $\text{cm}^2/\text{gmol/ohm}$

η - viscosity, poise

ϕ_i - the fraction of total particle mass with diameter
from d_i to d_{i+1}

[] - concentration, M

SUPERSCRIPT

o - ion pair, degrees

SUBSCRIPTS

b - bulk

cal - calculated

exp - experimented

s - surface

(s) - solid

APPENDIX E
FORTRAN PROGRAM LISTINGS

PROGRAM I

MASS TRANSFER MODEL WITH CO₂ FINITE RATE

REACTION

Program I calculates the rate of CaCO₃ dissolution with the reversible finite rate CO₂ differential equation and chemical equilibria relations given in Chapter III. The bulk solution compositions are calculated by specifying the solution pH, P_{CO₂}, Ca⁺⁺ concentration and particle diameter. By specifying a given range for β (the dissolution flux) and the [CaCO₃]_s, the CO₂ differential equation is solved numerically by a 4th-order Runge Kutta Method. Due to the nonlinearity of the equation, a trial and error on [H⁺] is made on each step size. The calculation stops when the [CO₂]_{bulk} converges to the specified value.

Input Data

Diffusivities, equilibrium and rate constants, P_{CO₂}, pH, particle diameter, [CaCO₃]_{surface}, and a guessed range for β .

Output Data

Echo prints input, β , rate of dissolution, and concentration profile of each chemical species versus the dimensionless distance, x.

PROGRAM LIMSDIS(TTY,INPUT=TTY,OUTPUT)

```

C*****THIS PROGRAM CALCULATE THE RATE OF LIMESTONE DISSOLUTION BY*****
C***** A MASS TRANSFER MODEL USING SPHERICAL GEOMETRY*****
C*****DIMENSION APH(10),APCO2(10)
DIMENSION ACTP(10),BCTP(10),ZI(10),GAMMA(15)
DIMENSION AC02(120)
DIMENSION CC03(120),CCAC03(120),CC02(120),CCA(120),CH(120)
DIMENSION CHC03(120),DX(120)
DIMENSION COH(120),CS03(120),CHS03(120),CAA(120),CH2A(120)
DIMENSION CHA(120)
COMMON/DIFF/DHC03,DC03,DH,DC02,DCA,DCAC03
COMMON/DIFF2/DS03,DHS03,DOH,DA,DH2A,DHA
COMMON/RATEK/K1,K2,K3,KF,KA1,KA2,KHS03,KW
COMMON/CONST/ALPH1,ALPH2,ALPH3,ALPH4,ALPH5
COMMON/CONSUR/HCO3S,C03S,CAS,HS,C02S
COMMON/RAD/RO,BETA
COMMON/EPS/EPS1,EPS2
COMMON/END/Y0,YF
COMMON/DRATE/KA,KB,KC
COMMON/COUNT/NJ
COMMON/INDEX/NK
COMMON/END2/Y01,YF1
COMMON/SURF/CC03,CCAC03,CC02,CCA,CH,CHC03,DX
COMMON/SURF2/COH,CS03,CHS03,CAA,CH2A,CHA
COMMON/CANC/C02,C03,HCO3,CAC03,H,CA,CAC03S
COMMON/CANC2/S03,HS03,OH,A,H2A,HA
COMMON/BULK/C02B,C03B,HCO3B,CAC03B,HB,CAB
COMMON/BULK2/S03B,HS03B,OHB,AB,H2AB,HAB
COMMON/ADD/KD
REAL K1,K2,K3,KW,KF,KA1,KA2,KHS03
REAL KD,KS

```

```

C*****DIFFUSIVITIES IN CM2/SEC*****
C*****CAC03S SURFACE CONCENTRATION OF ION PAIR AT*****
C*****SOLID LIQUID INTERPHASE*****

```

```

DATA DC02,DHC03,DC03,DCA/2.0E-5,1.2E-5,7.0E-6,7.9E-6/
DATA DH,DCAC03,CAC03S/9.3E-5,7.5E-6,6.204E-6/
DATA DS03,DHS03,DOH,DA/7.1E-6,1.19E-5,5.27E-5,7.05E-6/
DATA DH2A,DHA/1.19E-5,1.09E-5/
DATA KA1,KA2,KW,KHS03/3.548E-5,0.0,1.0E-14,6.24E-8/
DATA EPS1,EPS2/1.0E-6,1.0E-25/

```

```

C*****ERROR CRITERIA FOR CONVERGENCE*****
EPS1           EPS2
*****
```

```

C*****ACTP,BCTP ACTIVITIES COEFFICIENT PARAMETERS*****
C*****FOR MODIFIED DEBYE-HUCKEL EQUATION*****

```

```

DATA(ACTP    (I),I=1,9)/6.0,4.5,4.5,4.5,4.5,4.5,3.,3.,3./
DATA(BCTP    (I),I=1,9)/0.4,0.1,0.0,0.,0.,0.,0.3,0.3,0.3/

```

```

C*****HK      HENRY'S CONSTANT FOR CO2 IN WATER*****
C*****UI      EMPIRICAL CONSTANT FOR UNCHARGED SPECIES IN *****
C*****          DEBYE-HUCKEL EQUATION *****
C*****CI      IONIC STRENGTH OF SOLUTION *****
C*****ACONS,B TEMPERATURE CONSTANTS IN THE MODIFIED DEBYE-HUCKEL EQUATION*****
C*****ZI      IONIC VALENCIES *****

```

```

DATA HK,UI,CI,ACONS,B/0,0305,0,076,0,3,0,512,0,312/
DATA (ZI(I),I=1,9)/1.,2.,1.,2.,2.,1.,1.,2.,1./
DATA K1,K2,K3,KF/1,34E7,4,45E-7,6,3E-4,2,6E-2/
DATA KD/4,69E-11/
DATA KS/4,0E-4/

C*****INPUT DATA*****
C****AT      TOTAL BUFFER CONCENTRATION(GMOLES/LITER) *****
C****S03T    TOTAL SULFITE CONCENTRATION(GMOLES/LITER) *****
C****BETA1,BETA2 TRIAL INTERVALS FOR THE DISSOLUTION FLUX *****
C****(GMOLES-CM2/LITER-SEC) *****
C****NI      NUMBER OF PH AND PCO2 DATA PAIR *****
C****APCO2,APH   PH & PARTIAL PRESSURE OF CO2(ATM) *****
C****R0      PARTICLE DIAMETER(MICRO-METER) *****
C****CA      CALCIUM CONCENTRATION OF BULK SOLUTION *****
C****(GMOLES/LITER) *****
C*****ION PAIR *****
C*****ACTIVITY COEFFICIENTS*****COMPONENTS*****
C
C      GAMMA(1)          H+
C      GAMMA(2)          CA++
C      GAMMA(3)          HC03-
C      GAMMA(4)          CO3--
C      GAMMA(5)          SO3--
C      GAMMA(6)          HS03-
C      GAMMA(7)          OH-
C      GAMMA(8)          A--
C      GAMMA(9)          HA-
C      GAMMA(10)         CO2
C      GAMMA(11)         H2A
C      GAMMA(12)         CACO3(ION PAIR)

C*****ACTIVITY COEFFICIENTS*****COMPONENTS*****
C
21  GAMMA(I)=10.**(WA*(-WC/WB+CI*BCTP(I)))
DO 22 I=10,12
22  GAMMA(I)=10.**(UI*CI)
DO 3 J=1,NI
PH=APH(J)
PCO2=APCO2(J)
AH=10.**(-PH)
H=AH/GAMMA(1)
CO2=HK*PCO2
HB=H
CO2B=CO2
AACO2=CO2*GAMMA(10)
AHCO3=K2*AACO2/AH
HC03=AHCO3/GAMMA(3)
HC03B=HC03
ACO3=KD*AHCO3/AH
CO3=ACO3/GAMMA(4)

```

```

C03B=C03
ACA=CA*GAMMA(2)
CAB=CA
ACAC03=ACAC03/K3
CAC03=ACAC03/GAMMA(12)
CAC03B=CAC03
SKF=KF
SK1=K1
SK2=K2
SK3=K3
SKA1=KA1
SKD=KD
SKA2=KA2
SKHS03=KHS03
BETA1S=BETA1
BETA2S=BETA2

```

C*****REDEFINE EQUILIBRIUM AND RATE CONSTANT IN TERMS OF *****
C*****CONCENTRATIONS*****
C*****EQUILIBRIUM CONSTANT*****REACTION*****

```

C          K1           CACO3(ION PAIR) + H+ = CA++ + HC03-
C          K2           CO2 + H2O = H+ + HC03-
C          K3           CACO3(ION PAIR) = CA++ + CO3--
C          KHSO3        HS03- = H+ + SO3--
C          KW           H2O = H+ + OH-
C          KD           HC03- = H+ + CO3--
C          KS           CASO3(ION PAIR) = CA++ + SO3--
C          KA1          H2A = H+ + HA-
C          KA2          HA- = H+ + A--

```

C*****RATE CONSTANT***REACTION***
 C KF CO₂ + H₂O = H⁺ + HCO₃⁻

```

KF=KF*GAMMA(10)
K1=(K1*GAMMA(1)*GAMMA(12))/(GAMMA(2)*GAMMA(3))
K2=(K2*GAMMA(10))/(GAMMA(1)*GAMMA(3))
K3=K3*GAMMA(12)/(GAMMA(2)*GAMMA(4))
KHS03=(KHS03*GAMMA(6))/(GAMMA(5)*GAMMA(1))
KHS03=KHS03*(1.+GAMMA(2)*GAMMA(5))*CA/(GAMMA(12)*KS)
KW=KW/(GAMMA(1)*GAMMA(7))
KD=KD*GAMMA(3)/(GAMMA(1)*GAMMA(4))

```

```

DHB=KW/HB
HAB=AT/(1.+HB/KA1+KA2/HB)
H2AB=HAB*HB/KA1
AB=AT-HAB-H2AB
S03B=KHS03*KS03T/(HB+KHS03)
HS03B=S03T-S03B
PRINT 234
234 FORMAT(1H1,6X,*INPUT DATA*,//,6X,*DIFFUSIVITIES(CM2/SEC)*,/)
PRINT 235
235 FORMAT(10X,*C02*,11X,*HC03-* ,11X,*CO3-* ,11X,*CA+-*,13X,*HH*,9X,
1*CACO3(ION PAIR)*,/)
PRINT 102,DC02,DHC03,DC03,DCA,DH,DCACO3
PRINT 236
236 FORMAT(10X,*OH-* ,11X,*S03-* ,11X,*HS03-* ,11X,*A--*,11X,*H2A*,11X,
1*HA-*,/)
PRINT 102,DOH,DS03,DHS03,DA,DH2A,DHA
102 FORMAT(3X,6E15.3,/)
PRINT 237
237 FORMAT(10X,*K1*,14X,*K2*,14X,*K3*,14X,*KF*,/)
PRINT 103,K1,K2,K3,KF
PRINT 238

```

```

238 FORMAT(10X,*KA1*,14X,*KA2*,14X,*KW*,/)
PRINT 103,KA1,KA2,KW
103 FORMAT(3X,4E15.4,/)
PRINT 251
251 FORMAT(10X,*PH*,11X,*PCO2(ATM.)*,5X,*PARTICLE DIAMETER(CM)*,/)
PRINT 105,PH,PCO2,R0
105 FORMAT(3X,3E15.3)
BETA=BETA1
111 FORMAT(6X,E15.4)
CALL CONVERG(S)
PRINT 111,S
S1=S
BETA=BETA2
CALL CONVERG(S)
PRINT 111,S
S2=S
F1=S1-CO2B
F2=S2-CO2B
IF(F1*F2.GT.0.) GO TO 50
FSAVE=F1
DO 32 JJ=1,30
TRUEB=BETA2-F2*(BETA2-BETA1)/(F2-F1)
BETA=TRUEB
CALL CONVERG(S)
PRINT 111,S
FW=S-CO2B
ERR=ABS((BETA1-BETA2)/BETA1)/2.
IF(ERR.LE.0.001) GO TO 60
IF(ABS(FW).LE.1.0E-8) GO TO 60
IF(FW*F1.LT.0.) GO TO 31
BETA1=TRUEB
F1=FW
IF(FW*FSAVE.GT.0.) F2=F2/2.
FSAVE=FW
GO TO 32
31 BETA2=TRUEB
F2=FW
IF(FW*FSAVE.GT.0.) F1=F1/2.
FSAVE=FW
32 CONTINUE
GO TO 60
50 PRINT 33
33 FORMAT(1HO,10X,*NO CONVERGENCE*,/)
GO TO 200
60 CONTINUE
PRINT 239
239 FORMAT(//,6X,*OUTPUT DATA*,/,1X,*1ST LINE*,4X,*X*,11X,*CO2*,11X,
1*HC03-* ,11X,*CO3--*,11X,*CA++*,13X,*H+*,6X,*CAC03(ION PAIR)*)
PRINT 240
240 FORMAT(//,1X,*2ND LINE*,15X,*OH-* ,11X,*SO3-* ,11X,*HS03-* ,11X,
1*HA-* ,11X,*H2A*,11X,*HA-* ,//)
DO 34 I=1,101,5
PRINT 35,DX(I),CC02(I),CHC03(I),CC03(I),CCA(I),CH(I),CCAC03(I)
PRINT 38,COH(I),CS03(I),CHS03(I),CAA(I),CH2A(I),CHA(I)
38 FORMAT(21X,6E15.5)
35 FORMAT(6X,7E15.5)
34 CONTINUE
PRINT 37,TRUEB
37 FORMAT(3X,E15.4)
RATEII=-TRUEB/(1000.*R0)
PRINT 36,RATED
36 FORMAT(3X,*RATE OF DISSOLUTION=*,E15.5,*MOLE/SQ.CM SEC*,/)
DCC02=CC02(1)-CC02(101)
DCHC03=CHC03(1)-CHC03(101)
DCCA=CCA(1)-CCA(101)
DCH=CH(1)-CH(101)

```

```

DCCACO=CCACO3(1)-CCACO3(101)
DCCO3=CO3(1)-CCO3(101)
DCOH=COH(1)-COH(101)
DCSO3=CSO3(1)-CSO3(101)
DCHSO3=CHSO3(1)-CHSO3(101)
DCCAA=CAA(1)-CAA(101)
DCH2A=CH2A(1)-CH2A(101)
DCHA=CHA(1)-CHA(101)
DIC02=DCO2*DCC02
DIHC03=DHC03*DCHC03
DICA=DCA*DCCA
DIH=DH*DCH
DICACO=DCCACO*DCACO3
DICO3=DCO3*ICCO3
DIOH=DOH*DCOH
DISO3=DSO3*DCS03
DIHSO3=DHSO3*DCHSO3
DIAA=DCCAA*DIA
DIH2A=DH2A*DCH2A
DIHA=DHA*DCHA
PRINT 11
11 FORMAT(//,6X,*DIFFERENCE BETWEEN SURFACE & BULK CONCENTRATION
1 FOR EACH SPECIES(GMOLE/LITER)*,/)
PRINT 38,DCCO2,DIHC03,DCCO3,DCCA,DCH,DCCACO
PRINT 38,DCOH,DCSO3,DCHSO3,DCCAA,DCH2A,DCHA
PRINT 12
12 FORMAT(//,6X,*FLUX CONTRIBUTION FOR EACH SPECIES(GMOLE-CM2/LITER-S
1EC)*,/)
PRINT 38,DIC02,DIHC03,DICO3,DICA,DIH,DICACO
PRINT 38,DIOH,DISO3,DIHSO3,DIAA,DIH2A,DIHA
CA=CAB
KD=SKD
K1=SK1
K2=SK2
K3=SK3
KF=SKF
KA1=SKA1
KA2=SKA2
KHSO3=SKHSO3
BETA1=BETA1S
BETA2=BETA2S
3 CONTINUE
200 STOP
END
SUBROUTINE SURCONE(BETA,HYS)
```

C*****SURCONE CALCULATE THE CONCENTRATION OF SPECIES AT THE LIMESTONE
 C*****SURFACE
 C*****BY THE SPECIFIED CACO3(ION PAIR) CONCENTRATION AT THE LIMESTONE
 C*****INTERPHASE

```

COMMON/CONST/ALPH1,ALPH2,ALPH3,ALPH4,ALPH5
COMMON/CONSUR/HCO3S,C03S,CAS,HS,C02S
COMMON/AID/KD
COMMON/CANC/C02,C03,HCO3,CACO3,H,CA,CACO3S
COMMON/CANC2/S03,HS03,OH,A,H2A,HA
COMMON/DIFF/DHC03,DC03,DH,DCO2,DCA,DCACO3
COMMON/DIFF2/DSO3,DHSO3,DOH,DA,DH2A,DHA
COMMON/BULK/C02B,C03B,HCO3B,CACO3B,HB,CAB
COMMON/BULK2/S03B,HS03B,OHB,AB,H2AB,HAB
COMMON/EPS/EPS1,EPS2
COMMON/RATEK/K1,K2,K3,KF,KA1,KA2,KHSO3,KW
REAL K1,K2,K3,KA1,KA2,KHSO3,KW
ALPH1=DCO2*C02B+DHCO3*HC03B+DCACO3*CACO3B+DCO3*C03B-BETA
ALPH2=DCA*CAB+DCACO3*CACO3B-BETA
ALPH3=DH*HB+DHCO3*HC03B+2.*DCO2*C02B+DHA*HAB+2.*DH2A*H2AB-DOH
```

```

1*DHB-D503*S03B
ALPH4=DH2A*K2AB+DHA*KAB+DA*KAB
ALPH5=DHS03*KHS03B+D503*S03B
CAS=(ALPH2-DCAC03*CAC03S)/DCA
C03S=K3*CAC03S/CAS
W=DC03*C03S+DCAC03*CAC03S
H1=HB
H2=HB/1000.
CALL CALC(H1,F1,W)
CALL CALC(H2,F2,W)
IF(F1*F2.GT.0.) GO TO 50
FSAVE=F1
DO 20 J=1,30
H=H2-F2*(H2-H1)/(F2-F1)
CALL CALC(H,FW,W)
ERR=ABS((H1-H2)/H1)/2.
IF(ERR.LE.EPS1) GO TO 60
IF(ABS(FW).LE.EPS2) GO TO 60
IF(FW*F1.LT.0.) GO TO 10
H1=H
F1=FW
IF(FW*FSAVE.GT.0) F2=F2/2.
FSAVE=FW
GO TO 20
10 H2=H
F2=FW
IF(FW*FSAVE.GT.0) F1=F1/2.
FSAVE=FW
20 CONTINUE
50 PRINT 3
3 FORMAT(1HO,10X,*SURCONE DO NOT CONVERGE*,/)
60 CALL CALC(H,F,W)
HYS=H
RETURN
END
SUBROUTINE CALC(HY,F,W)

```

*****THE SUBROUTINE CALC EVALUATE THE CO₂ SURFACE CONCENTRATION

```

COMMON/DIFF/DHC03,DC03,DH,DC02,DCA,DCAC03
COMMON/DIFF2/D503,DHS03,D0H,DA,DH2A,DHA
COMMON/RATEK/K1,K2,K3,KF,KA1,KA2,KHS03,KW
COMMON/CONST/ALPH1,ALPH2,ALPH3,ALPH4,ALPH5
COMMON/CANC/C02,C03,HCO3,CAC03,H,CA,CAC03S
COMMON/ADD/KD
COMMON/CONSUR/HCO3S,C03S,CAS,HS,C02S
COMMON/RAD/RD,BETA
REAL KA1,KA2,KHS03,KW,K1,K2,K3
REAL KD
H=HY
OH=KW/H
H2A=ALPH4/(DH2A*(1.+DHA*KA1/(DH2A*KH)+KA1*KA2*DA/(DH2A*KH)))
HA=KA1*KH2A/H
A=KA1*KA2*KH2A/(KH)
HS03=ALPH5/(DHS03+D503*KHS03/H)
S03=KHS03*KHS03/H
HCO3=K1*KH*CAC03S/CAS
C03=KD*KHCO3/H
C02=(ALPH1-W-DHC03*HCO3)/DC02
C02S=C02
F=DH*KH+DHA*KH+2.*DH2A*KH2A-D0H*KH-D503*S03-2.*W-DHC03*HCO3-ALPH3+
12.*ALPH1
RETURN
END
SUBROUTINE FIND(HYD0,X)

```

C*****SUBROUTINE FIND CALCULATE THE CONCENTRATION OF SPECIES USING
C*****HYDROGEN CONCENTRATION CALCULATE IN SUBROUTINE CONVERG

```

COMMON/DIFF/DHC03,DC03,OH,DC02,DCA,DCAC03
COMMON/DIFF2/DS03,DHS03,DOH,DA,DH2A,DHA
COMMON/RATEK/K1,K2,K3,KF,KA1,KA2,KHS03,KW
COMMON/ADD/KD
COMMON/CANC/C02,C03,HCO3,CACO3,H,CA,CAC03S
COMMON/CANC2/S03,H03,OH,A,H2A,HA
COMMON/CONST/ALPH1,ALPH2,ALPH3,ALPH4,ALPH5
COMMON/RAD/RO,BETA
REAL K1,K2,K3,KA1,KA2,KHS03,KW
REAL KD
H=HYD0
OH=KW/H
H2A=ALPH4/(DH2A*(1.+DHA*KA1/(DH2A*H)+KA1*KA2*DA/(DH2A*KH*H)))
A=KA1*KA2*KH2A/(H*H)
HA=KA1*KH2A/H
HS03=ALPH5/(DHS03+DS03*KHS03/H)
S03=KHS03*KHS03/H
HC03=(ALPH3-DH*H-2.*DC02*C02-DHA*HA-2.*DH2A*KH2A+DOH*KOH+
1*DS03*S03)/DHC03
C03=KD*HC03/H
CAC03=(ALPH2+BETAXX)/(DCA*K3/C03+DCAC03)
CA=(ALPH2+BETAXX-DCAC03*CAC03)/DCA

RETURN
END
SUBROUTINE CONVERG(S)

```

C*****SUBROUTINE CONVERG EMPLOYS SUBROUTINES SURCONE,SIMPKUT,ROOT, & FIND
C*****UNTIL CONVERGENCE FOR BETA SATISFIED THE CALCULATED BULK
C*****CONCENTRATION OF C02 IN THE SOLUTION

```

DIMENSION ZA(15,4),ZB(15,1),T(4,1),WK(10)
DIMENSION CC03(120),CCAC03(120),CC02(120),CCA(120),CH(120)
DIMENSION CHCO3(120),DX(120)
DIMENSION COH(120),CS03(120),CHS03(120),CAA(120),CH2A(120)
DIMENSION CHA(120)
COMMON/CANC/C02,C03,HCO3,CACO3,H,CA,CAC03S
COMMON/CANC2/S03,H03,OH,A,H2A,HA
COMMON/RATEK/K1,K2,K3,KF,KA1,KA2,KHS03,KW
COMMON/ADD/KD
COMMON/SURF/CC03,CCAC03,CC02,CCA,CH,CHCO3,DX
COMMON/COUNT/NJ
COMMON/SURF2/COH,CS03,CHS03,CAA,CH2A,CHA
COMMON/INDEX/NK
COMMON/EPS/EPS1,EPS2
COMMON/END/Y0,YF
COMMON/CONST/ALPH1,ALPH2,ALPH3,ALPH4,ALPH5
COMMON/RAD/RO,BETA
COMMON/DIFF/DHC03,DC03,OH,DC02,DCA,DCAC03
COMMON/END2/Y01,YF1
COMMON/DKRATE/KA,KB,KC
COMMON/BULK/C02B,C03B,HCO3B,CACO3B,HB,CAB
COMMON/CONSUR/HCO3S,C03S,CAS,HS,C02S
REAL KA,KB,KC
REAL K1,K2,K3,KA1,KA2,KHS03,KW
CALL SURCONE(BETA,HS)
YF=HS*3,
Y0=HS/3,
AO=0,
BO=C02S
CO=0,
STEP=0.01
I=0
-----
```

```

42 CALL SIMPKUT(A0,B0,CO,STEP,CONC,FLUX,A14,A11,B11,C11,I)
NJ=NJ+1
A0=A11+STEP
B0=B11+CONC
CO=C11+FLUX
IF(A14.LE.0.87) GO TO 42
DO 50 I=1,15
ZA(I,1)=1.
ZA(I,2)=DX(I+70)
ZA(I,3)=DX(I+70)**2
ZA(I,4)=DX(I+70)**3
ZB(I,1)=CC02(I+70)
50 CONTINUE
CALL OFIMA3(ZA,15,ZB,15,15,1,4,T,4,WK,IER)
DIST=0.84
DO 10 J=86,101
DX(J)=DIST+0.01
DIST=DX(J)
CC02(J)=((T(4,1)*DX(J)+T(3,1))*DX(J)+T(2,1))*DX(J)+T(1,1)
X=DX(J)
C02=CC02(J)
CALL ROOT(X,C02)
CC03(J)=C03
CCAC03(J)=CAC03
CHC03(J)=HC03
CH(J)=H
CCA(J)=CA
COH(J)=OH
CS03(J)=S03
CHS03(J)=HS03
CAA(J)=A
CH2A(J)=H2A
CHA(J)=HA
S=CC02(101)
10 CONTINUE
RETURN
END
SUBROUTINE SIMPKUT(A0,B0,CO,STEP,CONC,FLUX,A14,A11,B11,C11,I)

*****SIMPKUT APPLY THE 4TH-ORDER RUNGE KUTTA METHOD TO SOLVE THE 2ND
*****ORDER CO2 DIFFERENTIAL RATE EQUATION

DIMENSION CC03(120),CCAC03(120),CC02(120),CCA(120),CH(120)
DIMENSION CHC03(120),DX(120)
DIMENSION COH(120),CS03(120),CHS03(120),CAA(120),CH2A(120)
DIMENSION CHA(120)
COMMON/DIFF/DHC03,DC03,DH,DC02,DCA,DCAC03
COMMON/DIFF2/DS03,DHS03,DOH,DA,DH2A,DHA
COMMON/RATEK/K1,K2,K3,KF,KA1,KA2,KHS03,KW
COMMON/CONST/ALPH1,ALPH2,ALPH3,ALPH4,ALPH5
COMMON/RAD/RO,BETA
COMMON/END/Y0,YF
COMMON/COUNT/NJ
COMMON/CANC/C02,C03,HC03,CAC03,H,CA,CAC03S
COMMON/CANC2/S03,HS03,OH,A,H2A,HA
COMMON/SURF/CC03,CCAC03,CC02,CCA,CH,CHC03,DX
COMMON/SURF2/COH,CS03,CHS03,CAA,CH2A,CHA
COMMON/ADD/KD
REAL K1,K2,K3,KF,KA1,KA2,KHS03,KW
A11=A0
A12=A11+STEP/2.
A13=A12
A14=A11+STEP
B11=B0
C11=CO
CALL ROOT(A11,B11)

```

```

D11=-KF*(H*HC03/K2-B11)/(DC02*(1.-A11)**4/(RO*RO))
I=I+1
DX(I)=A11
CC02(I)=B11
CHC03(I)=HC03
CC03(I)=CO3
CCA(I)=CA
CH(I)=H
CCAC03(I)=CAC03
COH(I)=OH
CS03(I)=S03
CHS03(I)=HS03
CAA(I)=A
CH2A(I)=H2A
CHA(I)=HA
B12=B11+C11*STEP/2,
C12=C11+D11*STEP/2,
CALL ROOT(A11,B11)
D12=-KF*(H*HC03/K2-B12)/(DC02*(1.-A12)**4/(RO*RO))
B13=B11+C12*STEP/2,
C13=C11+D12*STEP/2,
CALL ROOT(A11,B11)
D13=-KF*(H*HC03/K2-B13)/(DC02*(1.-A13)**4/(RO*RO))
B14=B11+C13*STEP
C14=C11+D13*STEP
CALL ROOT(A11,B11)
D14=-KF*(H*HC03/K2-B14)/(DC02*(1.-A14)**4/(RO*RO))
CONC=STEP/6.*(C11+C12*2.+2.*C13+C14)
FLUX=STEP/6.*(B11+2.*D12+2.*D13+D14)
RETURN
END
SUBROUTINE ROOT(X,CAB0)

```

*****ROOT IS A MODIFIED HALVE-INTERVAL METHOD USE TO EVALUATED THE
 *****SOLUTION COMPOSITON ONCE A CO₂ COMPOSITION IS CALCULATE BY
 *****SIMPKUT
 *****THE INTERVAL OF H⁺ CONCENTRATION BETWEEN THE BULK & SURFACE
 *****ARE USED

```

COMMON/END/YO,YF
COMMON/EPS/EPS1,EPS2
COMMON/CONST/ALPH1,ALPH2,ALPH3,ALPH4,ALPH5
COMMON/RAD/RO,BETA
COMMON/DIFF/DHC03,DC03,DH,DC02,DCA,DCAC03
COMMON/DIFF2/DS03,DHS03,DOH,DA,DH2A,DHA
COMMON/RATEK/K1,K2,K3,KF,KA1,KA2,KHS03,KW
COMMON/CANC/C02,CO3,HC03,CAC03,H,CA,CAC03S
COMMON/ADD/KD
COMMON/CANC2/S03,HS03,DH,A,H2A,HA
REAL K1,K2,K3,KF,KA1,KA2,KHS03,KW
REAL KD
CO2=CAB0
E=ALPH3-ALPH1-BETAXX
H1=YO
CALL FIND(H1,X)
F1=DH*K1+DC02*CO2+DHAKA+2.*DH2A*KH2A-DOH*OH-DS03*S03-DCAC03*CAC03-
1DC03*CO3-E
H2=YF
CALL FIND(H2,X)
F2=DH*K2+DC02*CO2+DHAKA+2.*DH2A*KH2A-DOH*OH-DS03*S03-DCAC03*CAC03-
1DC03*CO3-E
IF(F1*F2,GT,0.) GO TO 50
FSAVE=F1
DO 20 J=1,30
H=H2-F2*(H2-H1)/(F2-F1)

```

```
H3=H
CALL FIND(H3,X)
FW=DH*X+DC02*C02+DHA*HA+2.*DH2A*H2A-DOH*OH-DS03*S03-DCAC03*CAC03
1-DC03*C03-E
ERR=ABS((H1-H2)/H1)/2.
IF(ERR.LE.EPS1) GO TO 60
IF(ABS(FW),LE,EPS2) GO TO 60
IF(FW*F1,LT,0.) GO TO 10
H1=H
F1=FW
IF(FW*FSAVE,GT,0.) F2=F2/2,
FSAVE=FW
GO TO 20
10 H2=H
F2=FW
IF(FW*FSAVE,GT,0.) F1=F1/2,
FSAVE=FW
20 CONTINUE
50 PRINT 3
3 FORMAT(1HO,10X,*NO SOLUTION IN THE RANGE FOR ROOT*,/)
GO TO 63
40 HNG=H
CALL FIND(HNG,X)
Y0=H/2.
YF=H*2.
63 RETURN
END
```

PROGRAM II

MASS TRANSFER MODEL NEGLECTING CO₂ REACTION

Program II is a modification of program I. It neglects the CO₂ finite rate reaction by assuming [CO₂]_{surface} = [CO₂]_{bulk}. This program simulates rate data at low P_{CO₂} since CO₂ reaction is insignificant. It also saves computer time and has better convergence.

Input and output as in program I

```

PROGRAM LIMSDIS(TTY,INPUT=TTY,OUTPUT)

*****THIS PROGRAM CALCULATE THE RATE OF LIMESTONE DISSOLUTION BY*****
***** A MASS TRANSFER MODEL USING SPHERICAL GEOMETRY*****
*****DIMENSION APH(10),APCO2(10)
DIMENSION ACTP(10),BCTP(10),ZI(10),GAMMA(15)
DIMENSION AC02(120)
DIMENSION CC03(120),CAC03(120),CC02(120),CAA(120),CH(120)
DIMENSION CHC03(120),DX(120)
DIMENSION COH(120),CS03(120),CHS03(120),CAA(120),CH2A(120)
DIMENSION CHA(120)
COMMON/DIFF/DHC03,DC03,DH,DC02,DCA,DCAC03
COMMON/DIFF2/DS03,DHS03,DOH,DA,DH2A,DHA
COMMON/RATEK/K1,K2,K3,KF,KA1,KA2,KHS03,KW
COMMON/CONST/ALPH1,ALPH2,ALPH3,ALPH4,ALPH5
COMMON/CONSUR/HCO3S,C03S,CAS,HS,C02S
COMMON/RAI/RO,BETA
COMMON/EPS/EPS1,EPS2
COMMON/END/Y0,YF
COMMON/DRATE/KA,KB,KC
COMMON/COUNT/NJ
COMMON/INDEX/NK
COMMON/END2/Y01,YF1
COMMON/SURF/CC03,CCAC03,CC02,CAA,CH,CHC03,DX
COMMON/SURF2/COH,CS03,CHS03,CAA,CH2A,CHA
COMMON/CANC/C02,C03,HCO3,CAC03,H,CA,CAC03S
COMMON/CANC2/S03,HS03,OH,A,H2A,HA
COMMON/BULK/C02B,C03B,HCO3B,CAC03B,HB,CAB
COMMON/BULK2/S03B,HS03B,OHB,AB,H2AB,HAB
COMMON/ADD/KD
REAL K1,K2,K3,KW,KF,KA1,KA2,KHS03
REAL KD,KS

*****DIFFUSIVITIES IN CM2/SEC*****
*****CAC03S SURFACE CONCENTRATION OF ION PAIR AT*****
*****SOLID LIQUID INTERPHASE*****

DATA DC02,DHC03,DC03,DCA/2.0E-5,1.2E-5,7.0E-6,7.9E-6/
DATA DH,DCAC03,CAC03S/9.3E-5,7.5E-6,6.204E-6/
DATA DS03,DHS03,DOH,DA/3.85E-6,1.19E-5,5.27E-5,7.05E-6/
DATA DH2A,DHA/1.19E-5,1.09E-5/
DATA KA1,KA2,KW,KHS03/4.02E-5,0.0,1.0E-14,6.24E-8/
DATA EPS1,EPS2/1.0E-6,1.0E-25/

*****ERROR CRITERIA FOR CONVERGENCE*****
EPS1           EPS2           *****

*****ACTP,BCTP ACTIVITIES COEFFICIENT PARAMETERS*****
*****FOR MODIFIED DEBYE-HUCKEL EQUATION***** 

DATA(ACTP  (I),I=1,9)/6.0,4.5,4.5,4.5,4.5,4.5,3.,3.,3./
DATA(BCTP  (I),I=1,9)/0.4,0.1,0.0,0.,0.,0.,0.3,0.3,0.3/

*****HK      HENRY'S CONSTANT FOR CO2 IN WATER*****
*****U1      EMFIRICAL CONSTANT FOR UNCHARGED SPECIES IN *****
*****          DEBYE-HUCKEL EQUATION *****
*****CI      IONIC STRENGTH OF SOLUTION *****
*****ACONS,B TEMPERATURE CONSTANTS IN THE MODIFIED *****
*****          DEBYE-HUCKEL EQUATION*****

```

```

*****ZI          IONIC VALENCIES      *****
DATA HK,UI,CI,ACONS,B/0.0305,0.076,0.3,0.512,0.312/
DATA (ZI(I),I=1,9)/1.,2.,1.,2.,2.,1.,1.,2.,1./
DATA K1,K2,K3,KF/1.34E7,4.45E-7,6.3E-4,2.6E-2/
DATA KB/4.69E-11/
DATA KS/4.0E-4/

*****INPUT DATA*****
*****AT          TOTAL BUFFER CONCENTRATION(GMOLES/LITER) *****
*****S03T        TOTAL SULFITE CONCENTRATION(GMOLES/LITER) *****
*****BETA1,BETA2 TRIAL INTERVALS FOR THE DISSOLUTION FLUX *****
*****          (GMOLES-CM2/LITER-SEC) *****
*****NI          NUMBER OF PH AND PCO2 DATA PAIR *****
*****APCO2,APH  PH & PARTIAL PRESSURE OF CO2(ATM) *****
*****RO          PARTICLE DIAMETER(MICRO-METER) *****
*****CA          CALCIUM CONCENTRATION OF BULK SOLUTION *****
*****          (GMOLES/LITER) *****
*****READ,AT,S03T
*****READ,BETA1,BETA2
*****READ, NI
*****READ, CA,RO
*****DO 2 K=1,NI
*****READ ,APCO2(K),APH(K)
2  CONTINUE
*****DO 21 I=1,9
*****WA=ACONS*ZI(I)*ZI(I)
*****WC=SQRT(CI)
*****WB=1.+B*ACTP(I)*WC

*****ACTIVITY COEFFICIENTS*****COMPONENTS*****
C      GAMMA(1)          H+
C      GAMMA(2)          CA++-
C      GAMMA(3)          HC03-
C      GAMMA(4)          CO3--_
C      GAMMA(5)          SO3--_
C      GAMMA(6)          HS03-
C      GAMMA(7)          OH-
C      GAMMA(8)          A--_
C      GAMMA(9)          HA-
C      GAMMA(10)         CO2
C      GAMMA(11)         H2A
C      GAMMA(12)         CACO3(ION PAIR)

*****21  GAMMA(I)=10.**(WA*(-WC/WB+CI*BCTP(I)))
*****22  GAMMA(I)=10.**(UI*CI)
*****DO 3 J=1,NI
*****PH=APH(J)
*****PCO2=APCO2(J)
3  CONTINUE
*****AH=10.**(-PH)
*****H=AH/GAMMA(1)
*****CO2=HK*PCO2
*****HE=H
*****CO2B=CO2
*****AACO2=CO2*GAMMA(10)
*****AHCO3=K2*AACO2/AH
*****HC03=AHCO3/GAMMA(3)
*****HC03B=HC03

```

```

ACO3=K1*AHCO3/AH
CO3=ACO3/GAMMA(4)
CO3B=CO3
ACA=CA*GAMMA(2)
CAB=CA
ACACO3=ACA*ACO3/K3
CACO3=ACACO3/GAMMA(12)
CACO3B=CACO3

C*****REDEFINE EQUILIBRIUM AND RATE CONSTANT IN TERMS OF *****
C*****CONCENTRATIONS*****EQUILIBRIUM CONSTANT*****REACTION*****
C
      K1          CACO3(ION PAIR) + H+ = CA++ + HC03-
C      K2          CO2 + H2O = H+ + HC03-
C      K3          CACO3(ION PAIR) = CA++ + CO3--
C      KHS03       HS03- = H+ + SO3--
C      KW          H2O = H+ + OH-
C      KD          HC03- = H+ + CO3--
C      KS          CASO3(ION PAIR) = CA++ + SO3--
C      KA1         H2A = H+ + HA-
C      KA2         HA- = H+ + A--
C

C*****RATE CONSTANT*****REACTION*****
C      KF          CO2 + H2O = H+ + HC03-
C

KF=KF*GAMMA(10)
K1=(K1*GAMMA(1)*GAMMA(12))/(GAMMA(2)*GAMMA(3))
K2=(K2*GAMMA(10))/(GAMMA(1)*GAMMA(3))
K3=K3*GAMMA(12)/(GAMMA(2)*GAMMA(4))
RKHS03=(KHS03*GAMMA(6))/(GAMMA(5)*GAMMA(1))
KHS03=RKHS03*(1.+GAMMA(2)*GAMMA(5)*CA/(GAMMA(12)*KS))
KW=KW/(GAMMA(1)*GAMMA(7))
KD=KD*GAMMA(3)/(GAMMA(1)*GAMMA(4))
DHB=KW/HB
HAB=AT/(1.+HB/KA1+KA2/HB)
H2AB=HAB*HB/KA1
AB=AT-HAB-H2AB
SO3B=KHS03*SO3T/(HB+KHS03)
HS03B=SO3T-SO3B
PRINT 234
234 FORMAT(1H1,6X,*INPUT DATA*,//,6X,*DIFFUSIVITIES(CM2/SEC)*,/)
PRINT 235
235 FORMAT(10X,*CO2*,11X,*HC03-* ,11X,*CO3--*,11X,*CA++*,13X,*H*,9X,
1*CACO3(ION PAIR)*,/)
PRINT 102,DCO2,DHC03,DCO3,DCA,DH,DCACO3
PRINT 236
236 FORMAT(10X,*OH-* ,11X,*SO3--*,11X,*HS03-* ,11X,*A--*,11X,*H2A*,11X,
1*XHA-*),/
PRINT 102,DOH,DSO3,DHS03,DA,DH2A,DHA
102 FORMAT(3X,6E15.3,/)
PRINT 237
237 FORMAT(10X,*K1*,14X,*K2*,14X,*K3*,14X,*KF*,/)
PRINT 103,K1,K2,K3,KF
PRINT 238
238 FORMAT(10X,*KA1*,14X,*KA2*,14X,*KW*,12X,*KHS03*,/)
PRINT 103,KA1,KA2,KW,KHS03
103 FORMAT(3X,4E15.4,/)
PRINT 251
251 FORMAT(10X,*PH*,11X,*PCO2(ATM.)*,5X,*PARTICLE DIAMETER(CM)*,/)
PRINT 105,PH,PCO2,R0
105 FORMAT(3X,3E15.3)
PRINT 239

```

```

239 FORMAT(7X,*OUTPUT*,//,6X,*BULK CONCENTRATIONS(G-MOLE/L)*,/)
PRINT 235
PRINT 102,C02B,HC03B,C03B,CAB,HB,CAC03B
PRINT 236
PRINT 102,OHB,S03B,HS03B,AB,H2AB,HAB
CALL SURCONE(BETA1)
CALL PHI(CAC03,CAC03S,SIDE1)
CALL SURCONE(BETA2)
CALL PHI(CAC03,CAC03S,SIDE2)
IF(SIDE1*SIDE2.GT.1.) GO TO 187
M=0
120 BETA=(BETA2+BETA1)/2+
CALL SURCONE(BETA)
CALL PHI(CAC03,CAC03S,SIDEN)
IF(SIDE1*SIDEN.LT.1.) BETA2=BETA
IF(SIDE2*SIDEN.LT.1.) BETA1=BETA
DELT=ABS((BETA1-BETA2)/BETA1)
IF(DELT.LT.0.0003) GO TO 188
IF (M.EQ.25) GO TO 187
M=M+1
GO TO 120
188 PRINT 241
241 FORMAT(13X,*SURFACE CONCENTRATION(G-MOLE/L)*,/)
PRINT 235
PRINT 102,C02,HC03,C03,CA,H,CAC03
PRINT 236
PRINT 102,OH,S03,HS03,A,H2A,HA
PRINT 37,BETA
37 FORMAT(//,3X,E15,4)
RATED=-BETA/(1000.*R0)
PRINT 36,RATED
36 FORMAT(//,3X,*RATE OF DISSOLUTION=*,E15,5,*G-MOLE/SQ.CM SEC*,/)
DCC02=C02-C02B
DCHC03=HC03-HC03B
DCCA=CA-CAB
DCH=H-HB
DCCACO=CAC03-CAC03B
DCC03=C03-C03B
DCOH=OH-OHB
DCS03=S03-S03B
DCHS03=HS03-HS03B
DCCAA=A-AB
DCH2A=H2A-H2AB
DCHA=HA-HAB
DICO2=DC02*DCC02
DIHC03=DHC03*DCHC03
DICA=DCA*DCCA
DIH=DH*DCH
DICACO=DCCACO*DCAC03
DICO3=DC03*DCC03
DIOH=DOH*DCOH
DIS03=DS03*DCS03
DIHS03=DHS03*DCHS03
DIAA=DCCAA*DA
DIH2A=DH2A*DCH2A
DIHA=DHA*DCHA
PRINT 11
11 FORMAT(//,6X,*DIFFERENCE BETWEEN SURFACE AND BULK CONCENTRATION
FOR EACH CHEMICAL SPECIES*,/)
PRINT 235
PRINT 102,DCC02,DCHC03,DCC03,DCCA,DCH,DCCACO
PRINT 236
PRINT 102,DCOH,DCS03,DCHS03,DCCAA,DCH2A,DCHA
PRINT 12
12 FORMAT(//,6X,*FLUX CONTRIBUTION FOR EACH SPECIES*,/)
PRINT 235

```

```

PRINT 102,DIC02,DIHC03,DIC03,DICA,DIH,DICACO
PRINT 236
PRINT 102,DI0H,DIS03,DIHS03,DIAA,DIH2A,DIHA
187 STOP
END

SUBROUTINE PHI(CAC03,CAC03S,SIDE)
IF(CAC03.LT.CAC03S) SIDE=1
IF(CAC03.GT.CAC03S) SIDE=-1
RETURN
END
SUBROUTINE SURCONE(BETA)
COMMON/CONST/ALPH1,ALPH2,ALPH3,ALPH4,ALPH5
COMMON/CONSUR/HC03S,C03S,CAS,HS,C02S
COMMON/CANC/C02,C03,HC03,CAC03,H,CA,CAC03S
COMMON/CANC2/S03,HS03,OH,Ay,H2Ay,HA
COMMON/DIFF/DHC03,DC03,DH,DC02,DCA,DCAC03
COMMON/DIFF2/DS03,DHS03,DOH,DA,DH2A,DHA
COMMON/BULK/C02B,C03B,HC03B,CAC03B,HB,CAB
COMMON/BULK2/S03B,HS03B,OHB,AB,H2AB,HAB
COMMON/EPS/EPS1,EPS2
COMMON/RATEK/K1,K2,K3,KF,KA1,KA2,KHS03,KW
COMMON/ADID/KD
REAL KD
REAL K1,K2,K3,KA1,KA2,KHS03,KW
ALPH1=DC02*C02B+DHC03*HC03B+DCAC03*CAC03B+DC03*C03B-BETA
ALPH2=DCAXCAB+DCAC03*CAC03B-BETA
ALPH3=DH*HB+DHC03*HC03B+2.*DC02*C02B+DHA*HAB+2.*DH2A*H2AB-DOH
1*OHB-DS03*S03B
ALPH4=DH2A*H2AB+DHA*HAB+DA*AB
ALPH5=DHS03*HS03B+DS03*S03B
H1=HB
H2=HB/1.0E4
CALL FIND(BETA,H1,F1)
CALL FIND(BETA,H2,F2)
IF(F1*F2.GT.0.) GO TO 50
FSAVE=F1
DO 20 J=1,25
H=H2-F2*(H2-H1)/(F2-F1)
CALL FIND(C02,H,FW)
ERR=ABS((H1-H2)/H1)/2.
IF(ERR.LE.EPS1) GO TO 60
IF(ABS(FW).LE.EPS2) GO TO 60
IF(FW*F1.LT.0.) GO TO 10
H1=H
F1=FW
IF(FW*FSAVE.GT.0.) F2=F2/2.
FSAVE=FW
GO TO 20
10 H2=H
F2=FW
IF(FW*FSAVE.GT.0.) F1=F1/2.
FSAVE=FW
20 CONTINUE
50 PRINT 3
3 FORMAT(1HO,10X,*FIND DO NOT CONVERGE*,/)
60 CALL FIND(BETA,H,F)
CAC03=CA*HC03/(K1*H)
C03=KD*HC03/H
RETURN
END

SUBROUTINE FIND(BETA,HYS,F)
COMMON/DIFF2/DS03,DHS03,DOH,DA,DH2A,DHA
COMMON/DIFF/DHC03,DC03,DH,DC02,DCA,DCAC03

```

```
COMMON/CANC/C02,C03,HC03,CAC03,H,CA,CAC03S
COMMON/CANC2/S03,HS03,OH,A,H2A,HA
COMMON/RATEK/K1,K2,K3,KF,KA1,KA2,KHS03,KW
COMMON/CONST/ALPH1,ALPH2,ALPH3,ALPH4,ALPH5
COMMON/ADD/KD
REAL K1,K2,K3,KD
REAL KA1,KA2,KHS03,KW
H=HYS
OH=KW/H
H2A=ALPH4/(DH2A*(1.+DHAKA1/(DH2A*H)+KA1*KAA2*DA/(DH2A*KH)))
HA=KA1*KH2A/H
A=KA1*KAA2*KH2A/(H*KH)
HS03=ALPH5/(DHS03+DS03*KHS03/H)
S03=KHS03*HS03/H
HC03=(ALPH1-DC02*C02)/(DHCO3+DCACO3*CA*KD/(H*K3)+DC03*KD/H)
F=DHKH+DHCO3*HC03+2.*DC02*C02+DHAKH+2.*DH2A*KH2A-DOH*OH-DS03*S03
1-ALPH3
RETURN
END
```

PROGRAM III

MASS TRANSFER MODEL FOR CALCULATING SURFACE

 CaCO_3° and CaSO_3° CONCENTRATIONS

Program III is the same as program II, except that an experimental β is used to backcalculate the $[\text{CaCO}_3^\circ]$ and $[\text{CaSO}_3^\circ]$ at the limestone surface.

Input and output same as in program II

```

PROGRAM LIMSDIS(TTY,INPUT=TTY,OUTPUT)

C*****THIS PROGRAM CALCULATE THE RATE OF LIMESTONE DISSOLUTION BY*****
*
C***** A MASS TRANSFER MODEL USING SPHERICAL GEOMETRY*****
*
C*****DIMENSION APH(10),APCO2(10)
DIMENSION ACTP(10),BCTP(10),ZI(10),GAMMA(15)
DIMENSION AC02(120)
DIMENSION CC03(120),CCAC03(120),CC02(120),CCA(120),CH(120)
DIMENSION CHC03(120),DX(120)
DIMENSION COH(120),CS03(120),CHS03(120),CAA(120),CH2A(120)
DIMENSION CHA(120)
COMMON/DIFF/DHC03,DC03,DH,DC02,DCA,DCAC03
COMMON/DIFF2/DS03,DHS03,D0H,D0A,DH2A,DHA
COMMON/RATEK/K1,K2,K3,KF,KA1,KA2,KHS03,KW
COMMON/CONST/ALPH1,ALPH2,ALPH3,ALPH4,ALPH5
COMMON/CONSUR/HCO3S,C03S,CAS,HS,C02S
COMMON/RAD/RO,BETA
COMMON/EPS/EPS1,EPS2
COMMON/END/Y0,YF
COMMON/DKRATE/KA,KB,KC
COMMON/COUNT/NJ
COMMON/INDEX/NK
COMMON/END2/Y01,YF1
COMMON/SURF/CC03,CCAC03,CC02,CCA,CH,CHC03,DX
COMMON/SURF2/COH,CS03,CHS03,CAA,CH2A,CHA
COMMON/CANC/C02,C03,HCO3,CAC03,H,CA,CAC03S
COMMON/CANC2/S03,HSO3,OH,A,H2A,HA
COMMON/BULK/C02B,C03B,HCO3B,CAC03B,HB,CAB
COMMON/BULK2/S03B,HSO3B,OHB,AB,H2AB,HAB
COMMON/AID/KD
REAL K1,K2,K3,KW,KF,KA1,KA2,KHS03
REAL KD,KS

C*****DIFFUSIVITIES IN CM2/SEC*****
*
C*****CAC03S SURFACE CONCENTRATION OF ION PAIR AT*****
*
C*****SOLID LIQUID INTERPHASE*****
*
DATA DC02,DHC03,DC03,DCA/2.0E-5,1.2E-5,7.0E-6,7.9E-6/
DATA DH,DCAC03,CAC03S/9.3E-5,7.5E-6,6.204E-6/
DATA DS03,DHS03,D0H,D0A/3.85E-6,1.19E-5,5.27E-5,7.05E-6/
DATA DH2A,DHA/1.19E-5,1.09E-5/
DATA KA1,KA2,KW,KHS03/3.548E-5,0.071.0E-14,6.24E-8/
DATA EPS1,EPS2/1.0E-6,1.0E-25/

C*****ERROR CRITERIA FOR CONVERGENCE*****
*
C*****EPS1 EPS2 *****
*
C*****ACTP,BCTP ACTIVITIES COEFFICIENT PARAMETERS*****
*
C*****FOR MODIFIED DEBYE-HUCKEL EQUATION*****
*
DATA(ACTP (I),I=1,9)/6.0,4.5,4.5,4.5,4.5,4.5,3.,3.,3./
DATA(BCTP (I),I=1,9)/0.4,0.1,0.0,0.,0.,0.3,0.3,0.3/

```

```

C*****HK      HENRY'S CONSTANT FOR CO2 IN WATER*****
*
C*****UI      EMPIRICAL CONSTANT FOR UNCHARGED SPECIES IN ****
*
C*****      DEBYE-HUCKEL EQUATION      ****
*
C*****CI      IONIC STRENGTH OF SOLUTION      ****
*
C*****ACONS,B TEMPERATURE CONSTANTS IN THE MODIFIED*****
*
C*****DEBYE-HUCKEL EQUATION*****
*
C*****ZI      IONIC VALENCIES      ****
*
DATA HK,UI,CI,ACONS,B/0.0305,0.076,0.3,0.512,0.312/
DATA (ZI(I),I=1,9)/1.,2.,1.,2.,2.,1.,1.,2.,1./
DATA K1,K2,K3,KF/1.34E7,4.45E-7,6.3E-4,2.6E-2/
DATA KD/4.69E-11/
DATA KS/4.0E-4/

C*****INPUT DATA*****
*
C*****AT      TOTAL BUFFER CONCENTRATION(GMOLES/LITER) ****
*
C*****S03T    TOTAL SULFITE CONCENTRATION(GMOLES/LITER) ****
*
C*****BETA1,BETA2 TRIAL INTERVALS FOR THE DISSOLUTION FLUX ****
*
C*****      (GMOLES-CM2/LITER-SEC) ****
*
C*****NI      NUMBER OF PH AND PCO2 DATA PAIR ****
*
C*****APCO2,APH    PH & PARTIAL PRESSURE OF CO2(ATM) ****
*
C*****RO      PARTICLE DIAMETER(MICRO-METER) ****
*
C*****CA      CALCIUM CONCENTRATION OF BULK SOLUTION ****
*
C*****      (GMOLES/LITER) ****
*
C**********
*
READ,AT,S03T
READ,BETA
READ,NI
READ,CA,RO
DO 2 K=1,NI
  READ,APCO2(K),APH(K)
2 CONTINUE
DO 21 I=1,9
  WA=ACONS*ZI(I)*ZI(I)
  WC=SQRT(CI)
  WB=1.+B*ACTP(I)*WC

C*****ACTIVITY COEFFICIENTS*****COMPONENTS*****
**
C*****GAMMA(1)          H+
C*****GAMMA(2)          CA++
C*****GAMMA(3)          HC03-
C*****GAMMA(4)          CO3--

```

```

C      GAMMA(5)          S03--
C      GAMMA(6)          HS03-
C      GAMMA(7)          OH-
C      GAMMA(8)          A--
C      GAMMA(9)          HA-
C      GAMMA(10)         CO2
C      GAMMA(11)         H2A
C      GAMMA(12)         CACO3(ION PAIR)

C*****REDEFINE EQUILIBRIUM AND RATE CONSTANT IN TERMS OF *****
*
C*****CONCENTRATIONS*****
*
C*****EQUILIBRIUM CONSTANT*****REACTION*****
*
C      K1                 CACO3(ION PAIR) + H+ = CA++ + HC03-
C      K2                 CO2 + H2O = H+ + HC03-
C      K3                 CACO3(ION PAIR) = CA++ + CO3--
C      KHS03              HS03- = H+ + S03--
C      KW                 H2O = H+ + OH-
C      KD                 HC03- = H+ + CO3--
C      KS                 CASO3(ION PAIR) = CA++ + SO3--
C      KA1                H2A = H+ + HA-
C      KA2                HA- = H+ + A--


C*****RATE CONSTANT*****REACTION*****
*
C      KF                 CO2 + H2O = H+ + HC03-


KF=KF*GAMMA(10)
K1=(K1*GAMMA(1)*GAMMA(12))/(GAMMA(2)*GAMMA(3))
K2=(K2*GAMMA(10))/(GAMMA(1)*GAMMA(3))
K3=K3*GAMMA(12)/(GAMMA(2)*GAMMA(4))

```

```

RKHS03=(KHS03*GAMMA(6))/(GAMMA(5)*GAMMA(1))
KHS03=RKHS03*(1.+GAMMA(2)*GAMMA(5)*CA/(GAMMA(12)*KS))
KW=KW/(GAMMA(1)*GAMMA(7))
KD=KD*GAMMA(3)/(GAMMA(1)*GAMMA(4))
OHB=KW/HB
HAB=AT/(1.+HB/KA1+KA2/HB)
H2AB=HAB*HB/KA1
AB=AT-HAB-H2AB
S03B=KHS03*S03T/(HB+KHS03)
HS03B=S03T-S03B
PRINT 234
234 FORMAT(1H1,6X,*INPUT DATA*,//,6X,*DIFFUSIVITIES(CM2/SEC)*,/)
PRINT 235
235 FORMAT(10X,*C02*,11X,*HC03-* ,11X,*C03--*,11X,*CA++*,13X,*H*,9X,
1*CAC03(ION PAIR)*,/)
PRINT 102,DCO2,DHC03,DC03,DCA,DH,DCAC03
PRINT 236
236 FORMAT(10X,*OH-* ,11X,*S03--*,11X,*HS03-* ,11X,*A--*,11X,*H2A*,11X
,1*HA-* ,)
PRINT 102,D0H,DS03,DHS03,DA,DH2A,DHA
102 FORMAT(3X,6E15.3,/)
PRINT 237
237 FORMAT(10X,*K1*,14X,*K2*,14X,*K3*,14X,*KF*,/)
PRINT 103,K1,K2,K3,KF
PRINT 238
238 FORMAT(10X,*KA1*,14X,*KA2*,14X,*KW*,12X,*KHS03*,/)
PRINT 103,KA1,KA2,KW,KHS03
103 FORMAT(3X,4E15.4,/)
PRINT 251
251 FORMAT(10X,*PH*,11X,*PC02(ATM.)*,5X,*PARTICLE DIAMETER(CM)*,/)
PRINT 105,PH,PC02,R0
105 FORMAT(3X,3E15.3)
PRINT 239
239 FORMAT(7X,*OUTPUT*,//,6X,*BULK CONCENTRATIONS(G-MOLE/L)*,/)
PRINT 235
PRINT 102,C02B,HC03B,C03B,CAB,HB,CAC03B
PRINT 236
PRINT 102,OHB,S03B,HS03B,AB,H2AB,HAB
CALL SURCONE(BETA)
PRINT 241
241 FORMAT(13X,*SURFACE CONCENTRATION(G-MOLE/L)*,/)
PRINT 235
PRINT 102,C02,HC03,C03,CA,H,CAC03
PRINT 236
PRINT 102,OH,S03,HS03,A,H2A,HA
PRINT 37,BETA
37 FORMAT(//,3X,E15.4)
RATED=-BETA/(1000.*R0)
PRINT 36,RATED
36 FORMAT(//,3X,*RATE OF DISSOLUTION=*,E15.5,*G-MOLE/SQ.CM SEC*,/)
DCC02=C02-C02B
DCHC03=HC03-HC03B
DCCA=CA-CAB
DCH=H-HB
DCCAC0=CAC03-CAC03B
DCC03=C03-C03B
DCOH=OH-OHB
DCS03=S03-S03B
DCHS03=HS03-HS03B
DCCAA=A-AB
DCH2A=H2A-H2AB
DCHA=HA-HAB
DICO2=DC02*DCC02

```

```

DIHC03=DHC03*DCHC03
DICA=ICA*DCCA
DIH=DH*DCH
DICACO=DCCACO*DCACO3
DCO3=DC03*DCC03
DOH=DOH*DCOH
DSO3=DS03*DCS03
DH503=DHS03*DCHS03
DIAA=DCCAA*DA
DH2A=DH2A*DCH2A
DIHA=DHA*DCHA
PRINT 11
11 FORMAT(//,6X,*DIFFERENCE BETWEEN SURFACE AND BULK CONCENTRATION
FOR EACH CHEMICAL SPECIES*,//)
PRINT 235
PRINT 102,DCC02,DCHC03,DCC03,DCCA,DCH,DCCACO
PRINT 236
PRINT 102,DCOH,DCS03,DCHS03,DCCAA,DCH2A,DCHA
PRINT 12
12 FORMAT(//,6X,*FLUX CONTRIBUTION FOR EACH SPECIES*,/)
PRINT 235
PRINT 102,DC02,DIHC03,DC03,DICA,DIH,DICACO
PRINT 236
PRINT 102,DOH,DSO3,DH503,DIAA,DH2A,DIHA
STOP
END

SUBROUTINE SURCONE(BETA)
COMMON/CONST/ALPH1,ALPH2,ALPH3,ALPH4,ALPH5
COMMON/CONSUR/HCO3S,C03S,CAS,HS,C02S
COMMON/CANC/C02,C03,HCO3,CACO3,H,CA,CACO3S
COMMON/CANC2/S03,HS03,OH,A,H2A,HA
COMMON/DIFF/DHC03,DC03,DH,DC02,ICA,DCACO3
COMMON/DIFF2/DSO3,DHS03,DOH,DA,DH2A,DIHA
COMMON/BULK/C02B,C03B,HCO3B,CACO3B,HB,CAB
COMMON/BULK2/S03B,HS03B,OH,B,H2AB,HAB
COMMON/EPS/EPS1,EPS2
COMMON/RATEK/K1,K2,K3,KF,KAI,KA2,KHS03,KW
COMMON/ADD/KD
REAL KD
REAL K1,K2,K3,KAI,KA2,KHS03,KW
ALPH1=DC02*C02B+DHC03*HCO3B+DCACO3*CACO3B+DC03*C03B-BETA
ALPH2=ICA*CAB+DCACO3*CACO3B-BETA
ALPH3=DH*HB+DHC03*HCO3B+2.*DC02*C02B+DHA*HAB+2.*DH2A*H2AB-DOH
1*OH-B-SO3B
ALPH4=DH2A*H2AB+DHA*HAB+DA*AB
ALPH5=DHS03*S03B+DSO3*S03B
H1=HB
H2=HB/1.0E4
CALL FIND(BETA,H1,F1)
CALL FIND(BETA,H2,F2)
IF(F1*F2.GT.0.) GO TO 50
FSAVE=F1
DO 20 J=1,25
H=H2-F2*(H2-H1)/(F2-F1)
CALL FIND(CO2,H,FW)
ERR=ABS((H1-H2)/H1)/2.
IF(ERR.LE.EPS1) GO TO 60
IF(ABS(FW).LE.EPS2) GO TO 60
IF(FW*F1.LT.0.) GO TO 10
H1=H
F1=FW
IF(FW*FSAVE.GT.0.) F2=F2/2.
FSAVE=FW
GO TO 20
10 H2=H

```

```

      F2=FW
      IF(FW*FSAVE.GT.0.) F1=F1/2.
      FSAVE=FW
20  CONTINUE
50  PRINT 3
3   FORMAT(1HO,10X,*FIND DO NOT CONVERGE*,/)
60  CALL FIND(BETA,H,F)
      CAC03=CA*HC03/(K1*H)
      CO3=KD*HC03/H
      RETURN
      END

SUBROUTINE FIND(BETA,HYS,F)
COMMON/DIFF2/DS03,DHS03,DOH,DA,DH2A,DHA
COMMON/DIFF/DHC03,DC03,DH,DC02,DCA,DCAC03
COMMON/CANC/C02,C03,HC03,CAC03,H,CA,CAC03S
COMMON/CANC2/S03,H03,OH,A,H2A,HA
COMMON/RATEK/K1,K2,K3,KF,KA1,KA2,KHS03,KW
COMMON/CONST/ALPH1,ALPH2,ALPH3,ALPH4,ALPH5
COMMON/ADD/KD
REAL K1,K2,K3,KD
REAL KA1,KA2,KHS03,KW
H=HYS
OH=KW/H
H2A=ALPH4/(DH2A*(1.+DHA*KA1/(DH2A*H)+KA1*KA2*DA/(DH2A*KH)))
HA=KA1*KH2A/H
A=KA1*KA2*KH2A/(H*H)
HS03=ALPH5/(DHS03+DS03*KHS03/H)
S03=KHS03*HS03/H
HC03=(ALPH1-DC02*C02)/(DHC03+DCAC03*CA*KD/(H*K3)+DC03*KD/H)
F=DH*H+DHC03*HC03+2.*DC02*C02+DHA*HA+2.*DH2A*KH2A-DOH*OH-DS03*S03

1-ALPH3
PRINT 10,F
10  FORMAT(3X,E15.3)
      RETURN
      END

```

CC:

PROGRAM IV

MASS TRANSFER MODEL WITH EQUILIBRIUM SHIFT

OF CaSO_3° ON CaCO_3°

Program IV is similar to program II with the addition of $[\text{CaCO}_3^{\circ}]$ as a function of $[\text{CaSO}_3^{\circ}]$ at the limestone surface.

Input and output is the same as in program II

```

PROGRAM LIMSDIS(TTY,INPUT=TTY,OUTPUT)

C*****C*****C*****C*****C*****C*****C*****C*****C*****C*****C*****C
* THE PHYSICAL CONSTANTS USED IN THIS PROGRAM IS AT 55 DEGREE C
C*****C*****C*****C*****C*****C*****C*****C*****C*****C*****C*****C
*
C*****C*****C*****C*****C*****C*****C*****C*****C*****C*****C*****C
* THIS PROGRAM CALCULATE THE RATE OF LIMESTONE DISSOLUTION BY*****
* A MASS TRANSFER MODEL USING SPHERICAL GEOMETRY*****
* C*****C*****C*****C*****C*****C*****C*****C*****C*****C*****C*****C
*
DIMENSION APH(10),APCO2(10)
DIMENSION ACTP(10),BCTP(10),ZI(10),GAMMA(15)
DIMENSION AC02(120)
DIMENSION CC03(120),CCAC03(120),CC02(120),CCA(120),CH(120)
DIMENSION CHC03(120),DX(120)
DIMENSION COH(120),CS03(120),CHS03(120),CAA(120),CH2A(120)
DIMENSION CHA(120)
COMMON/DIFF/DHC03,DC03,DH,DC02,DCA,DCAC03
COMMON/DIFF2/DS03,DHS03,DOH,DA,DH2A,DHA
COMMON/RATE/K1,K2,K3,KF,KA1,KA2,KHS03,KW
COMMON/CONST/ALPH1,ALPH2,ALPH3,ALPH4,ALPH5
COMMON/CONSUR/HCO3S,C03S,CAS,HS,C02S
COMMON/RAD/R0,BETA
COMMON/EPS/EPS1,EPS2
COMMON/END/Y0,YF
COMMON/DKRATE/KA,KB,KC
COMMON/COUNT/NJ
COMMON/INDEX/NK
COMMON/END2/Y01,YF1
COMMON/SURF/CC03,CCAC03,CC02,CCA,CH,CHC03,DX
COMMON/SURF2/COH,CS03,CHS03,CAA,CH2A,CHA
COMMON/CANC/C02,C03,HCO3,CAC03,H,CA,CAC03S
COMMON/CANC2/S03,H03,OH,A,H2A,HA
COMMON/BULK/C02B,C03B,HCO3B,CAC03B,HB,CAB
COMMON/BULK2/S03B,H03B,OHB,AB,H2AB,HAB
COMMON/AID/KD
REAL K1,K2,K3,KW,KF,KA1,KA2,KHS03
REAL KD,KS

C*****C*****C*****C*****C*****C*****C*****C*****C*****C*****C*****C
* DIFFUSIVITIES IN CM2/SEC
* C*****C*****C*****C*****C*****C*****C*****C*****C*****C*****C*****C
* C*****C*****C*****C*****C*****C*****C*****C*****C*****C*****C*****C
* C*****C*****C*****C*****C*****C*****C*****C*****C*****C*****C*****C
* C*****C*****C*****C*****C*****C*****C*****C*****C*****C*****C*****C
DATA DC02,DHC03,DC03,DCA/3.89E-5,2.33E-5,1.36E-5,1.54E-5/
DATA DH,DCAC03/1.81E-4,1.46E-5/
DATA DS03,DHS03,DOH,DA/7.49E-6,1.46E-5,1.03E-4,1.37E-5/
DATA DH2A,DHA/2.32E-5,2.12E-5/
DATA KA1,KA2,KW,KHS03/0.,0.,7.26E-14,3.99E-8/
DATA EPS1,EPS2/1.0E-6,1.0E-25/

C*****C*****C*****C*****C*****C*****C*****C*****C*****C*****C*****C
* ERROR CRITERIA FOR CONVERGENCE
* C*****C*****C*****C*****C*****C*****C*****C*****C*****C*****C*****C
* C*****C*****C*****C*****C*****C*****C*****C*****C*****C*****C*****C
* C*****C*****C*****C*****C*****C*****C*****C*****C*****C*****C*****C
* C*****C*****C*****C*****C*****C*****C*****C*****C*****C*****C*****C
C*****C*****C*****C*****ACTP,BCTP ACTIVITIES COEFFICIENT PARAMETERS
*
```

```

*****FOR MODIFIED DEBYE-HUCKEL EQUATION*****
*
DATA(ACTP   (I),I=1,9)/6.0,4.5,4.5,4.5,4.5,4.5,3.,3.,3./
DATA(BCTP   (I),I=1,9)/0.4,0.1,0.0,0.,0.,0.3,0.3,0.3/
*
C*****HK      HENRY'S CONSTANT FOR CO2 IN WATER*****
*
C*****UI      EMPIRICAL CONSTANT FOR UNCHARGED SPECIES IN ****
*
C*****      DEBYE-HUCKEL EQUATION ****
*
C*****CI      IONIC STRENGTH OF SOLUTION ****
*
C*****ACONS,B TEMPERATURE CONSTANTS IN THE MODIFIED*****
*
C*****DEBYE-HUCKEL EQUATION*****
*
C*****ZI      IONIC VALENCIES ****
*
DATA HK,UI,CI,ACONS,B/0.0168,0.076,0.3,0.543,0.336/
DATA (ZI(I),I=1,9)/1.,2.,1.,2.,1.,1.,2.,1./
DATA K1,K2,K3,KF/6.43E6,5.12E-7,4.51E-4,0.127/
DATA KD/7.02E-11/
DATA KS/2.81E-4/
*
C*****INPUT DATA*****
*
C*****AT      TOTAL BUFFER CONCENTRATION(GMOLES/LITER) ****
*
C*****SO3T    TOTAL SULFITE CONCENTRATION(GMOLES/LITER) ****
*
C*****BETA1,BETA2 TRIAL INTERVALS FOR THE DISSOLUTION FLUX ****
*
C*****      (GMOLES-CM2/LITER-SEC) ****
*
C*****NI      NUMBER OF PH AND PCO2 DATA PAIR ****
*
C*****APCO2,APH    PH & PARTIAL PRESSURE OF CO2(ATM) ****
*
C*****RO      PARTICLE DIAMETER(MICRO-METER) ****
*
C*****CA      CALCIUM CONCENTRATION OF BULK SOLUTION ****
*
C*****      (GMOLES/LITER) ****
*
READ,AT,SO3T
READ,BETA1,BETA2
READ,NI
READ,CA,RO
DO 2 K=1,NI
READ,APCO2(K),APH(K)
2 CONTINUE
DO 21 I=1,9
WA=ACONS*ZI(I)*ZI(I)
WC=SQRT(CI)
WB=1.+B*ACTP(I)*WC

*****
ACTIVITY COEFFICIENTS*****COMPONENTS*****

```

```

**  

C      GAMMA(1)          H+  

C      GAMMA(2)          CA++  

C      GAMMA(3)          HC03-  

C      GAMMA(4)          CO3--  

C      GAMMA(5)          SO3--  

C      GAMMA(6)          HS03-  

C      GAMMA(7)          OH-  

C      GAMMA(8)          A--  

C      GAMMA(9)          HA-  

C      GAMMA(10)         CO2  

C      GAMMA(11)         H2A  

C      GAMMA(12)         CAC03(ION PAIR)  

*****  

**  

21  GAMMA(I)=10.**(WA*(-WC/WB+CI*BCTP(I)))  

DO 22 I=10,12  

22  GAMMA(I)=10.**((UI*CI)  

DO 3 J=1,NI  

PH=APH(J)  

PCO2=APCO2(J)  

3  CONTINUE  

AH=10.**(-PH)  

H=AH/GAMMA(1)  

CO2=HK*PCO2  

HB=H  

CO2B=CO2  

AACO2=CO2*GAMMA(10)  

AHCO3=K2*AACO2/AH  

HC03=AHCO3/GAMMA(3)  

HC03B=HC03  

ACO3=KD*AHCO3/AH  

CO3=ACO3/GAMMA(4)  

CO3B=CO3  

ACA=CA*GAMMA(2)  

CAB=CA  

ACACO3=ACA*ACO3/K3  

CACO3=ACACO3/GAMMA(12)  

CACO3B=CACO3  

*****  

*REDEFINE EQUILIBRIUM AND RATE CONSTANT IN TERMS OF *****  

*  

*****CONCENTRATIONS*****  

*  

*****EQUILIBRIUM CONSTANT*****REACTION*****  

*  

C      K1           CAC03(ION PAIR) + H+ = CA++ + HC03-  

C      K2           CO2 + H2O = H+ + HC03-  

C      K3           CAC03(ION PAIR) = CA++ + CO3--  

C      KHS03        HS03- = H+ + SO3--  

C      KW           H2O = H+ + OH-  

C      KD           HC03- = H+ + CO3--  

C      KS           CASO3(ION PAIR) = CA++ + SO3--  

C      KA1          H2A = H+ + HA-  

C      KA2          HA- = H+ + A--  

*****RATE CONSTANT*****REACTION*****  

*  

C      KF           CO2 + H2O = H+ + HC03-  

*****  

*
```

```

KF=KF*GAMMA(10)
K1=(K1*GAMMA(1)*GAMMA(12))/(GAMMA(2)*GAMMA(3))
K2=(K2*GAMMA(10))/(GAMMA(1)*GAMMA(3))
K3=K3*GAMMA(12)/(GAMMA(2)*GAMMA(4))
RKHS03=(KHS03*GAMMA(6))/(GAMMA(5)*GAMMA(1))
KHS03=RKHS03*(1.+GAMMA(2)*GAMMA(5)*CA/(GAMMA(12)*KS))
KW=KW/(GAMMA(1)*GAMMA(7))
KD=KD*GAMMA(3)/(GAMMA(1)*GAMMA(4))
OHB=KW/HB
HAB=AT/(1.+HB/KA1+KA2/HB)
H2AB=HAB*HB/KA1
AB=AT-HAB-H2AB
S03B=KHS03*S03T/(HB+KHS03)
HS03B=S03T-S03B
PRINT 234
234 FORMAT(1H1,6X,*INPUT DATA*,//,6X,*DIFFUSIVITIES(CM2/SEC)*,/)
PRINT 235
235 FORMAT(10X,*C02*,11X,*HC03-* ,11X,*C03--*,11X,*CA++*,13X,*HH*,9X,
1*CACO3(ION PAIR)*,/)
PRINT 102,DC02,DHC03,DC03,BCA,DH,DCACO3
PRINT 236
236 FORMAT(10X,*OH-* ,11X,*S03--*,11X,*HS03-* ,11X,*A--*,11X,*H2A*,11X
1*HA-* ,/)
PRINT 102,DOH,DS03,DHS03,DA,DH2A,DHA
102 FORMAT(3X,6E15.3,/)
PRINT 237
237 FORMAT(10X,*K1*,14X,*K2*,14X,*K3*,14X,*KF*,/)
PRINT 103,K1,K2,K3,KF
PRINT 238
238 FORMAT(10X,*KA1*,14X,*KA2*,14X,*KW*,12X,*KHS03*,/)
PRINT 103,KA1,KA2,KW,KHS03
103 FORMAT(3X,4E15.4,/)
PRINT 251
251 FORMAT(10X,*PH*,11X,*PC02(ATM.)*,5X,*PARTICLE DIAMETER(CM)*,/)
PRINT 105,PH,PC02,R0
105 FORMAT(3X,3E15.3)
PRINT 239
239 FORMAT(7X,*OUTPUT*,//,6X,*BULK CONCENTRATIONS(G-MOLE/L)*,/)
PRINT 235
PRINT 102,C02B,HC03B,C03B,CAB,HB,CACO3B
PRINT 236
PRINT 102,OHB,S03B,HS03B,AB,H2AB,HAB
CALL SURCONE(BETA1)
CALL PHI(S03,CACO3,SIDE1)
CALL SURCONE(BETA2)
CALL PHI(S03,CACO3,SIDE2)
IF(SIDE1*SIDE2.GT.1.) GO TO 187
M=0
120 BETA=(BETA2+BETA1)/2.
CALL SURCONE(BETA)
PRINT 660,S03,CACO3
660 FORMAT(4X,2E15.4)
CALL PHI(S03,CACO3,SIDEN)
IF(SIDE1*SIDEN.LT.0.) BETA2=BETA
IF(SIDE2*SIDEN.LT.0.) BETA1=BETA
DELT=ABS((BETA1-BETA2)/BETA1)
IF(DELT.LT.0.0003) GO TO 188
IF (M.EQ.25) GO TO 187
M=M+1
GO TO 120
188 PRINT 241
241 FORMAT(13X,*SURFACE CONCENTRATION(G-MOLE/L)*,/)

```

```

PRINT 235
PRINT 102,C02,HC03,C03,CA,H,CAC03
PRINT 236
PRINT 102,OH,S03,HS03,A,H2A,HA
PRINT 37,BETA
37 FORMAT(//,3X,E15.4)
RATED=-BETA/(1000.*R0)
PRINT 36,RATED
36 FORMAT(//,3X,*RATE OF DISSOLUTION=*,E15.5,*G-MOLE/SQ.CM.SEC*,/)
DCC02=C02-C02B
DCHC03=HC03-HC03B
DCCA=CA-CAB
DCH=H-HB
DCCACO=CAC03-CAC03B
DCC03=C03-C03B
DCOH=OH-OHB
DCS03=S03-S03B
DCHS03=HS03-HS03B
DCCAA=A-AB
DCH2A=H2A-H2AB
DCHA=HA-HAB
DICO2=DCO2*DCC02
DIHC03=DHC03*DCHC03
DICA=DCA*DCCA
DIH=DH*DCH
DICACO=DCCACO*DCCACO
DICO3=DCO3*DCC03
DIOH=DOH*DCOH
DIS03=DS03*DCS03
DIHS03=DHS03*DCHS03
DIAA=DCCAA*DA
DIH2A=DH2A*DCH2A
DIHA=DHA*DCHA
PRINT 11
11 FORMAT(//,6X,*DIFFERENCE BETWEEN SURFACE AND BULK CONCENTRATION

1FOR EACH CHEMICAL SPECIES*,//)
PRINT 235
PRINT 102,DCC02,DCHC03,DCC03,DCCA,DCH,DCCACO
PRINT 236
PRINT 102,DCOH,DCS03,DCHS03,DCCAA,DCH2A,DCHA
PRINT 12
12 FORMAT(//,6X,*FLUX CONTRIBUTION FOR EACH SPECIES*,/)
PRINT 235
PRINT 102,DIC02,DIHC03,DICO3,DICA,DIH,DICACO
PRINT 236
PRINT 102,DIOH,DIS03,DIHS03,DIAA,DIH2A,DIHA
187 STOP
END

SUBROUTINE PHI(S03,CAC03,SIDE)
IF(S03.LT.4.96E-5.AND.CAC03.LT.6.2E-6) SIDE=-1.
IF(S03.LT.4.96E-5.AND.CAC03.GT.6.2E-6) SIDE=1.
IF(S03.GE.4.96E-5) SIDE=ALOG10(CAC03)+10.76+1.29*ALOG10(S03)
RETURN
END
SUBROUTINE SURCONE(BETA)
COMMON/CONST/ALPH1,ALPH2,ALPH3,ALPH4,ALPH5
COMMON/CONSUR/HC03S,C03S,CAS,HS,C02S
COMMON/CANC/C02,C03,HC03,CAC03,H,CA,CAC03S
COMMON/CANC2/S03,HS03,OH,A,H2A,HA
COMMON/DIFF/DHC03,DC03,OH,DC02,DCA,DCCACO
COMMON/DIFF2/DS03,DHS03,DOH,DA,DH2A,DHA
COMMON/BULK/C02B,C03B,HC03B,CAC03B,HB,CAB
COMMON/BULK2/S03B,HS03B,OHB,AB,H2AB,HAB

```

```

COMMON/EPS/EPS1,EPS2
COMMON/RATEK/K1,K2,K3,KF,KA1,KA2,KHS03,KW
COMMON/ADD/KD
REAL KD
REAL K1,K2,K3,KA1,KA2,KHS03,KW
ALPH1=DC02*CO2B+DHCO3*HC03B+DCAC03*CAC03B+DC03*C03B-BETA
ALPH2=DCA*CAB+DCAC03*CAC03B-BETA
ALPH3=DH*HB+DHCO3*HC03B+2.*DC02*CO2B+DHA*HAB+2.*DH2A*H2AB-DOH
1*OHB-DS03*S03B
ALPH4=DH2A*KH2AB+DHA*KAB+DA*KAB
ALPH5=DHS03*KHS03B+DS03*S03B
H1=HB
H2=HB/1.0E4
CALL FIND(BETA,H1,F1)
CALL FIND(BETA,H2,F2)
IF(F1*F2.GT.0.) GO TO 50
FSAVE=F1
DO 20 J=1,25
H=H2-F2*(H2-H1)/(F2-F1)
CALL FIND(CO2,H,FW)
ERR=ABS((H1-H2)/H1)/2.
IF(ERR.LE.EPS1) GO TO 60
IF(ABS(FW).LE.EPS2) GO TO 60
IF(FW*F1.LT.0.) GO TO 10
H1=H
F1=FW
IF(FW*FSAVE.GT.0.) F2=F2/2.
FSAVE=FW
GO TO 20
10 H2=H
F2=FW
IF(FW*FSAVE.GT.0.) F1=F1/2.
FSAVE=FW
20 CONTINUE
50 PRINT 3
3 FORMAT(1H0,10X,*FIND DO NOT CONVERGE*,/)
60 CALL FIND(BETA,H,F)
CAC03=CA*HC03/(K1*H)
CO3=KD*HC03/H
RETURN
END

SUBROUTINE FIND(BETA,HYS,F)
COMMON/DIFF2/DS03,DHS03,DOH,DA,DH2A,DHA
COMMON/DIFF/DHCO3,DC03,DH,DC02,DCA,DCAC03
COMMON/CANC/CO2,CO3,HC03,CAC03,H,CA,CAC03S
COMMON/CANC2/S03,HS03,OH,A,H2A,HA
COMMON/RATEK/K1,K2,K3,KF,KA1,KA2,KHS03,KW
COMMON/CONST/ALPH1,ALPH2,ALPH3,ALPH4,ALPH5
COMMON/ADD/KD
REAL K1,K2,K3,KD
REAL KA1,KA2,KHS03,KW
H=HYS
OH=KW/H
H2A=ALPH4/(DH2A*(1.+DHA*KA1/(DH2A*H)+KA1*KA2*DA/(DH2A*H*H)))
HA=KA1*KH2A/H
A=KA1*KA2*KH2A/(H*H)
HS03=ALPH5/(DHS03+DS03*KHS03/H)
S03=KHS03*HS03/H
HC03=(ALPH1-DC02*CO2)/(DHCO3+DCAC03*CA*KD/(H*K3)+DC03*KD/H)
F=DH*H+DHCO3*HC03+2.*DC02*CO2+DHA*HA+2.*DH2A*H2A-DOH*OH-DS03*S03

1-ALPH3
RETURN
END

```

PROGRAM V

SIMPLIFIED MASS TRANSFER MODEL SUMMING DISSOLUTION
 RATE OVER PARTICLE SIZE DISTRIBUTION.

Program V calculates k_t versus fraction remaining F by the following equation:

$$F = \sum_{i=1}^n \phi_i \left(1 - \frac{k_t}{d_i d_{i+1}}\right)^{1.5}$$

For values of $\left(1 - \frac{k_t}{d_i d_{i+1}}\right) < 1$, set $F = 0$.

Input

ϕ_i particle size distribution and

d_i particle diameter from Coulter counter data
 and values of k_t

Output

Values of fraction remaining and k_t

```

PROGRAM MASS(TTY,INPUT=TTY,OUTPUT)
DIMENSION PHI(50),DP(50),DPSQ(50),F(50),KT(50),FR(100),DIFF(100)
DIMENSION D(50)
REAL KTL,KTH
REAL MN,KT
INTEGER TYPE(2)
DATA(KT(I),I=1,9)/.1,.2,.3,.4,.5,.6,.7,.8,.9/
DATA(KT(I),I=10,18)/1.,2.,3.,4.,5.,6.,7.,8.,9./
DATA(KT(I),I=19,27)/10.,20.,30.,40.,50.,60.,70.,80.,90./
DATA(KT(I),I=28,36)/100.,200.,300.,400.,500.,600.,700.,800.,900./
DATA(KT(I),I=37,45)/1000.,2000.,3000.,4000.,5000.,6000.,7000.,
18000.,9000./
READ 999,(TYPE(I),I=1,2)
999 FORMAT(2A10)
READ,N,DO2
READ,(PHI(I),I=1, N)
C
C
PRINT 888,((TYPE(I),I=1,2),DO2)
888 FORMAT(1H1,2X,*LIMESTONE TYPE *,2A10,5X,*GEOM MEAN DIAM FO FIRST
1COULTER INTERVAL*,E10.3,//,2X ,*COULTER DISTRIBUTION*,/)
PRINT 666
666 FORMAT(2X,*MEAN SQUARE DIAM*,9X,*WGT PER CENT*)
DO 555 I=1,N
DPSQ(I)=DO2*(1.58740)**(I-1)
PRINT 777,DPSQ(I),PHI(I)
777 FORMAT(2X,F15.3,20X,F8.3)
555 CONTINUE
SUM=0.
KTL=0.
KTH=0.
T50=1.0
PRINT 111
DO 3 J=1,45
DO 20 I=1, N
C EVALUATE THE PRODUCT OF PARTICLE DIAMETERS AT A SPECIFIED
C DIFFERENTIAL PARTICLE SIZE DISTRIBUTION
DP(I)=1.-KT(J)/DPSQ(I)
IF(DP(I).GT.0.) GO TO 30
GO TO 20
30 F(I)=DP(I)**1.5*PHI(I)
C THE ABOVE EXPRESSION CALCULATE THE FRACTION REMAINING FOR A SPECIFY KT
SUMF=F(I)
SUM=SUM+SUMF
IF (I.LT. N) GO TO 20
PRINT 5,KT(J),SUM
FR(J)=SUM
SUM=0.
20 CONTINUE
3 CONTINUE
111 FORMAT(1H1,9X,*KT*,20X,*PER CENT REMAINING*,//)
5 FORMAT(6X,F10.5,22X,F10.5)
DO 40 I=1,45
DIFF(I)=50.-FR(I)
IF(DIFF(I) .GT.-15. .AND. DIFF(I) .LT. 0.) GO TO 32
GO TO 99
32 KTL=KT(I)
99 IF(DIFF(I) .LT.15. .AND. DIFF(I) .GT. 0.) GO TO 31
GO TO 40
31 KTH=KT(I)

```

```

40      GO TO 96
CONTINUE
96      CONTINUE
IF(KTH .LT. 1.0) GO TO 50
RKT=KTL
DO 60 J=1,100
RINCR=(KTH-KTL)/100.
RKT=RKT+RINCR
SUM=0.
DO 70 I=1, N
DP(I)=1.-RKT/DPSQ(I)
IF(DP(I) .GT. 0.) GO TO 33
GO TO 70
F(I)=DP(I)**1.5*PHI(I)
SUMF=F(I)
SUM=SUM+SUMF
IF (I .LT. N) GO TO 70
ROD=SUM-50.
IF(ROD .LT. 0.1 .AND. ROD .GT.-0.1) GO TO 34
GO TO 60
34      T50=RKT
GO TO 80
70      CONTINUE
60      CONTINUE
IF(T50 .LT. 1.0) GO TO 50
80      PRINT 6
6       FORMAT(//,8X,*KT/KT50*,21X,*FRACTION REMAINING*,//)
DO 90 I=1,45
DIFF(I)=KT(I)/T50
PRINT 7,DIFF(I),FR(I)
FORMAT(6X,F10.5,22X,F10.5)
90      CONTINUE
PRINT 8
8       FORMAT(//,8X,*KT50*,21X,*PER CENT REMAINING*,//)
PRINT 9,T50,SUM
9       FORMAT(6X,F10.5,22X,F10.5)
GO TO 100
50      CONTINUE
PRINT 212
212    FORMAT(/,5X,*NO CONVERGENCE FOR KT50*)
100    STOP
END

```

LITERATURE CITED

- Albery, W.J., Greenwood, A.R., and Ribble, R.F., "Diffusion Coefficients of Carboxylic Acids," Trans. Far. Soc. 63, 360 (1967)
- Barton, P., and Vatanatham, T., "Kinetics of Limestone Neutralization of Acid Waters," Env. Sci. and Tech. 10, 262 (1976)
- Berner, R.A., and Morse, J.W., "Dissolution Kinetics of Calcium Carbonate in Sea Water IV. Theory of Calcite Dissolution," Amer. J. Sci. 274, 108 (1974)
- Cavanaugh, C.M., "Buffer Additives for Flue Gas Desulfurization Processes," M.S. Thesis, University of Texas at Austin, Austin, Texas (1978)
- Chang, C.S., and Rochelle, G.T., "SO₂ Absorption into Aqueous Solution," accepted for publication in AICHE Journal (1981)
- Erga, O., and Terjesen, S.G., "Kinetics of the Heterogeneous Reaction of Calcium Bicarbonate Formation, with Special Reference to Copper Ion Inhibition," Acta. Chem. Scand. 10, 872 (1956)
- Garrels, R.M., and Thompson, M.E., "A Chemical Model for Sea Water at 25°C and One Atmosphere Total Pressure," Am. J. Sci. 260, 57 (1962)

- Hamer, W.J., "Theorectical Mean Activity Coefficients of Strong Electrolytes in Aqueous Solution from 0° to 100° C," "National Standard Reference Series - National Bureau of Standards 24 (1968)
- Harned, H.S., and Bonner, F.T., "The First Ionization of Carbonic Acid in Aqueous Solution of Sodium Chloride," J. Am. Chem. Soc. 67, 1026 (1945)
- Harned, H.S., and Owen, B.B., "The Physical Chemistry of Electrolyte Solution," Third Edition, Reinhold, New York (1958)
- Harned, H.S., and Scholes, S.R.Jr., "The Ionization Constants of Bicarbonate from 0° to 50°," J. Am. Chem. Soc. 63, 1706 (1941)
- Jeffrey, G.H., and Vogel, A.I., "The Dissociation Constants of Organic Acids. Part XI. The Thermodynamic Primary Dissociation Constants of Some Normal Dibasic Acids," J. Chem. Soc. 21 (1935)
- Kaplan, N., "Proceedings: Flue Gas Desulfurization Symposium - 1973. An EPA Overview of Sodium-Based Double Alkali Processes. Part II. Status of Technology and Description of Attractive Schemes," EPA - 650/2-73-038b, p.1019 (1973)
- Kim, Y.K., Deming, M.E., and Hatfield, J.D., "Dissolution of Limestone in Simulated Slurries for Removal of Sulfur Dioxide from Stack Gas," Env. Sci. and Tech. 9, 943 (1975)

- Koss V., and Möller P., "Oberflächenzusammensetzung, Loslichkeit und Ionenaktivitätsprodukt von Calcit in fremdionenhaltigen Lösungen," Z. Anorg. Allg. Chem. 410, 165 (1974)
- Landolt-Bornstein Physikalisch-Chemische Tabellen, Bd. II-7 225, Spring-Verlag, Berlin, Germany (1960)
- Lewis, J.B., "Some Determination of Liquid-Phase Diffusion Coefficients by Means of The Improved Diaphragm Cell," J. Appl. Chem. 5, 228 (1955)
- Lowell, P.S., Ottmers, D.M., Schwitzgebel, K., Strange, T. I., and Deberry, D.W., "A Theoretical Description of the Limestone Injection - Wet Scrubbing Process," PB 193-029, U.S. Environment Protection Agency (1970)
- Morse, J.W., "Dissolution Kinetics of Calcium Carbonate in Sea Water III: A New Method for the Study of Carbonate Reaction Kinetics," Amer. J. Sci. 274, 97 (1974)
- Nielsen, K.L., "Method in Numerical Analysis," 2nd Edition New York, MacMillian (1964)
- Ottmers, D., Phillips, J., Burklin, C., Corbett, W., Phillips, N., and Shelton, C., "A Theorectical and Experimental Study of the Lime/Limestone Wet Scrubbing Process," EPA Report No. EPA-650/2-75-006 (1974)
- Pinsent, R.W., Pearson, L., and Roughton, F.J.W., "The Kinetics of Combination of Carbon Dioxide with Hydroxide Ions," Trans. Far. Soc. 52, 1512 (1956)

Plummer, L.N., and Wigley, T.M.L., "The Dissolution of Calcite in CO_2 -Saturated Solutions at 25°C and 1 atmosphere total pressure," Geochim. Cosmochim. Acta. 40, 191 (1976)

Plummer, L.N., Wigley, T.M.L., and Parkhurst, D.L., "The Kinetics of Calcite Dissolution in CO_2 -Water Systems at 5° to 60°C and 0.0 to 1.0 atm CO_2 ," Amer. J. Sci. 278, 179 (1978)

Rochelle, G.T., and King, C.J., "The Effects of Additives on Mass Transfer in CaCO_3 or CaO Slurry Scrubbing of SO_2 from Waste Gases," Ind. Eng. Chem. Fund. 16, 67 (1977)

Rochelle, G.T., and King, C.J., "Alternatives for Stack Gas Desulfurization by Throwaway Scrubbing," Chem. Eng. Prog. 74, 65 (1978)

Sherwood, T.K., Pigford, R.L., and Wilke, C.R., "Mass Transfer," McGraw-Hill (1975)

Sjöberg, E.L., "A Fundamental Equations for Calcite Dissolution Kinetics," Geochim. Cosmochim. Acta. 40, 441 (1976)

Smith, R.C., "Synthesis of Organic Acids for Stack Gas Desulfurization by Aqueous Scrubbing," M.S. Thesis, The University of Texas at Austin, Texas (1981)

Tartar, H.V., and Garretson, H.H., "The Thermodynamic Ionization Constants of Sulfurous Acid at 25°C ," J. Am. Chem. Soc. 63, 808 (1941)

Terjesen, S.G., Erga, O., Thersen, G., and Ve, A.,

"The Inhibitory Action of Metal Ions on the Formation of Calcium Bicarbonate by the Reaction of Calcite with Aqueous Carbonate. 11. Phase Boundary Processes as Rate Determining Steps in Reaction between Solids and Liquids,"

Chem. Eng. Sci. 14, 277 (1961)

Weems, W.T., "Enhanced Absorption of Sulfur Dioxide by Sulfite and Other Buffers," M.S. Thesis,
University of Texas, Austin, Texas (1981)

VITA

Pui-Kun Roland Chan was born in Kowloon, Hong Kong, on January 10, 1954, the son of Shui Tai Chan and Yee Cheong Chan. After completing his work at New Method College, Kowloon, Hong Kong, in 1973, he entered Contra Costa College at San Pablo, California. He received his Associate in Science in January, 1976. During the spring of 1976, he attended San Francisco State University, California. In September, 1976, he entered the University of Texas at Austin, where he received the degree of Bachelor of Science in Chemical Engineering in May, 1979. In September, 1979, he entered the Graduate School of the University of Texas at Austin.

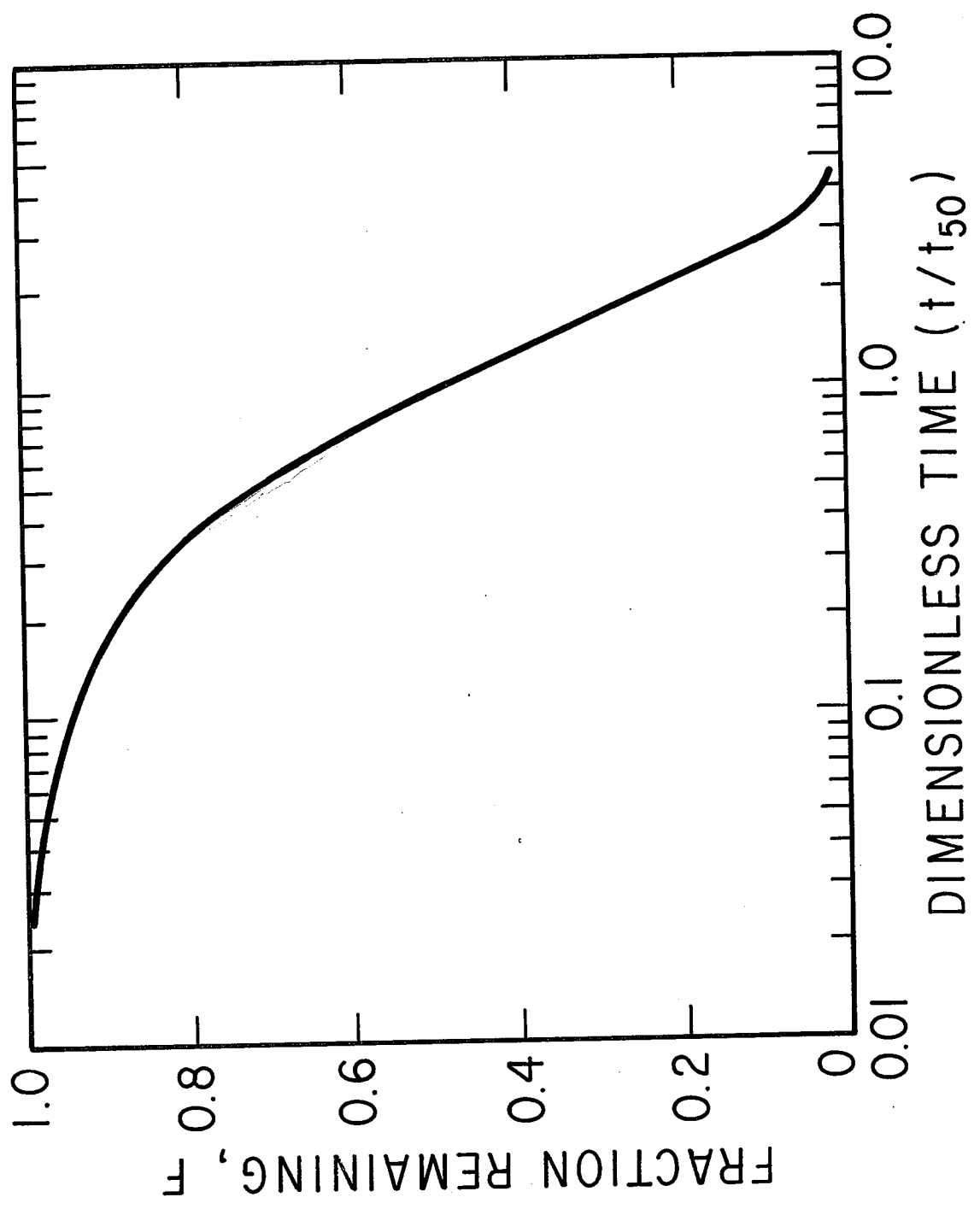
Permanent Address: 7 Whampoa Street
Kowloon. Hong Kong

This thesis was typed by the author

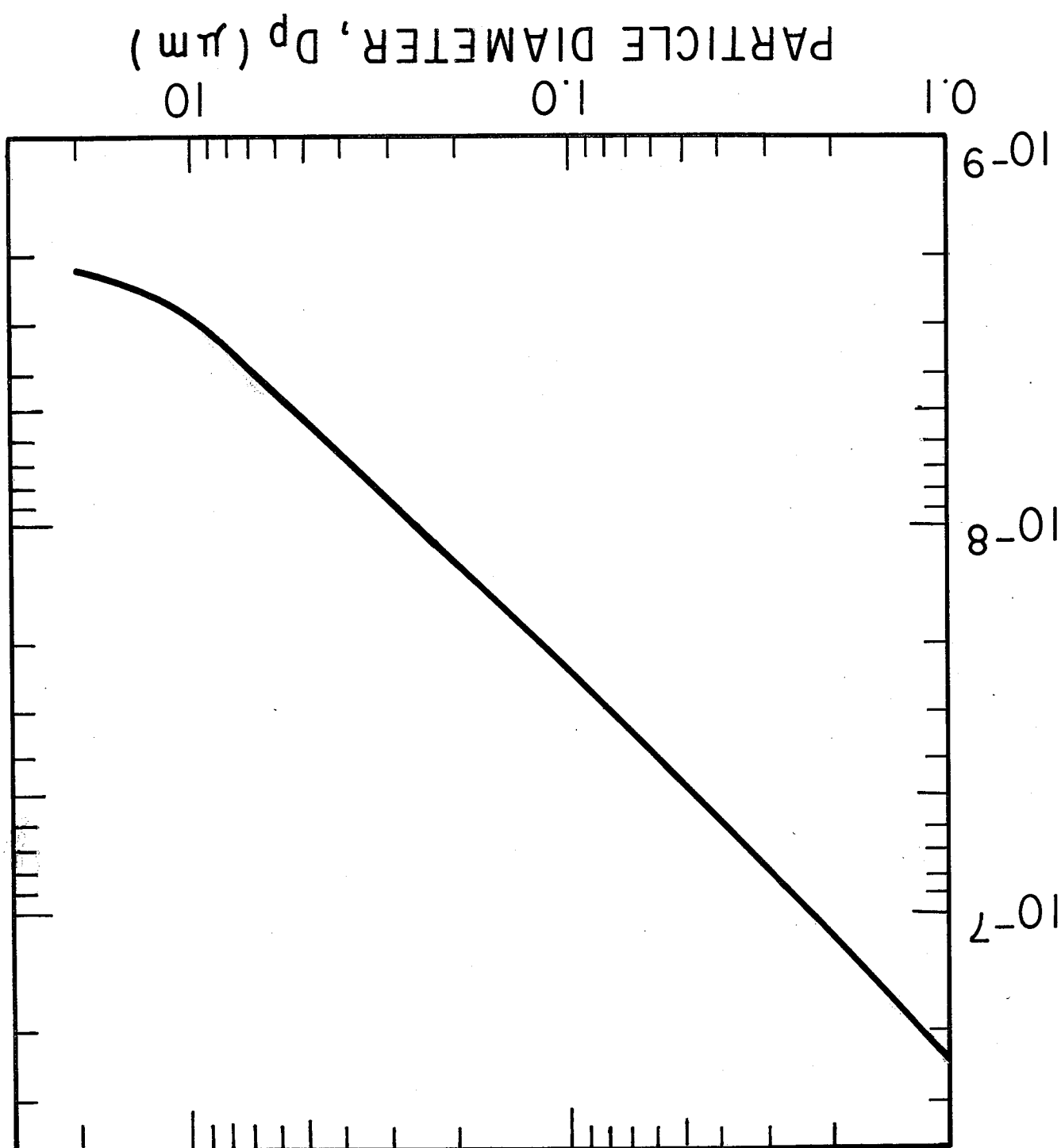
CaCO_3 DISSOLUTION IN SO_2 SCRUBBING SOLUTION
MASS TRANSFER ENHANCED BY
CHEMICAL REACTIONS

APPROVED:

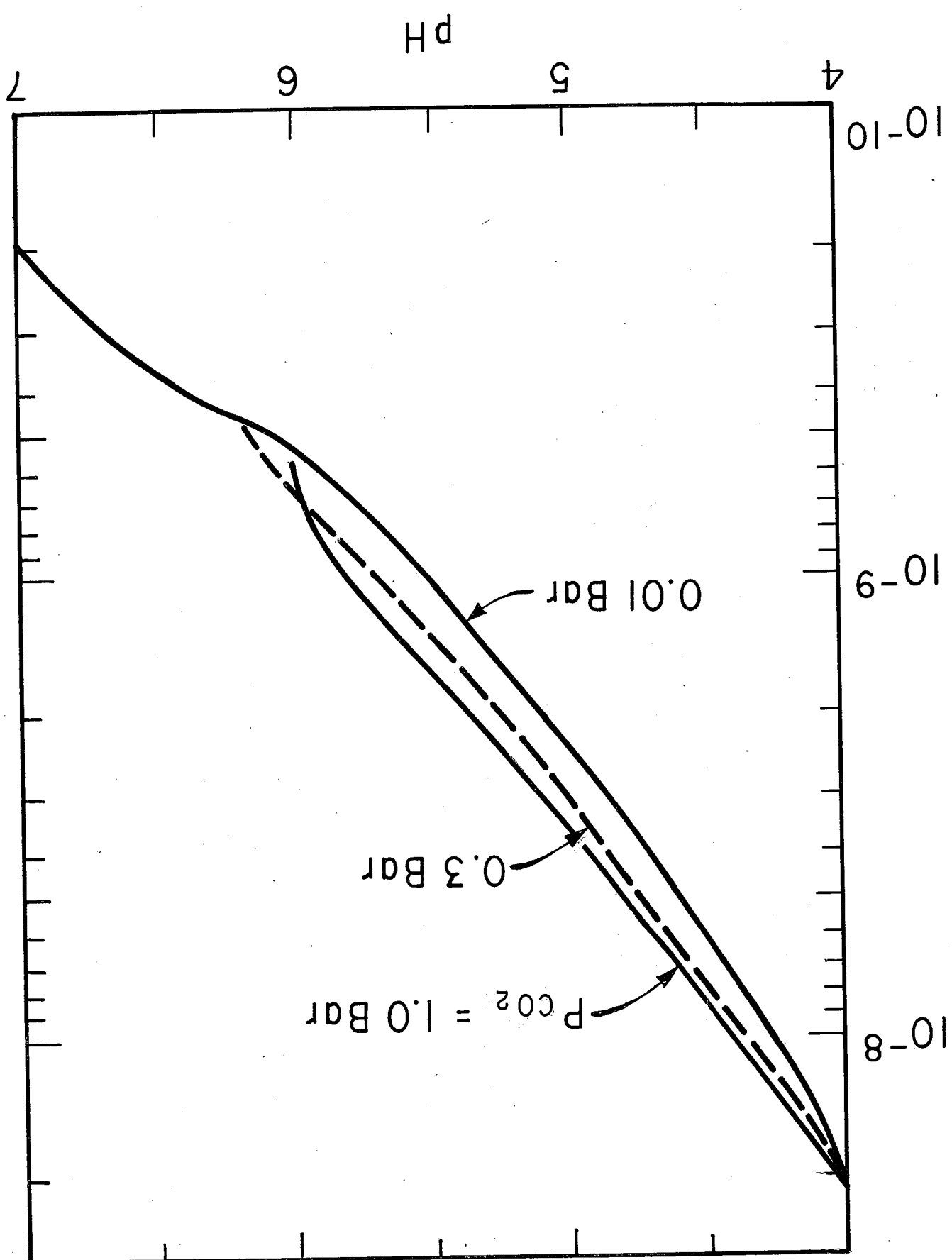
To my mother and in memory of my father

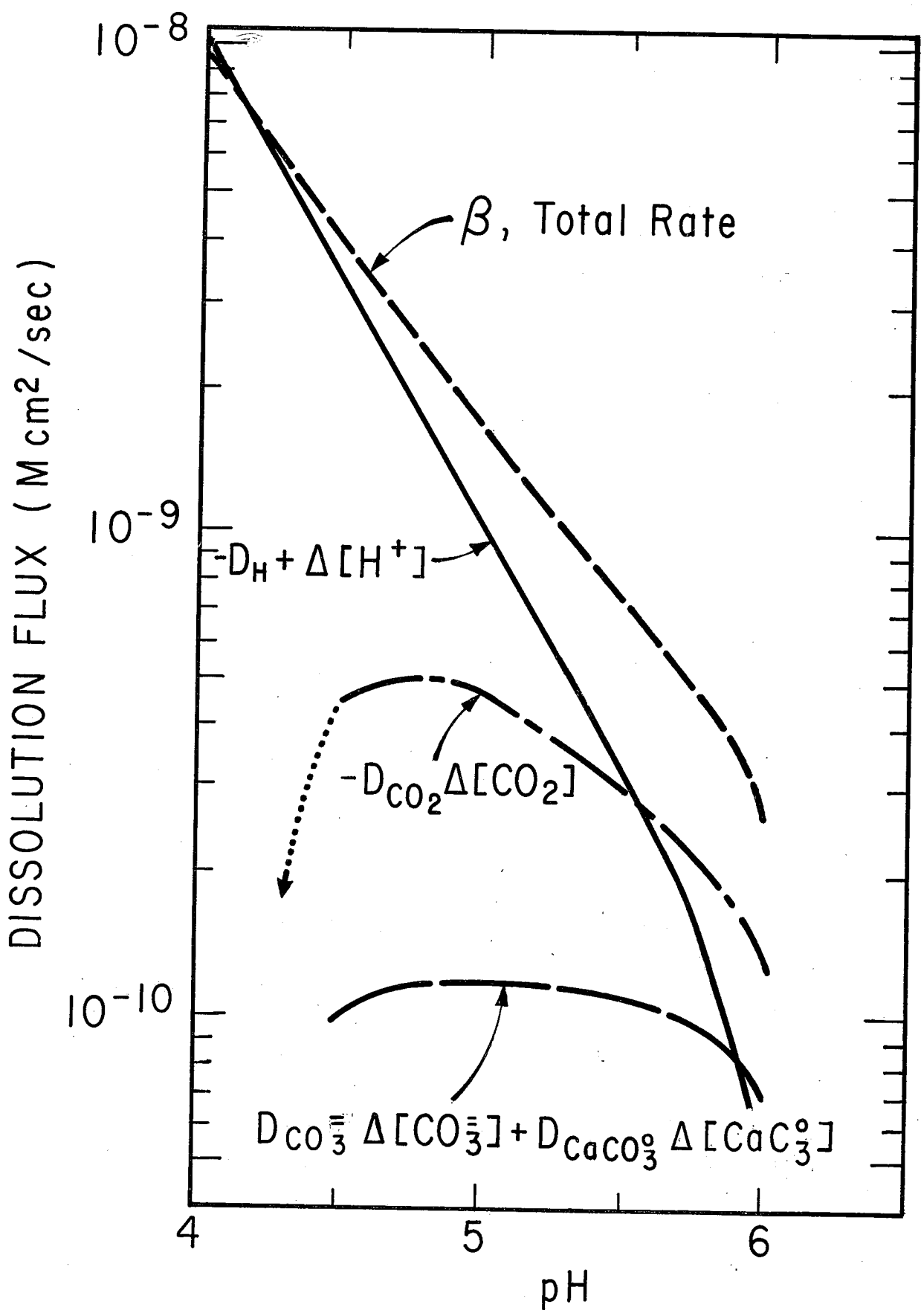


DISSOLUTION RATE (gmol/cm²-sec)



DISSOLUTION RATE (g mol/cm² - sec)





Dissolution Flux ($M \text{ cm}^{-2}/\text{sec}$)

DISSOLUTION RATE (g/mole/cm²/sec)

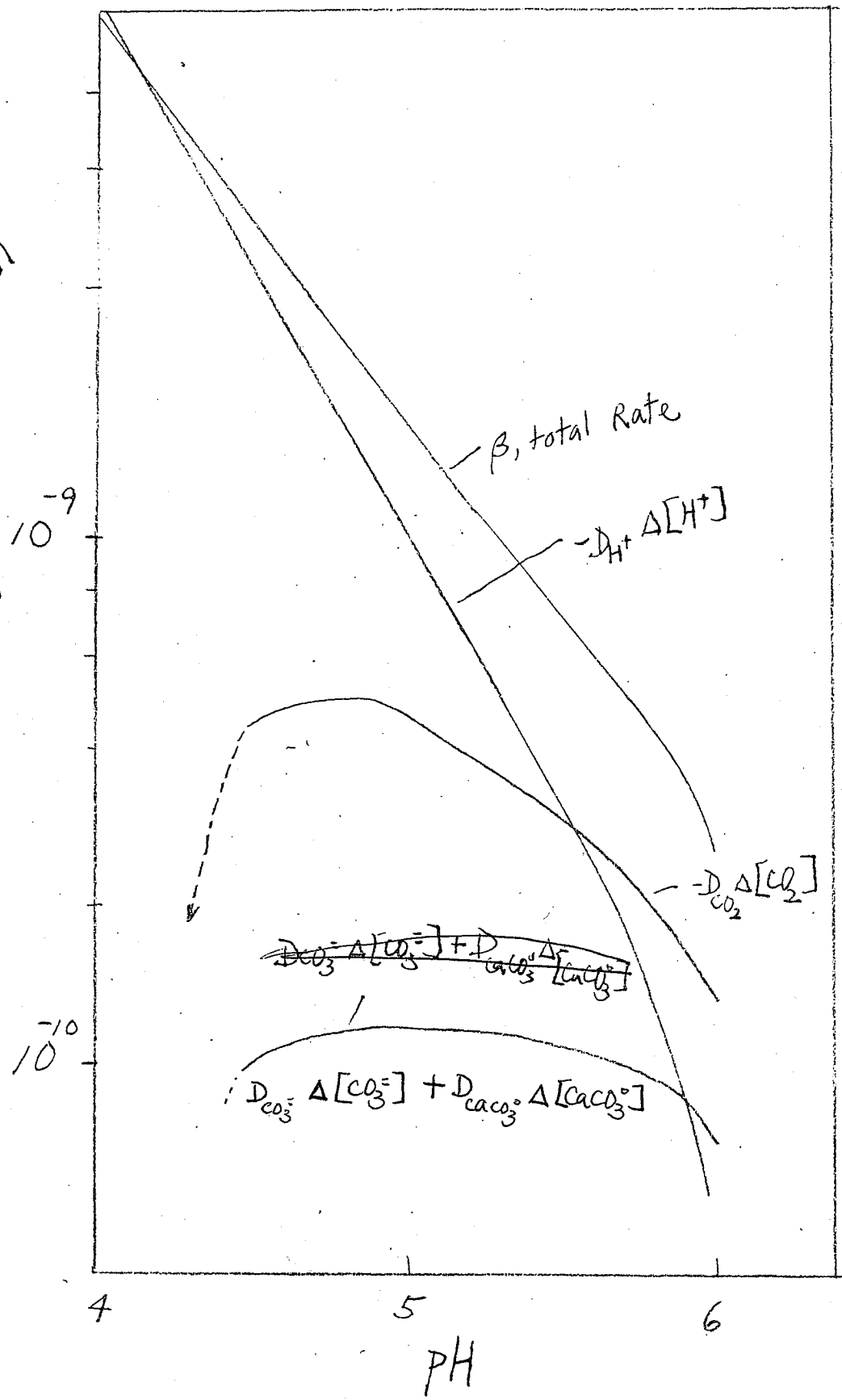


FIGURE 3-2: DISSOLUTION RATE
CONTRIBUTION From various
chemical species

$$P_{CO_2} = 1 \text{ atm}, [Ca^{2+}] = 0.01 \text{ M}, \beta = 8.8 \text{ L}$$

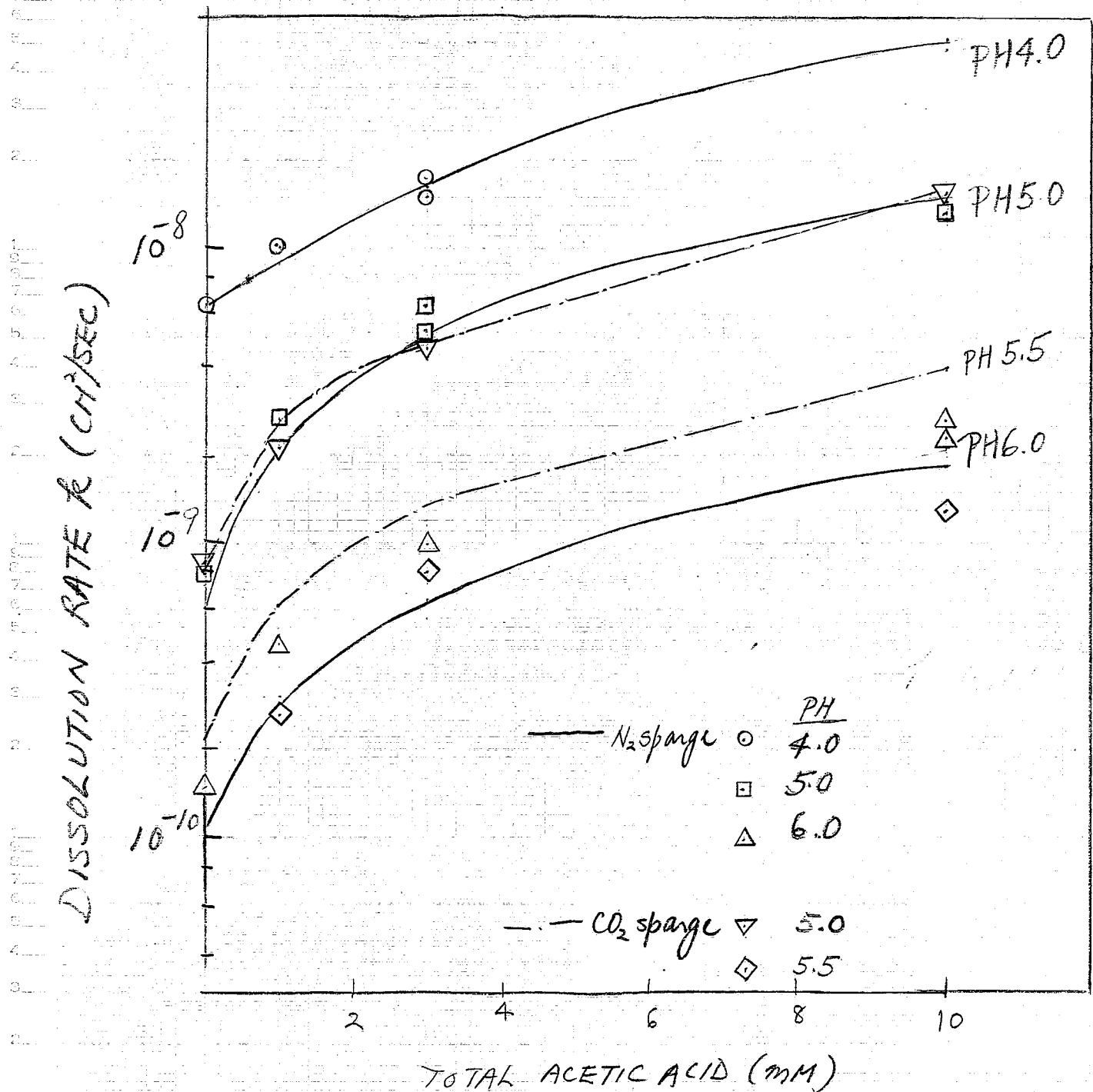


FIGURE 5-4 CaCO_3 DISSOLUTION at 25°C in 0.1M acetic acid - effect of Acetic acid.

FIGURE 5-9: CALCULATED SOLUTION COMPOSITION
AT CaCO_3 SURFACE; N_2 sparging,
 25°C .

